3D SEISMIC ATTRIBUTES ANALYSIS IN RESERVOIR CHARACTERIZATION: THE MORRISON NE FIELD & MORRISON FIELD, CLARK COUNTY KANSAS

by

ANDREW B. VOHS

B.S., University of Kansas, 2013

A THESIS

submitted in partial fulfillment of the requirements for the degree

MASTER OF SCIENCE

Department of Geology
College of Arts and Sciences

KANSAS STATE UNIVERSITY
Manhattan, Kansas

2016

Approved by:

Major Professor
Dr. Abdelmoneam Raef

Copyright

Abstract

Seismic reservoir characterization and prospect evaluation based 3D seismic attributes analysis in Kansas has been successful in contributing to the tasks of building static and dynamic reservoir models and in identifying commercial hydrocarbon prospects. In some areas, reservoir heterogeneities introduce challenges, resulting in some wells with poor economics. Analysis of seismic attributes gives insight into hydrocarbon presence, fluid movement (in time lapse mode), porosity, and other factors used in evaluating reservoir potential. This study evaluates a producing lease using seismic attributes analysis of an area covered by a 2010 3D seismic survey in the Morrison Northeast field and Morrison field of Clark County, KS. The target horizon is the Viola Limestone, which continues to produce from seven of twelve wells completed within the survey area. In order to understand reservoir heterogeneities, hydrocarbon entrapment settings and the implications for future development plans, a seismic attributes extraction and analysis, guided with geophysical well-logs, was conducted with emphasis on instantaneous attributes and amplitude anomalies. Investigations into tuning effects were conducted in light of amplitude anomalies to gain insight into what seismic results led to the completion of the twelve wells in the area drilled based on the seismic survey results. Further analysis was conducted to determine if the unsuccessful wells completed could have been avoided. Finally the study attempts to present a set of 3D seismic attributes associated with the successful wells, which will assist in placing new wells in other locations within the two fields, as well as promote a consistent understanding of entrapment controls in this field.

Table of Contents

List of Figures

List of Tables

Acknowledgements

I'd firstly like to thank everyone who made this research possible. Without vast amounts of help from these people I would not have been able to achieve the things I was aiming to achieve while at Kansas State University.

Thanks to the department faculty, students and staff at KSU who helped in so many ways during my time here. Special thanks to Dr. Abdelmoneam Raef for guiding me through this research and always being available to assist in any way possible. Thank you to Dr. Matthew Totten for initially setting up this project and making himself available to help in any way possible. Thank you to Dr. Sambhudas Chaudhuri for serving on my advisory committee and offering his assistance as well. Thank you to all of my professors previously mentioned as well as Dr. Kirk and Dr. Lambert who provided me with valuable information through coursework.

Special thanks to Dan Reynolds and Coral Coast Petroleum for providing the seismic data for this study and for being available to talk about their operation in that area. Also, thank you Adam Kennedy of Valhalla Exploration for providing digital well logs not available from the Kansas Geological Survey. And finally thank you to IHS and Rock Solid Images for providing the academic licenses for their software.

Chapter 1 - Introduction

1.1 Summary

3D seismic surveys are very useful in many exploration programs because of the high structural and stratigraphic resolution as well as the rock-properties trends that can be inferred based on seismic attributes. Analysis of seismic attributes such as root mean squared (RMS) amplitude, relative acoustic impedance, average energy and attenuation can indicate good hydrocarbon reservoir properties due to identifying lithofacies, higher porosities, structural and stratigraphic controls as well as paleotopography. Other, instantaneous attributes such as instantaneous phase, instantaneous frequency, thin bed indicator and normalized amplitude can aid in accurately tracking a horizon of interest throughout a seismic data volume, and in determining zones of hydrocarbon saturation. Using independent attributes, or a combination of attributes, one can evaluate a hydrocarbon reservoir. Relationships between attributes of seismic data and reservoir characterization and development have been recognized recently, for example, seismic amplitude, envelope, root mean square (RMS) amplitude, acoustic impedance and elastic impedance can all indicate changes in lithology, while layer thickness can be indicated by peak-to-trough thickness, peak frequency and bandwidth (Chopra & Marfurt, 2008). Spectral decomposition can aid in recognizing thinning and thickening beds by providing clear images of stratigraphic features that may not be discernable using just broadband data. This is done by providing a way to examine a geologic feature at any frequency (Subrahmanyam & Rao, 2008). Thickening and thinning of strata can be recognized by animating through a series of frequencies along an interpreted horizon allowing an interpreter to identify where strata are thinning and thickening (Chopra & Marfurt, 2008). Lateral continuity of events can be evaluated using

instantaneous attributes like instantaneous phase which is useful attribute in indicating lateral continuity of rock layers and making a detailed visualization of bedding configurations (IHS, 2012), and it can make weakly coherent events more clear (Taner et al, 1977). Normalized amplitude is also useful in confirming the lateral continuity of events and tracking horizons of interest by determining the direction of lateral continuity (IHS, 2012)

In analyzing various seismic attributes, this study will aim to determine whether the main control on well productivity in the study area is related to paleotopography and/or lithological heterogeneities as entrapment controls. The attributes analyzed will reflect this goal and an emphasis will be put on attributes that evaluate lithological heterogeneities and attributes that give insight into the thinning and thickening of layers generating paleotopographic traps.

In December of 2010 Coral Coast Petroleum obtained a permit to begin drilling for hydrocarbons within the Morrison Northeast field and Morrison field in Clark County, KS. The prospect within this field was based on a 3D seismic survey that predicted the presence of an economically viable hydrocarbon reservoir within the Viola limestone. Following the successful completion of Stephens 1, eleven more wells were completed within the field. Seven of the wells drilled are still producing oil and/or gas from the Viola limestone. One well (initially dry and abandoned in the Viola) produces from the Morrow, three wells were dry holes and a fifth unsuccessful well targeting the Viola within the survey also did not produce as predicted and was converted into a SWD well. The survey also includes the location of the Harden 4 well originally drilled by Berexeco, Inc. in 2007 that was a dry hole.

This study will aim to explain what attributes or seismic signatures led to the drilling of twelve wells in the area targeting the Viola. The study will also attempt to determine if attributes unique to producing wells can be applied to other locations within the Viola Limestone. Finally,

this study will attempt to determine if reprocessing seismic data could have avoided drilling the dry holes, and a poor producing well that was converted into a SWD well.

1.2 Study Area

The study area lies within the Hugoton embayment of Kansas which is a northern shelf-like extension of the Anadarko basin. The Hugoton embayment is bounded by uplifted areas on the west by the Sierra Grande Arch, north by the Central Kansas Uplift, and east by the Pratt Anticline as seen in Figure 1-1(Ball 1991). The area covered by the 3D seismic survey is located in Clark County, KS in the southwestern portion of the state as seen in Figure 1-2. A 3D seismic survey that lead to the drilling of twelve wells within the study area in the Morrison Northeast field and Morrison field. Figure 1-3 shows the location of the study in east-central Clark County. The twelve wells within the area covered by the seismic data volume drilled by Coral Coast Petroleum LC and one by Berexeco, Inc. are shown in Figure 1-4.

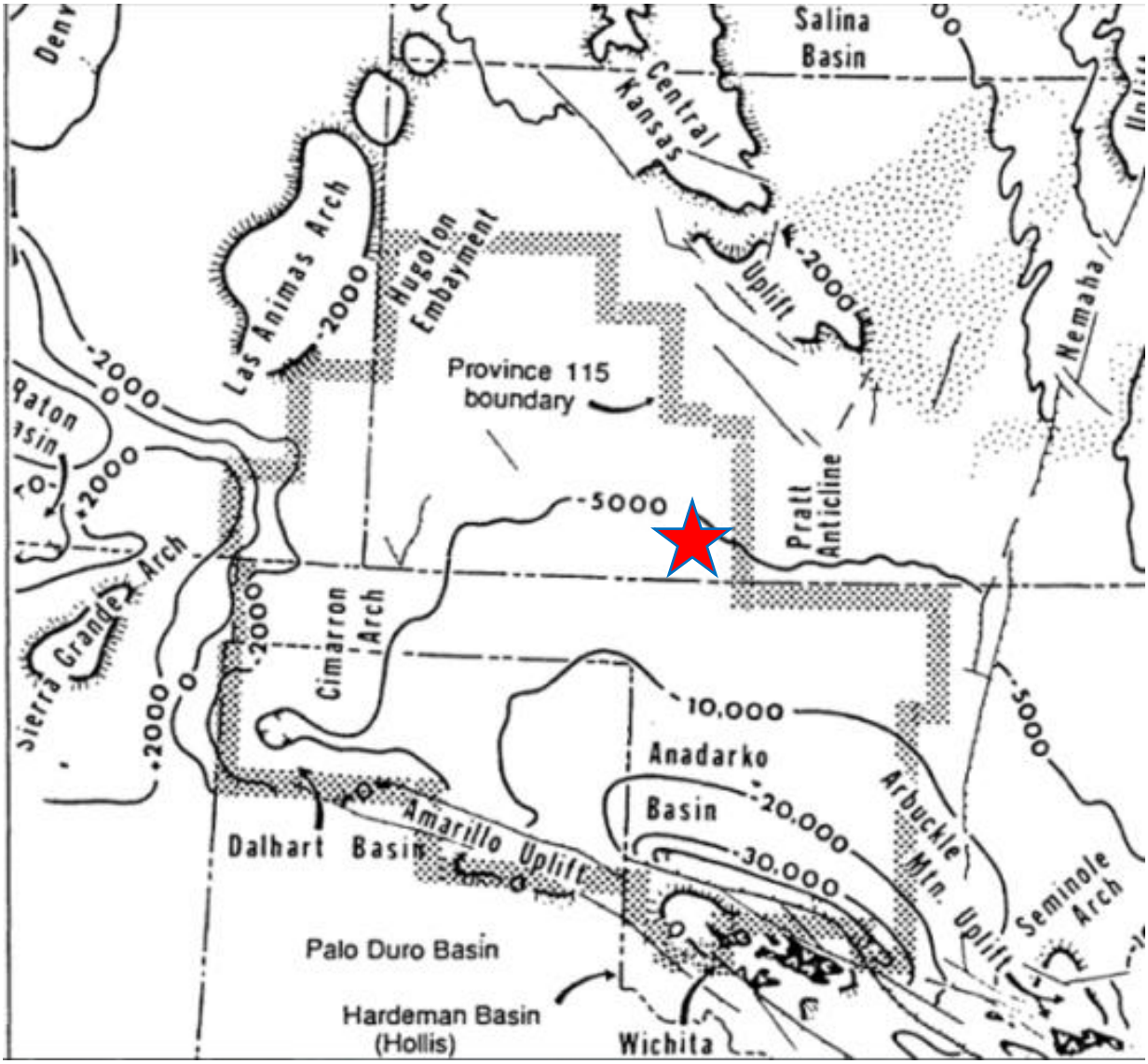

Figure 1-1 Anadarko Basin map. Red star indicates approximate location of the study area within Clark County, KS. (Adjusted from Ball, 1991).

Figure 1-2 County map of Kansas. Yellow star indicates location of Clark County, KS. (Adjusted from www.kshs.org, 2015).

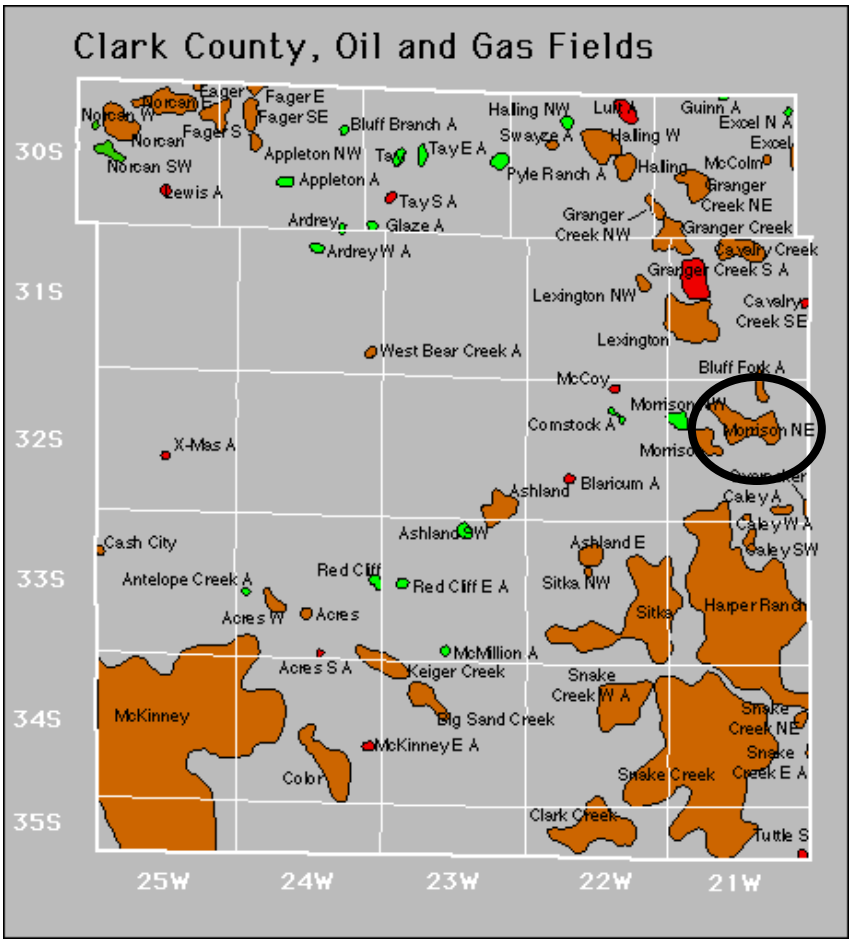

Figure 1-3 Southern Clark County KS map. The Morrison NE and Morrison fields where the wells were drilled are circled (KGS, 2014).

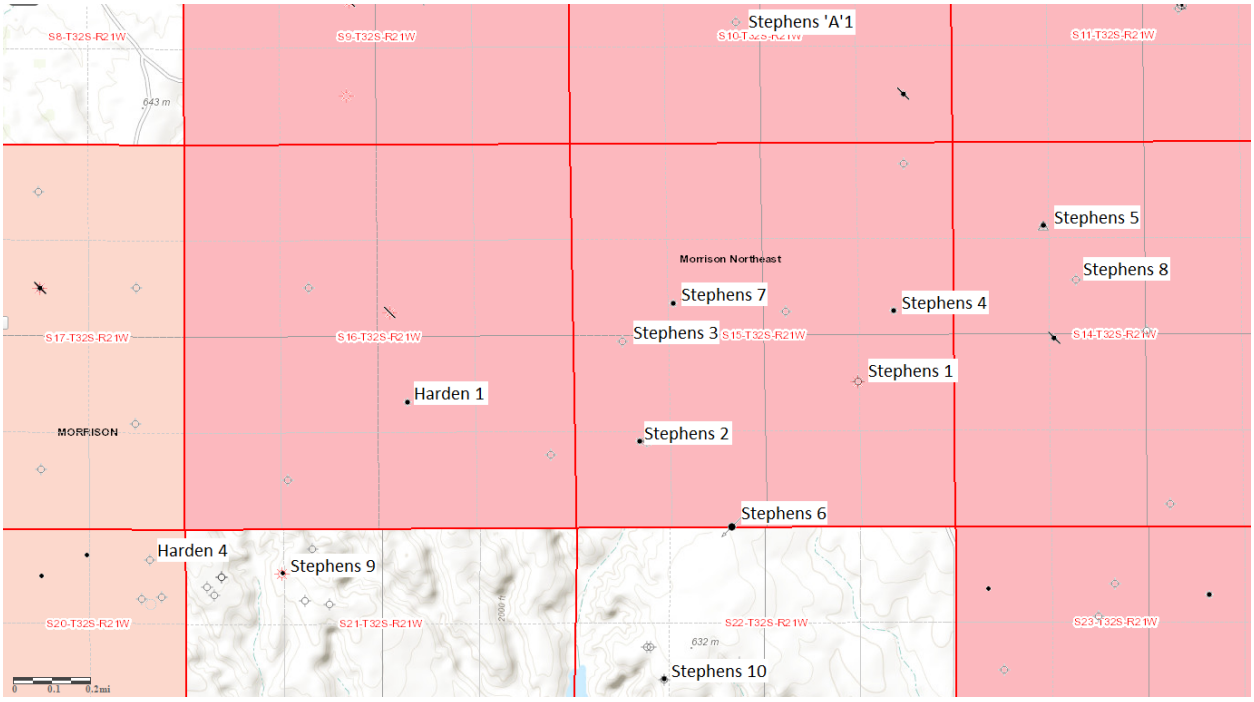

Figure 1-4 Study area within the southern portion of the Morrison NE and north east portion of the Morrison fields with the twelve wells drilled within the 3D seismic survey labeled (Adjusted from KGS, 2015). Harden 4 was drilled by Berexeco, Inc., Stephens 1-10, 'A' 1 and Harden 1 were drilled by Coral Coast Petroleum, LLC.

1.3 Field History

The first well in the area was drilled in 1954 and produced oil from formations within the Morrowan stage (Figure 1-5). From 1954 to 1966 19,734 barrels of oil were produced from the field. Below is a chart of production since 1966 within the Morrison Northeast field of Clark County, Kansas, which the majority of the survey area is within (KGS, 2015). Small amounts of oil and gas were produced between 1973 and 2011 with a spike in gas production from the mid 80's through the early 90's. In 2011 Coral Coast Petroleum began production within the Viola limestone with great success. Seven wells drilled within the area covered by this seismic survey targeting the Viola were successful

oil and gas producing wells (Tables 1-1 & 1-2). This success could lead to additional wells drilled into the Viola limestone throughout this 3D seismic survey area.

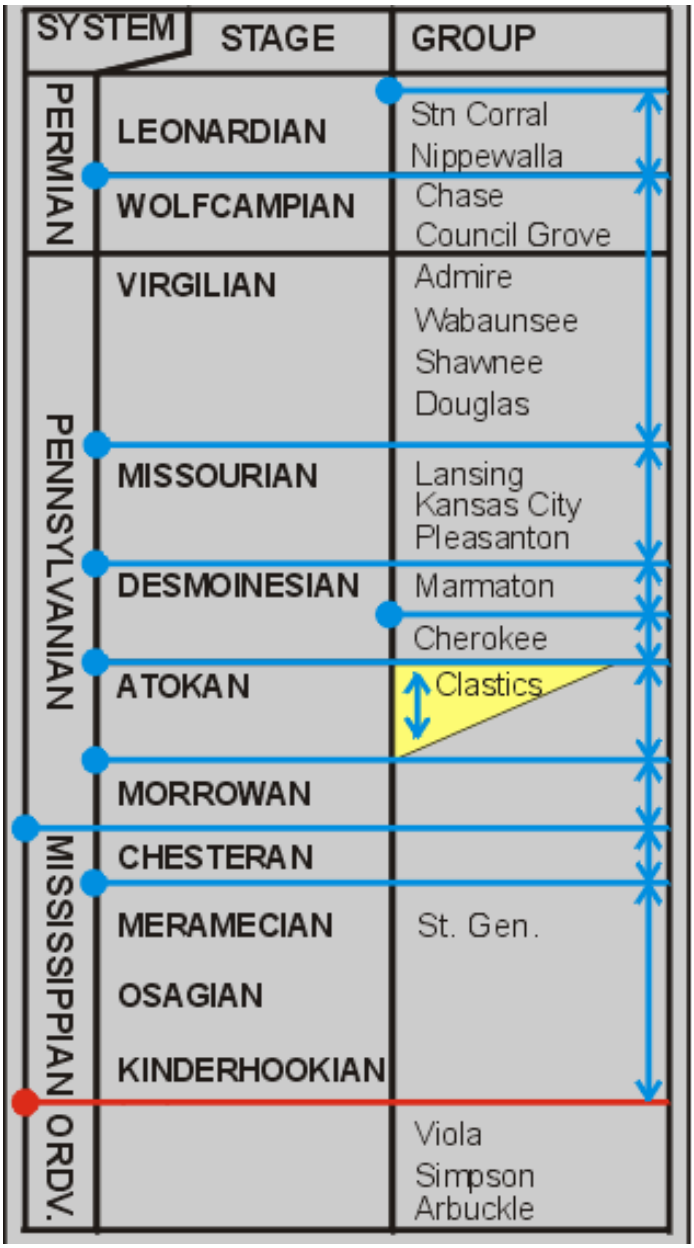

Figure 1-5 Stratigraphic column of the Morrison NE field (KGS 2015).

Year	Oil			Gas		
	Production (bbls)	Wells	Cumulative (bbls)	Production (mcf)	Wells	Cumulative (mcf)
1966	2,152	2	19,734	-	-	0
1967	2,031	3	21,765	-	-	0
1968	1,411	2	23,176	3,224,056	3	3,224,056
1969	1,498	2	24,674	54,952	2	3,279,008
1970	1,411	2	26,085	62,871	2	3,341,879
1971	982	2	27,067	8,935	2	3,350,814
1972	-	-	27,067	4,196	1	3,355,010
1973	-	-	27,067	-	-	3,355,010
1974	-	-	27,067	-	-	3,355,010
1975	-	-	27,067	-	-	3,355,010
1976	-	-	27,067	-	-	3,355,010
1977	-	-	27,067	-	-	3,355,010
1978	-	-	27,067	-	-	3,355,010
1979	-	-	27,067	-	-	3,355,010
1980	-	-	27,067	-	-	3,355,010
1981	-	-	27,067	-	-	3,355,010
1982	-	-	27,067	-	-	3,355,010
1983	-	-	27,067	7,120	1	3,362,130
1984	127	1	27,194	78,740	1	3,440,870
1985	-	-	27,194	27,251	1	3,468,121
1986	-	-	27,194	17,916	1	3,486,037
1987	-	-	27,194	12,409	1	3,498,446
1988	-	-	27,194	24,276	1	3,522,722
1989	-	-	27,194	37,147	1	3,559,869
1990	140	1	27,334	105,602	3	3,665,471
1991	-	-	27,334	114,727	2	3,780,198
1992	51	1	27,385	266	1	3,780,464
1993	-	-	27,385	-	-	3,780,464
1994	-	-	27,385	1,163	1	3,781,627
1995	-	-	27,385	-	-	3,781,627
1996	-	-	27,385	-	-	3,781,627
1997	-	-	27,385	-	-	3,781,627
1998	-	-	27,385	-	-	3,781,627
1999	-	-	27,385	-	-	3,781,627
2000	-	-	27,385	-	-	3,781,627
2001	-	-	27,385	-	-	3,781,627
2002	-	-	27,385	-	-	3,781,627

2003	-	-	27,385	-	-	3,781,627
2004	-	-	27,385	-	-	3,781,627
2005	-	-	27,385	-	-	3,781,627
2006	-	-	27,385	-	-	3,781,627
2007	-	-	27,385	-	-	3,781,627
2008	-	-	27,385	-	-	3,781,627
2009	-	-	27,385	5,182	2	3,786,809
2010	-	-	27,385	-	-	3,786,809
2011	47,065	2	74,450	34,163	2	3,820,972
2012	105,605	5	180,055	121,659	4	3,942,631
2013	68,568	6	248,623	179,069	5	4,121,700
2014	30,148	6	278,732	92,610	5	4,214,310
2015*	8,954	7	287,725	26,169	4	4,243,479

*Through 7-2015

Table 1-1 Production history of the Morrison NE field showing increase in activity following the completion of the 3D seismic survey (KGS 2015).

Well	Year	Oil Production (bbls)	Gas Production (mcf)
Stephens 1***	2011	44,694	34,163
	2012	8,066	113,997
	2013	2,081	109,555
	2014	799	83,198
	2015	478*	25,240**
Stephens 2***	2011	2,371	N/A
	2012	42,803	
	2013	19,395	
	2014	6,312	
	2015	1,248**	
Stephens 3	2011	D&A	D&A
Stephens 4***	2012	46,430	N/A
	2013	18,113	
	2014	11,151	
	2015	2,286**	
Stephens 5	2012	3,992	2,648
	2013	494-Converted to SWD	
Stephens 6	2013	6,701	10,938
	2014	1,608	4,560
	2015	306*	1,709**
Stephens 7	2013	15,293	21,465
	2014	636	
	2015	140****	240**
Stephens 8	2013	D&A	D&A
Stephens 9	2013		3,373
	2014	124	155,408
	2015		61,161**
Stephens 10	2013	N/A	N/A
Stephens ‘A’1	2011	D&A	D&A
Harden 1	2012	4,384	5,014
	2013	13,191	48,049
	2014	1,265	639*****
	2015*	166	
Harden 4	2007	D&A	D&A

*Through 5-2015, **Through 7-2015, ***Combined gas production of Stephens 1,2&4, ****Through 2-2015, *****Through 8-2014, ******Through 5-2014.

Table 1-2 Production data for the 13 wells drilled within the 3D seismic survey area (KGS 2015).

1.4 Paleotopographic Traps

Viola production within the study area is not necessarily structurally controlled. Production is controlled by preservation of the upper Viola which lies below an erosional unconformity separating it from the Maquoketa above. The upper Viola contains the porous dolomite that is associated with production. The result of this erosional unconformity is that the Viola produces from a paleotopographic trap (Richardson, 2013).

1.5 Purpose

The purpose of this study is to determine what specific seismic attributes successfully locate paleotopographic or stratigraphic traps within the Viola limestone and provide discriminating trends for the drilling results of the thirteen wells covered by the 3D seismic survey. The study will also develop a prospect analysis based on drilling results, well log analysis, and 3D seismic attributes analysis. This prospect analysis will aid in determining whether or not the controlling factor(s) in the success of wells targeting the Viola limestone in this field is simply paleogeographic heterogeneities within the field, lithological heterogeneities in the Morrison NE field or a combination of the two. Determining the extent of the seismic attributes that indicate hydrocarbon reservoirs could benefit future operations in this area. In addition, this study will attempt to determine if reprocessing the 3D seismic data could have avoided drilling the dry hole seen in Stephens 3, 8, ‘A’1, Harden 4 and the poor production that lead to Stephens 5 being converted into a SWD well.

Chapter 2- Literature Review

2.1 Geological Review

The zone of interest in this study within the Morrison NE field includes Upper Ordovician Maquoketa limestone, the Middle Ordovician stage Viola and Simpson groups and the Lower Ordovician/Cambrian Arbuckle group. These four formations are important to the study because the Maquoketa and the Simpson bound the Viola limestone above and below, and the Arbuckle forms an easy to recognize seismic reflection that aids in locating the horizons of interest. The producing formation of the wells within the 3D seismic survey is the Middle Ordovician Viola limestone. Recognizing these strata on well logs and in seismic sections is crucial in moving forward with this study to ensure horizons picked and attribute analysis is carried out at the correct time depth in the seismic section. A stratigraphic column of the study area is displayed in Figure 2-1.

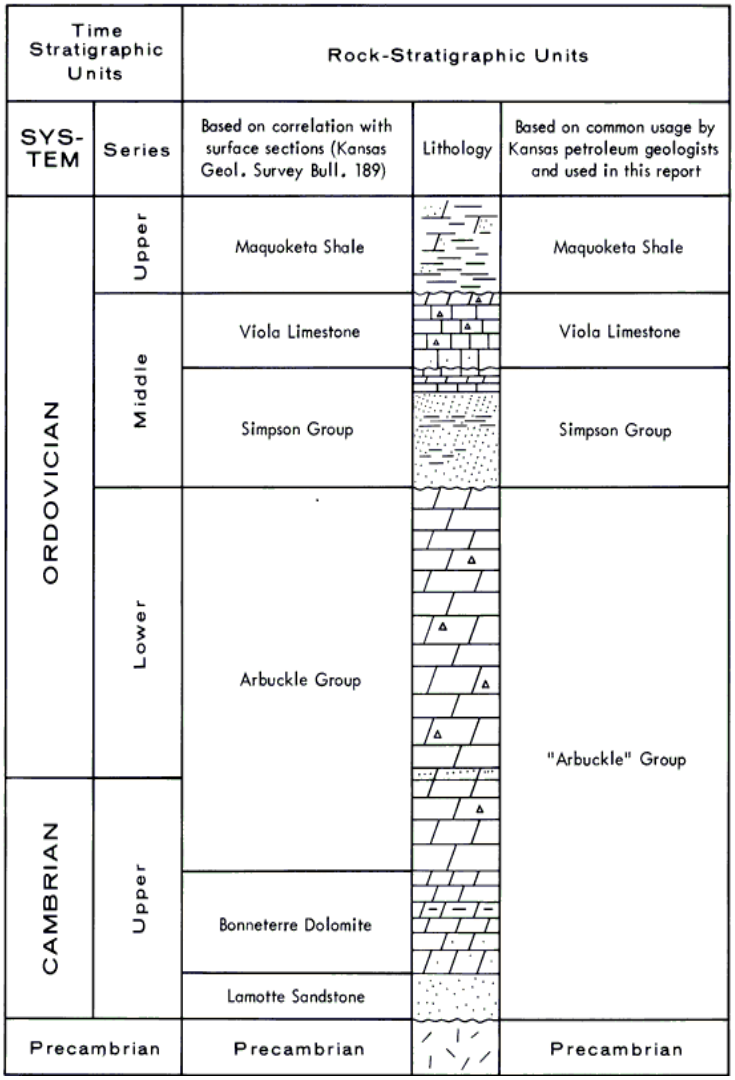

Figure 2-1 Stratigraphic column showing the formations of interest in the study area (Cole, 1975)

2.1-1 Maquoketa Shale

The Upper Ordovician Maquoketa shale is a limestone in the study area that is a difficult to recognize but important unit with regard to Viola limestone production in the Morrison NE field. This limestone serves as the seal above the Viola limestone in the study area. The Maquoketa is a cream to light gray, dense limestone with no visible porosity and a thickness of

about 20 to 25 feet within the study area. This dense non-porous rock makes an excellent seal for the petroleum system in the area (KGS, 2015).

2.1-2 Simpson Formation

The Middle Ordovician Simpson formation marks the bottom of the Viola limestone and is divided into three parts, shale and limestone represent the top of the formation, below that is the upper Simpson sand followed by the lower Simpson sand. The top portion of the Simpson formation consists of two hard and blocky shale deposits with a layer of soft, chalky fossiliferous limestone that has poor porosity in between the two shale layers. This top portion is underlain by the upper Simpson sand which consists of a fine-grained, poorly sorted, sub-rounded sandstone consisting mostly of quartz with abundant shale inclusions. The upper sand also contains a thick (~60 feet) shale layer similar to what is seen in the top portion of the Simpson formation. The base of the Simpson formation consists of a medium-coarse grained, sub-rounded quartz sandstone that is about 15 feet thick throughout the study area (KGS, 2015).

2.1-3 Viola Limestone

The producing formation of the wells within the 3D seismic survey is the Ordovician Viola limestone. The Viola limestone was deposited in the middle Ordovician period in a warm tropical marine setting (Figure 2-3), and is a medium to coarse crystalline vuggy dolomite containing scattered chert throughout with a thickness of about 175 to 200 feet within the study area. Vugs within the Viola exist mainly in the upper Viola and give it a good porosity/permeability which makes it an excellent reservoir rock for hydrocarbons to be stored (KGS, 2015). The Viola sits below an erosional unconformity separating it from the overlying

Maquoketa/Kinderhook section representing about 20 Ma of no deposition and subaerial exposure contributing to the formation of vugs that give the Viola its good porosity/permeability. Subaerial exposure is also responsible for generating the paleogeographic highs and lows within the Viola. Below this productive zone the Viola is more dense and crystalline showing no productive porosity/permeability ("C" zone). A model of a paleotopographic trap as shown in Figure 2-2 within the Viola is the result of this erosional unconformity (Richardson, 2013).

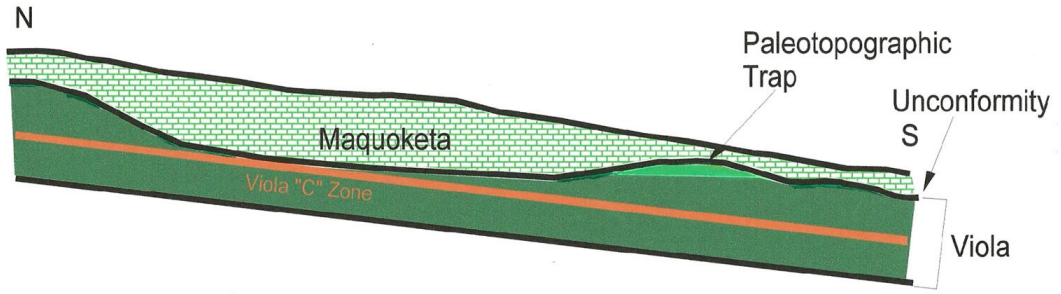

Figure 2-2 Idealized north-south cross section showing paleotopographic traps in the Viola limestone (Richardson, 2013).

2.1-4 Arbuckle Group

The lower Ordovician and Cambrian Arbuckle group is made up of dolomite, sandy/cherty dolomite and sandstone that exhibit high porosity and permeability. Arbuckle group rocks that exhibit shale only exists directly beneath shaly beds in the Simpson (Cole, 1975). The Arbuckle group is important to this study because of its seismic signature which is easy to pick up in the seismic data volume. This allows for accurate location and picking of other horizons of interest within the study area.

2.1-5 Depositional Environment

The Viola limestone was deposited during the Middle Ordovician period, a time period in which North America was located near the equator. During this time period, much of what is now the state of Kansas, and the majority of the continent was covered by an extensive epicontinental sea (Figure 2-3) (Barnes, 2004). Sedimentation during the Middle Ordovician was controlled by this epicontinental sea, as well as parts of the Transcontinental Arch that stretched across present day Kansas (Ross 1976 and St. Clair, 1981). Kansas was split by the Central Kansas Arch, which is part of the Transcontinental Arch, from northwest to southeast during the time of Viola deposition (Figure 2-4) (St. Clair, 1981). Uplifts, like the Central Kansas Arch created a shallow sea across the Southwest Kansas Basin, making an environment suitable for carbonate rocks to be deposited. Due to being deposited in this type of environment, the Viola is considered to be a shelf carbonate deposit. During the Middle Ordovician period, the epicontinental sea covering present day Kansas experienced two marine transgressions where sea level fell and rose again (Bornemann et al., 1982). Subaerial exposure of the Viola during these allowed for dissolution to occur within the upper Viola limestone, allowing the secondary, vuggy porosity to develop within the upper Viola, as well as paleotopographic highs and lows to be generated within the Viola.

2.1-5 a) Vuggy Porosity

Vuggy porosity can be defined as irregular holes that cut across grains and cement boundaries. Vugs and vuggy porosity are very common descriptive terms for describing porosity in carbonate rocks. Choquette and Pray (1970) describe a vug as a pore that is (1) somewhat equant, or not markedly elongated, (2) has a diameter greater than 1/16 mm and (3) is not fabric

selective. Vuggy porosity is usually a secondary porosity that occurs due to dissolution of the preexisting rock.

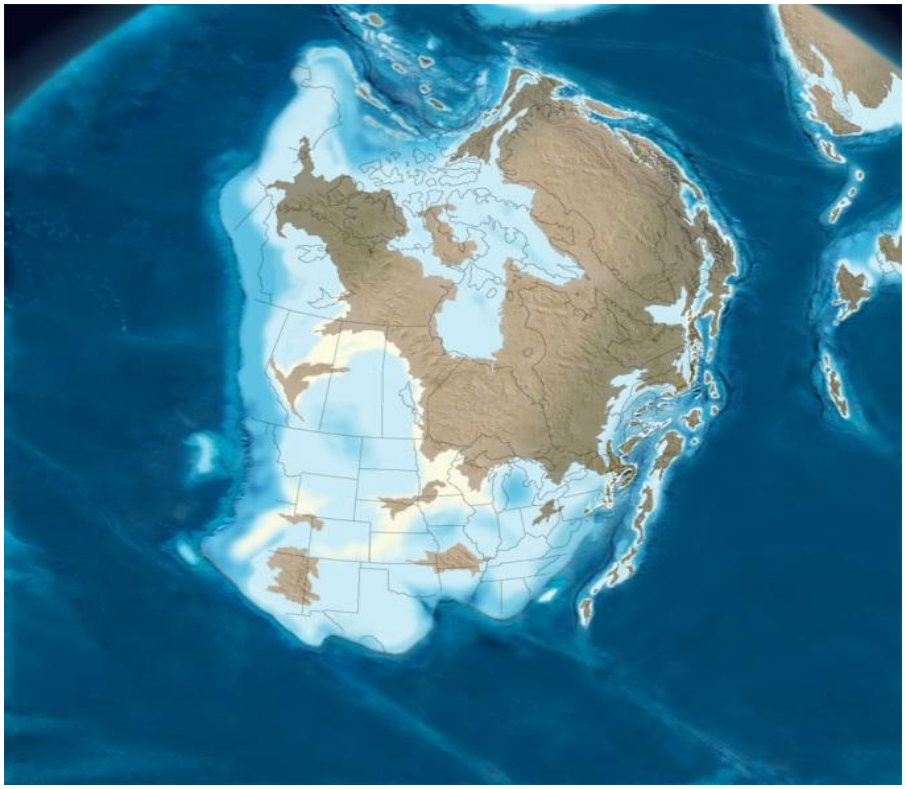

Figure 2-3 Shows a shallow epicontinental sea responsible for depositing the sediment that makes up the Middle Ordovician Viola in Kansas (Blakey, 2015).

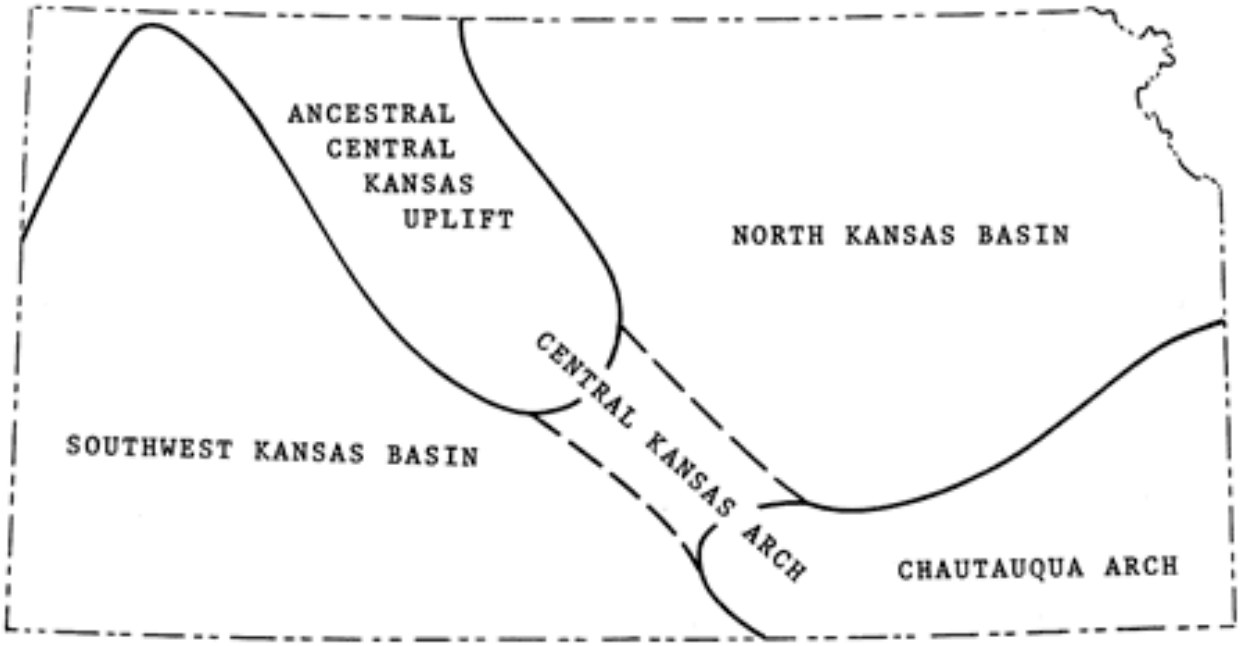

Figure 2-4 Structures present in Kansas during Viola deposition (from Merriam, 1963)

2.2 Seismic Attributes

Reflection seismology originated in the 1920's and slowly developed into the 1950's. A major breakthrough occurred in the 1960's and 1970's with the advent of digital recording and processing as well as the common midpoint stacking method. This is when reflection seismology became an important tool for the exploration geologist. Through the 1980's the quality of 2D seismic profiles increased but limitations in their ability to show complex structures posed a problem for interpretation. This problem with 3D resolution was solved by the introduction of 3D seismic acquisition and processing in the late 1980's. 3D seismic surveys have the ability to provide data that can be used to interpret stratigraphy, make detailed structural analysis and see fluid rock interactions (Cartwright & Huuse, 2005).

Seismic exploration aims to map the geologic features that are associated with the deposition, generation, migration, and entrapment of hydrocarbons, while seismic exploitation characterizes static and dynamic characteristics of hydrocarbon reservoirs. Seismic attributes measure characteristics of interest to petroleum exploration and exploitation. Good seismic attributes can be directly sensitive to the geologic feature or reservoir property of interest, or allow structural analysis of depositional environment to be defined allowing features or properties of interest to be inferred (Chopra & Marfurt, 2005).

Attributes analysis has been important to reflection seismology since the 1930's when travel times to coherent reflections began to be picked by geophysicists on seismic field records. As computer technology advanced, so did the evolution of seismic attributes. The 1960's brought digital recording which improved measurements of seismic amplitude as well as correlating strong amplitudes with presence of hydrocarbon in rock pores ("bright spots"). Early in the 1970's color printers were able to display reflection strength, frequency, phase and interval

velocity over black and white seismic records. Interpretation workstations provided interpreters in the 1980's the ability to quickly interact with data, integrating seismic traces with other information like well logs. With advances in computer technology, the 1990's brought on the industry adoption of 3D seismic attribute extractions. Associating attributes with 3D seismic sections moved attributes analysis away from seismic stratigraphy and more towards reservoir characterization and exploitation of hydrocarbon resources. As time progressed 3D seismic attributes analysis and development in rock physics research allowed for the direct relation of attributes to rock properties. Today large volumes of different data can be integrated and numerous seismic attributes can be calculated on a routine basis by seismic interpreters looking for geologic information from seismic data (Chopra & Marfurt. 2005).

More than fifty distinct seismic attributes can be calculated from seismic data and subsequently applied to interpretation of geologic structure, stratigraphy and rock/pore fluid properties. As seismic attributes continue to grow in number and variety, attempts have been made to classify them into families to better understand and apply them to hydrocarbon exploration and exploitation. A most recent classification scheme divides seismic attributes into general and specific categories. General attributes measure geometric, kinematic, dynamic, or statistical features from seismic data. Attributes in the general category include reflector amplitude, reflector time, reflector dip and azimuth, complex amplitude and frequency, generalized Hilbert attributes, illumination, edge detection/coherence, AVO, and spectral decomposition. General attributes are based on physical or morphological character of the data connected to lithology or geology thus they are 'generally' able to be applied from basin to basin all around the Earth. Specific attributes may correlate to a geologic feature or to reservoir productivity in a specific basin, but these correlations don't apply to other basins. Hundreds of

specific attributes are cited in literature, but many are sums, products, or combinations of general attributes being applied to a specific basin (Chopra & Marfurt, 2005).

Attributes are being used by geoscientists to map features on a scale as small as an individual reservoir to as large as an entire basin. Relationships between attributes of seismic data and reservoir characterization/development have been recognized recently, for example, seismic amplitude, envelope, root mean square (RMS) amplitude, acoustic impedance and elastic impedance can all indicate changes in lithology, while layer thickness can be indicated by peak-to-trough thickness, peak frequency and bandwidth. This use of seismic attributes has been increasing in energy companies, geoscience contractors, and in universities when looking to improve workflows using these well-established attributes as well as looking at previously unrecognized or overlooked geologic features. (Chopra & Marfurt, 2008).

Generally interpreters work with amplitude character based on a single dominant frequency which can be modified by thin-bed tuning (Chopra & Marfurt, 2008). Spectral decomposition can give clear images of stratigraphic feature that may not be discernable using just broadband data by providing a way to examine a geologic feature at any frequency (Subrahmanyam & Rao, 2008). Using spectral decomposition replaces the single input trace with a gather of traces corresponding to the spectral decomposition of the input attribute. The input to spectral decomposition is a seismic volume while the output is several volumes representing individual frequency bands. Spectral decomposition allows for structures with different frequency bands to be illuminated to see if a particular frequency band gives better resolution. Animating through a series of frequencies along an interpreted horizon allows an interpreted to identify where strata are thinning and thickening (Chopra & Marfurt, 2008).

2.2-1 Complex Seismic Trace

Processed seismic data is used to characterize reservoirs using both spatial and temporal variations in reflection amplitude, reflection phase and wavelet frequency. A complex seismic trace is required for generating certain seismic attributes because it introduces the concepts of instantaneous seismic amplitude, phase and frequency allowing for the generation of instantaneous seismic attributes. Instantaneous, when referring to seismic amplitude, phase and frequency, means that a value for each is calculated for every time sample along the seismic trace. This trace is referred to as a complex seismic trace, not because it is mathematically complex, but because it is generated using two inputs (1) a real part (actual or real seismic trace) and (2) an imaginary part (quadrature or imaginary seismic trace). The first input is a seismic trace which is the recorded curve from a seismograph, and is referred to as the actual seismic trace or real seismic trace (Taner et al, 1977). This is the first input in generating what is known as the complex seismic trace that is required when generating seismic attributes. The second input in generating the complex seismic trace is known as the quadrature trace or imaginary seismic trace (Taner et al, 1977). The imaginary seismic trace is calculated using the Hilbert transform of the real seismic trace. The Hilbert transform is a filter that is applied to stacked seismic data (real seismic trace) that rotates the phase angle by 90 degrees. This rotation of phase angles cause what would be a zero-crossing on the real seismic trace to be either a peak or trough on the imaginary trace, while peaks and troughs on the real seismic trace will be zero-crossings on the imaginary trace (Figure 2-5) (Partyka, 1999). The real seismic trace and imaginary seismic trace are then combined to generate the complex seismic trace, which preserves the amplitude spectrum of both of the seismic traces and is displayed in 3D as a helical

spiral along the time axis with the real seismic trace on one axis and the imaginary seismic trace on the other (Figure 2-6) (Taner et. al, 1977).

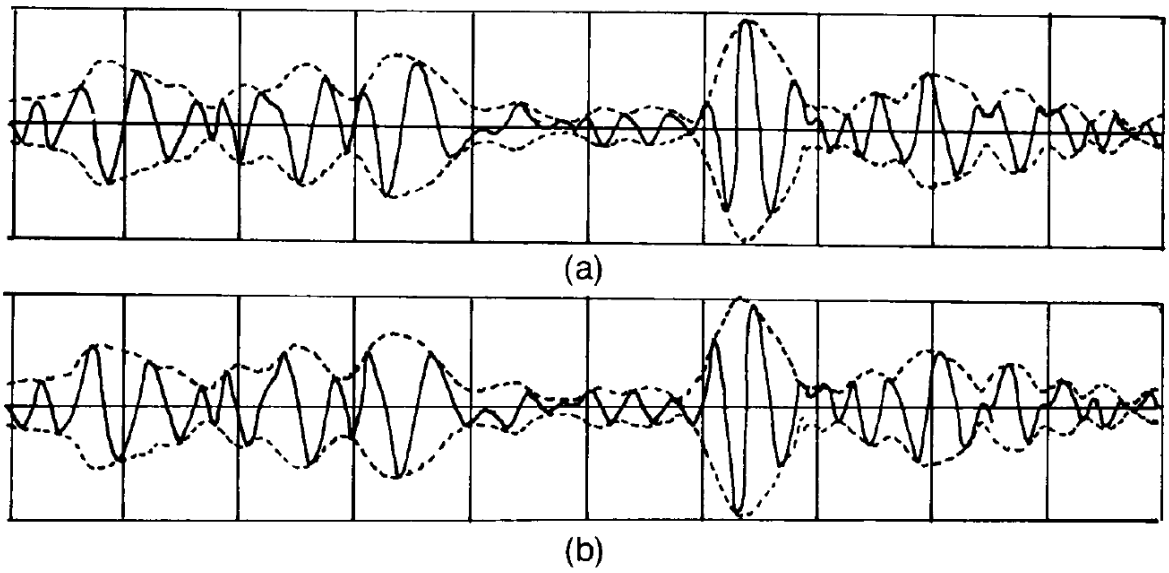

Figure 2-5 (a) Is the real seismic trace and (b) is the imaginary seismic trace. The x-axis is amplitude and the y-axis is two-way travel time. Note the zero-crossings in the real seismic trace result in peaks and troughs in the imaginary seismic trace, while peaks and troughs in the real seismic trace result in zero-crossings in the imaginary trace and vice versa. The dotted line is reflection strength (Taner et. al, 1977).

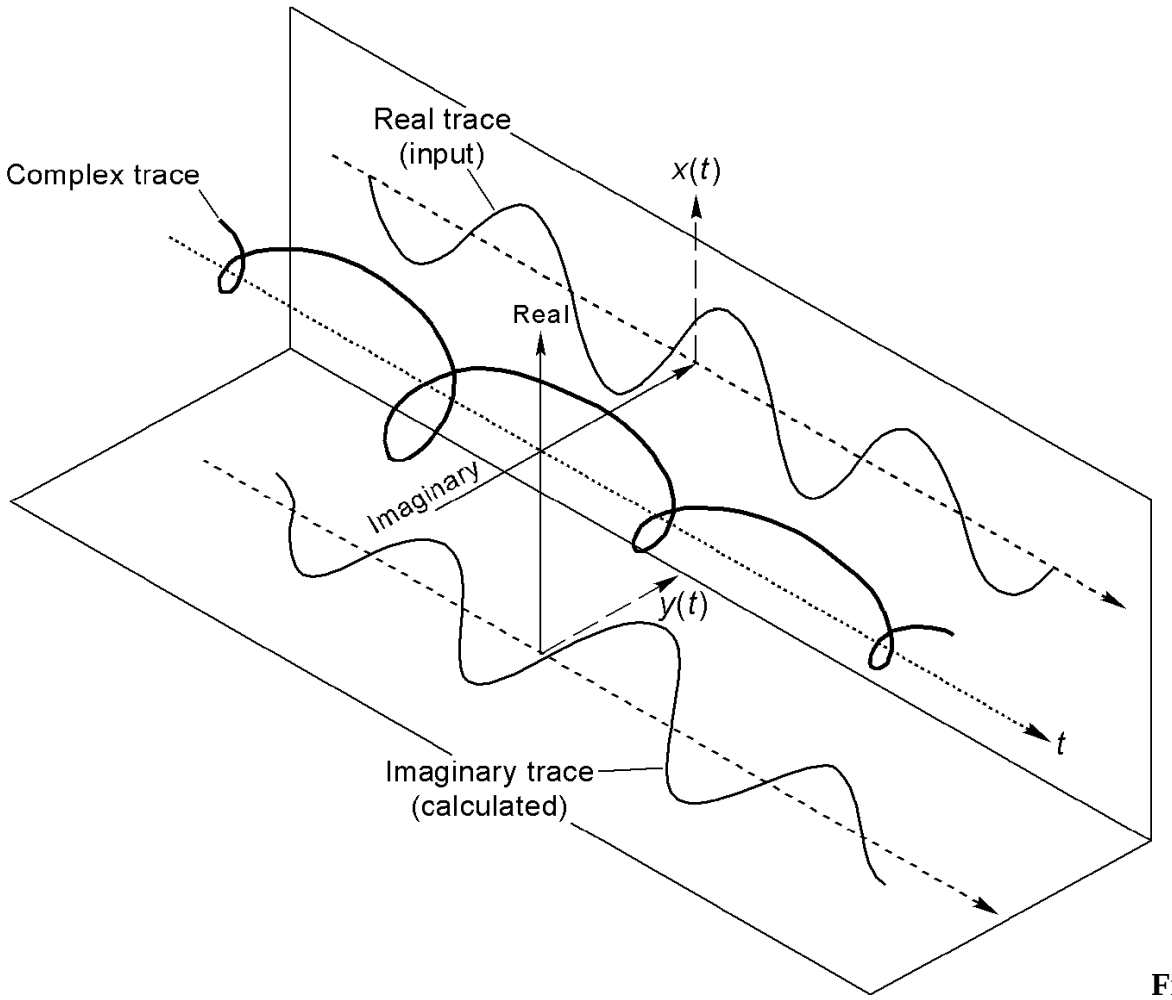

Figure 2-6 A diagram of a portion of an actual complex seismic trace showing the quadrature (imaginary) trace on the y-axis, the actual (real) seismic trace on the x-axis and the helical complex seismic trace on the time axis in 3D (BEG, 2015).

Chapter 3 - Data and Methods

3.1 Data Collected

The first step in beginning this study was to collect all available data for the zone of interest within the study area. Data collected included the 3D seismic survey, digital and paper well logs for the 12 wells drilled based off of the 3D seismic survey and the well drilled prior to the survey being completed within the area covered by the survey, details about each well (Table 3-1) and production data for the Morrison NE field (Tables 1-1 & 1-2). Coral Coast Petroleum acquired the seismic data in 2010, in the Morrison NE field, Clark County, Kansas and donated the survey for this study. Well and production data was available from the Kansas Geological Survey website.

Well Name	Elevation (ft)	Total Depth (ft)	Digital Logs	Tops	Status
Harden 1	2118 KB	6690	Yes	No	O&G
Harden 4	2134 KB	6777	Yes	No	D&A
Stephens 1	2050 GL	6840	Yes	Yes	O&G
Stephens 2	2063 KB	6750	No	Yes	O&G
Stephens 3	2065 KB	6760	Yes	Yes	D&A
Stephens 4	2049 KB	6760	Yes	Yes	O&G
Stephens 5	1988 KB	6675	Yes	No	SWD
Stephens 6	2067 KB	6518	No	No	O&G
Stephens 7	2044 KB	6610	Yes	No	O&G
Stephens 8	1984 KB	6866	Yes	No	D&A
Stephens 9	2122 KB	6812	Yes	Yes	O&G
Stephens 10	2055 KB	6760	Yes	Yes	O&G (Morrow)
Stephens 'A' 1	1997 KB	5340	Yes	No	D&A

Table 3-1 Data available for each well.

3.2 Methodology

3.2-1 3D Seismic interpretation platform and Data Loading

IHS Kingdom Suite and OpendTect software were used to complete this study. Kingdom Suite is a PC-based software application that can cover a wide range of geological and seismic interpretation workflows. Many companies of all different sizes use Kingdom Suite as their seismic interpretation software of choice. To learn more about IHS Kingdom suite go to:

www.ihs.com. OpendTect is an open source seismic interpretation software that is available for free. More information on OpendTect can be found at www.opendtect.org.

A 3D Seismic survey was uploaded into IHS Kingdom Suite software and a workflow was generated (Table 3-2). The survey parameters include 320 inlines running west to east and 380 crosslines running south to north with a bin spacing of 82.5 feet, covering an area of approximately seven and a half square miles. The sampling rate for this survey was approximately 2.0 milliseconds or 500 Hz, with adequate sampling of up to 250 Hz (Nyquist frequency) and a cut off frequency of 125 Hz with the dominant frequency being about 60 Hz as seen in the amplitude spectrum shown in Figure 3-1. The survey was uploaded as a SEGY file into Kingdom Suite using a seismic reference datum of 2200 feet and a replacement velocity of 11,000 feet per second. The projection system used for this survey was NAD 27, Southern Kansas, US foot. Once the 3D seismic survey was loaded well locations, elevations, total depths, digital logs, tops data and well statuses were also loaded into Kingdom Suite.

Step	Method Description
Step 1	Create new project and upload seismic survey and well data to Kingdom Suite
Step 2	Generate synthetic seismograms: seismic modeling and synthetic-to-seismic tie
Step 3	Seismic interpretation, horizon tracking and surface generation
Step 4	Generate seismic attributes and spectral decomposition, quality check horizons with Kingdom Suite
Step 5	Seismic attributes analysis in Kingdom Suite and OpendTect
Step 6	Digital well log analysis
Step 7	Multi-attributes space and cluster analysis in prospect evaluation

Table 3-2 3D seismic interpretation workflow.

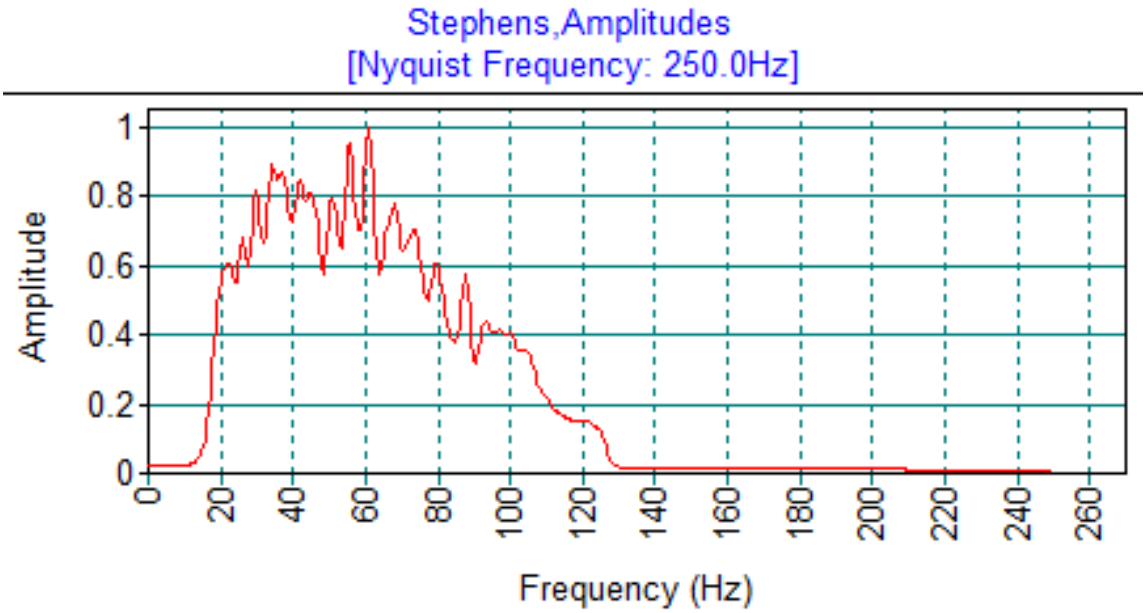

Figure 3-1 Amplitude spectrum for the Stephens Ranch 3D seismic survey.

3.2-2 1D Seismic modeling: Identifying stratigraphic seismic horizons

Raw seismic data is of limited to use to a seismic interpreter. Things like structure are possible to be interpreted using raw seismic data but no correlation to what formation is appearing at a particular time depth can be made using only raw seismic data. To tie actual formations of interest to the seismic data synthetic seismograms need to be generated. A synthetic seismogram produces seismic traces unique to specific layers or formations of interest in the subsurface when a seismic pulse is produced. Synthetics also allow to correlate well log data, which is sampled in feet, with seismic data which is sampled in two-way travel time. The main inputs for generating synthetic seismograms are seismic trace data at the borehole, time-depth relationship charts, acoustic or sonic logs for the borehole, density logs for the borehole and seismic wavelets extracted from the trace data or theoretical seismic wavelets. The well logs provide a smaller sampling interval outside of the vertical resolution of the seismic data when velocity and density are measured at the borehole. Velocity and density information is taken

from the well logs and configured to produce acoustic impedance which is shown in the equation below:

$$Z=\rho * \upsilon$$

where Z = acoustic impedance, ρ = density and υ = velocity within the layer of interest. The acoustic impedance and velocity information combine to produce a reflection coefficient related to time. To achieve a reflection coefficient, two assumptions are made. The first assumption is that the earth consists of horizontal layers with constant velocity, and the second is that the source of the seismic pulse generates a compressional plane wave that encounters layer boundaries at normal incidence producing no shear waves (Yilmaz, 1987). The reflection coefficient is the change in velocity and density, or acoustic impedance, between two boundaries (boundaries 1 & 2) and is calculating using the equation:

$$e(t)=\frac{(Z_2-Z_1)^2}{(Z_2+Z_1)^2}$$

where e(t) is the reflection coefficient, Z_1 is acoustic impedance in medium one and Z_2 is acoustic impedance in medium 2. This reflection coefficient is the ratio of change in acoustic impedance to twice the average in acoustic impedance across two boundaries. If Z_2 is greater than Z_1, then the reflection coefficient is positive. If Z_2 is less than Z_1, then the reflection coefficient is negative. After the reflection coefficient is calculated for all reflections in the seismic data, a seismic wavelet is extracted from the seismic trace data surrounding the borehole. This seismic wavelet is known as the source wavelet and it is assumed to be non-changing as it travels through the subsurface (Yilmaz, 1987). This wavelet will replicate itself according to the reflection coefficient. If the reflection coefficient is positive, the wavelet will exhibit positive polarity (a peak), and if the reflection coefficient is negative, the wavelet will exhibit negative or

reversed polarity (a trough). The source wavelet that is produced is then convolved with the reflection coefficient to produce the synthetic seismogram for the well following the convolutional model below:

$$x(t) = w(t) * e(t) + n(t)$$

where w(t) is the seismic wavelet, e(t) is the reflection coefficient, * signifies convolution, n(t) is random noise and x(t) is the synthetic seismogram. Random noise is caused by several sources such as wind, environment noise (e.g. passing truck) or geophones not secured to the ground properly. Two assumptions about the above equation must be made to generate a synthetic seismogram. The first is that the noise component n(t) is zero and the second is that the source waveform w(t) is known (Yilmaz, 1987). These assumptions produce the convolutional model for a seismogram that is free of noise below:

$$x(t) = w(t) * e(t)$$

where w(t) is the seismic wavelet, e(t) is the reflection coefficient, * signifies convolution and x(t) is the synthetic seismogram. Figure 3-2 gives a visual representation of the processes behind synthetic seismogram generation.

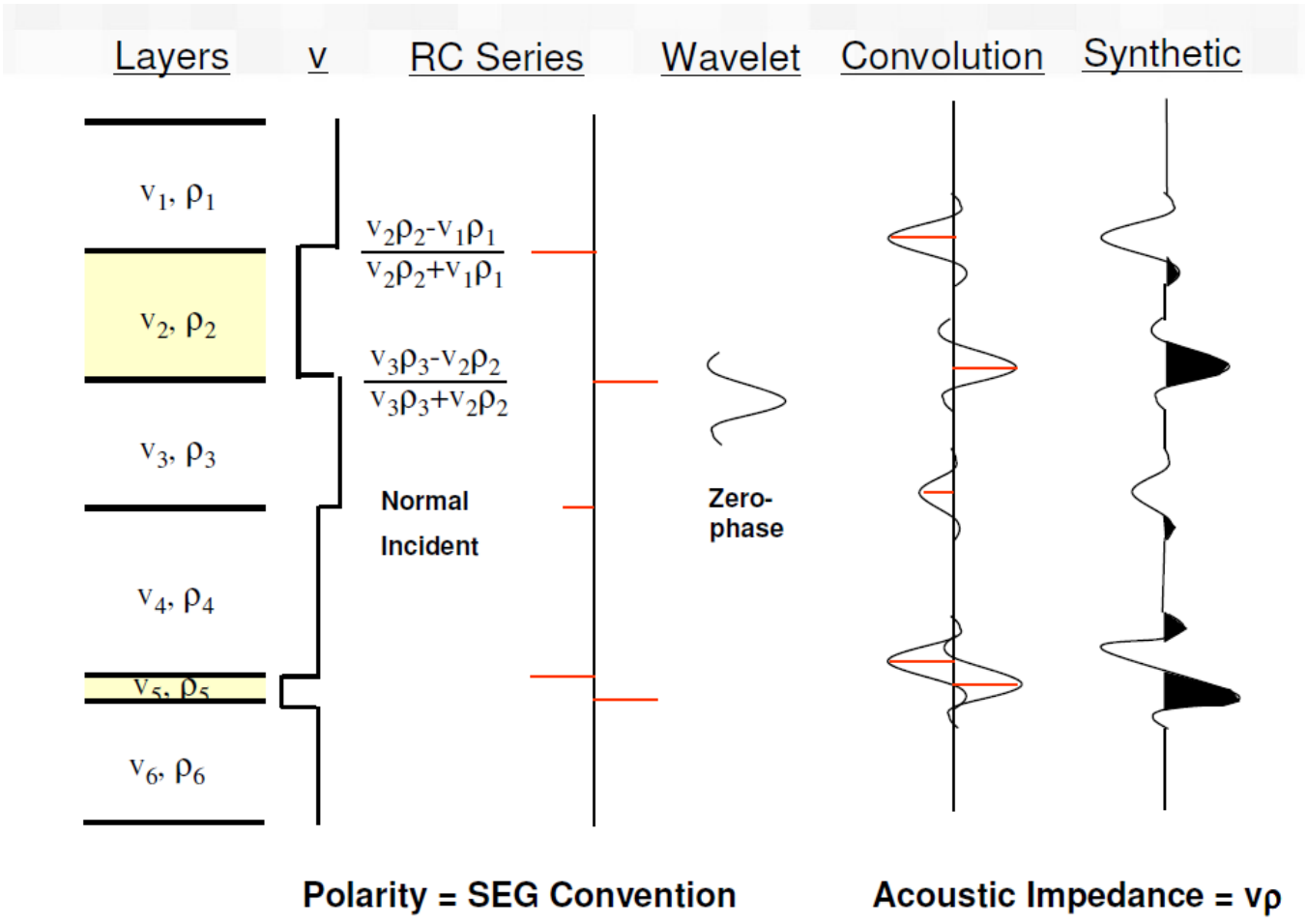

Figure 3-2 (SMT, 2013) Visual representation of the convolutional model for synthetic seismogram generation.

Synthetic seismograms, or synthetics, were generated for each well with digital well logs within the 3D seismic survey area. The synthetics were generated using digital density logs and sonic logs, time-depth charts, wavelets derived from the seismic data and seismic trace data around each well borehole with available digital well logs. Eight out of the thirteen wells within the area covered by the seismic survey resulted in acceptable synthetic seismograms. The wells with acceptable synthetics are; Stephens 1, Stephens 3, Stephens 4, Stephens, 5, Stephens 6, Stephens 7, Stephens 8 and Stephens 9 (Figure 3-3).

When generating synthetic seismograms, the initially generated synthetic does not match well to the seismic trace data well resulting in a poor correlation coefficient. Due to this problem, a synthetic interpretation step is required to match the generated synthetic to the seismic trace data. The first step in synthetic interpretation is the bulk shift. The bulk shift operation shifts the entire synthetic either up or down which will change the correlation coefficient and replacement velocity. It is important to be very careful when bulk shifting and observe all changes happening. Once the maximum correlation coefficient achievable using the bulk shift operation is reached, stretching and squeezing of the synthetic can be done as well to further improve the correlation coefficient. An acceptable correlation coefficient between seismic data at the borehole and synthetics is about 0.6 to 0.7 (Figure 3-3 a). Stretching and Squeezing must be done conservatively, to maintain accuracy in the final synthetic seismogram (3-3 a & b). Figure 3-3 also show the relationship between sonic logs, density logs, acoustic impedance values and reflectivity coefficients. These values all contribute to the generation of a synthetic seismogram.

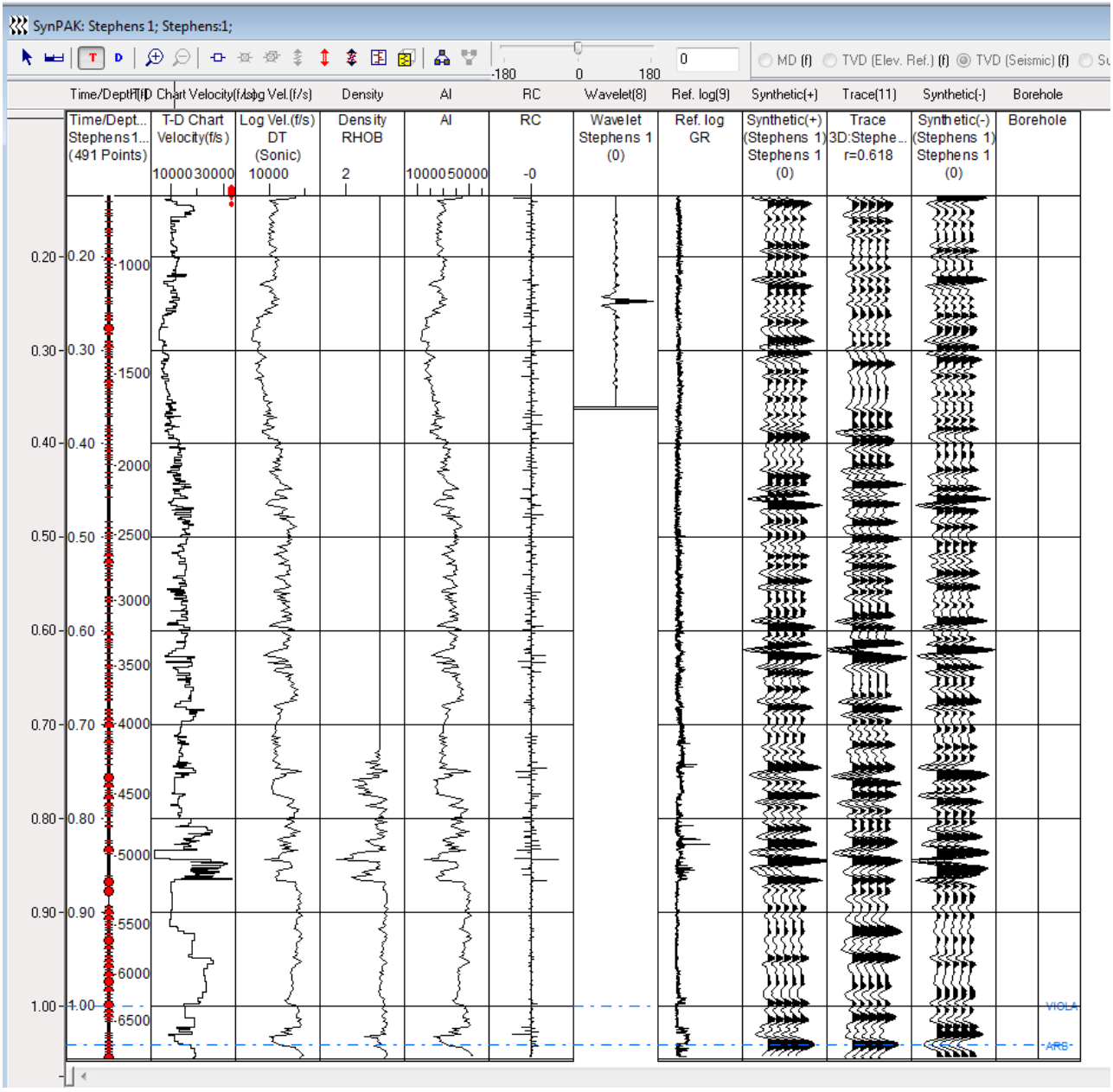

Figure 3-3 a) is a visual representation of synthetic generation using Kingdom Suite showing acoustic impedance as the product of velocity (DT) and density (RHOB) of particular horizons in the subsurface, reflection coefficients calculated from the ratio of the difference in acoustic impedance to twice the average acoustic impedance across two boundaries, reflection coefficient being convolved with the source wavelet, and individual wavelets being summed to generate a synthetic. Correlation coefficient value r=0.618 represents an acceptable correlation coefficient.

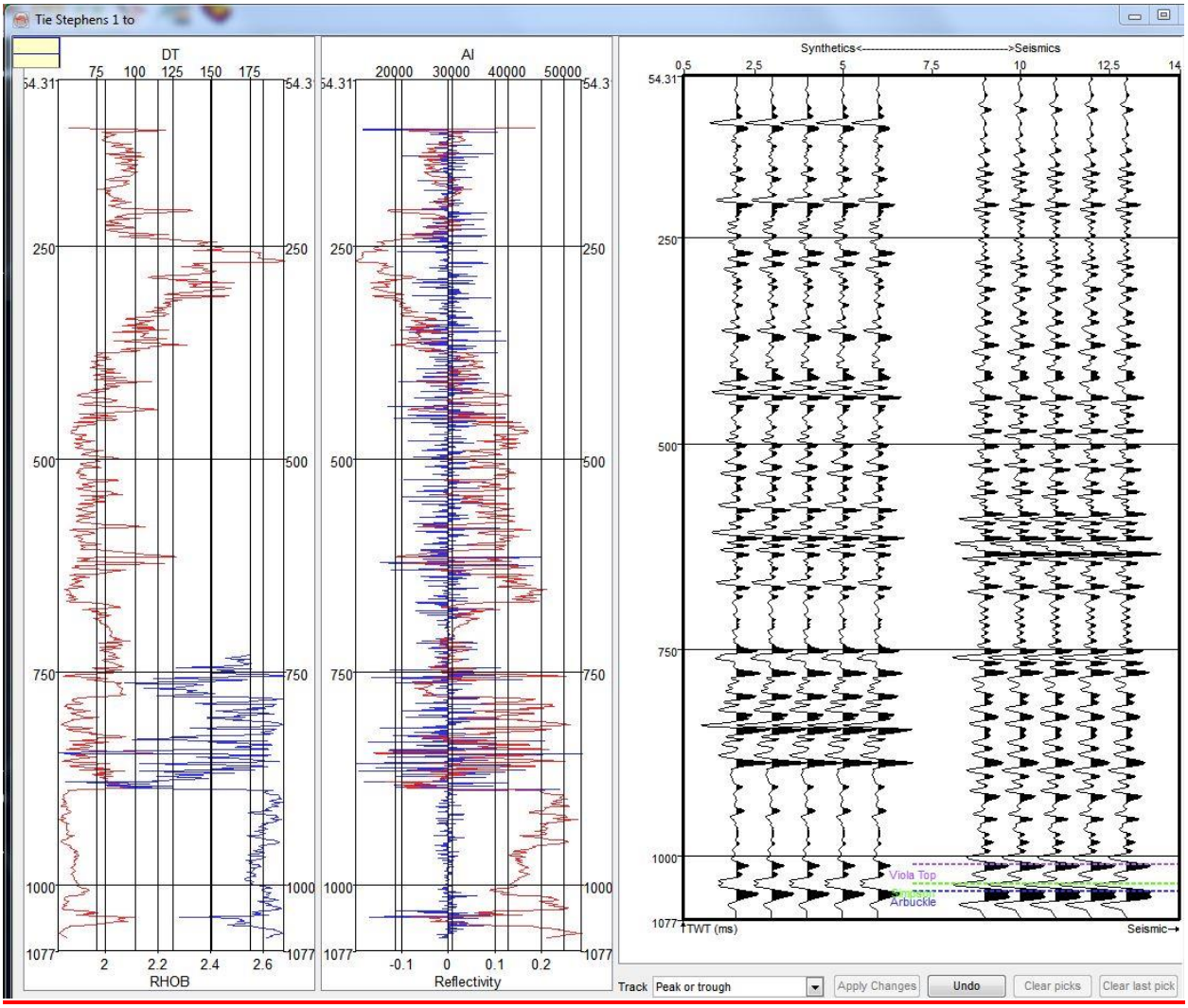

Figure 3-3 b) Synthetic to seismic tie for the Stephens 1 well using OpendTect Software (same well as Figure 3-3 a). This synthetic displays a good correlation between the generated synthetic and seismic trace data as well as the relationship between the sonic (DT) and density (RHOB) logs and the acoustic impedance (AI) and reflectivity values.

Figure 3-3 Generation of Synthetic Seismograms.

3.2-3 Formation Tops and Horizon Tracking

To determine where the formations of interest are present within the seismic data, formation top data has to be loaded into Kingdom Suite (Table 3-3). Formation top data can then be lain over synthetic seismograms (Figure 3-3 a & b) which can be lain over the seismic trace data (Figure 3-4) (Appendix B) allowing for the formation tops to be picked manually and

tracked through the entire seismic section (Figure 3-5). Auto picking of horizons in Kingdom is an option that allows horizons to be picked with greater speed but at the expense of high pick confidence (Figure 3-6). Auto picking is a good method to track horizons quickly. Examples of horizons that were easy to track in this study using auto picking are the Arbuckle and Simpson formations. The Arbuckle and Simpson formations are seen on the seismic trace data as very consistent high amplitude peak or very consistent low amplitude trough throughout the survey respectively (Figure 3-7). The Viola limestone formation is not a good candidate for auto picking due to changes in thickness/seismic resolution that result in inconsistent amplitudes marking its formation top within the seismic trace data. When auto picking is used on the Viola, the strongest reflection is traced throughout the survey. This reflection is the Viola 'C' zone which is not truncated by variations in paleotopography. Auto picking of this zone is shown in Figure 3-6. When the Viola limestone horizon is tracked manually and combined with instantaneous seismic attributes, a more accurate surface is generated.

Well	Kinderhook	Viola	Simpson	Arbuckle
Stephens ‘A’ 1	N/A	N/A	N/A	N/A
Stephens 1	6304	6383	6575	6697
Stephens 2	6314	6387	6584	N/A
Stephens 3	6314	6407	6572	6694
Stephens 4	6284	6370	6560	6683
Stephens 5	6190	6304	6482	6614
Stephens 6	6324	6398	N/A	N/A
Stephens 7	N/A	N/A	N/A	N/A
Stephens 8	6236	6344	6508	N/A
Stephens 9	6349	6458	6633	6764
Stephens 10	6310	6480	6586	6710
Harden 1	N/A	N/A	N/A	N/A
Harden 4	N/A	N/A	N/A	N/A

Table 3-3 Formation top data from logs.

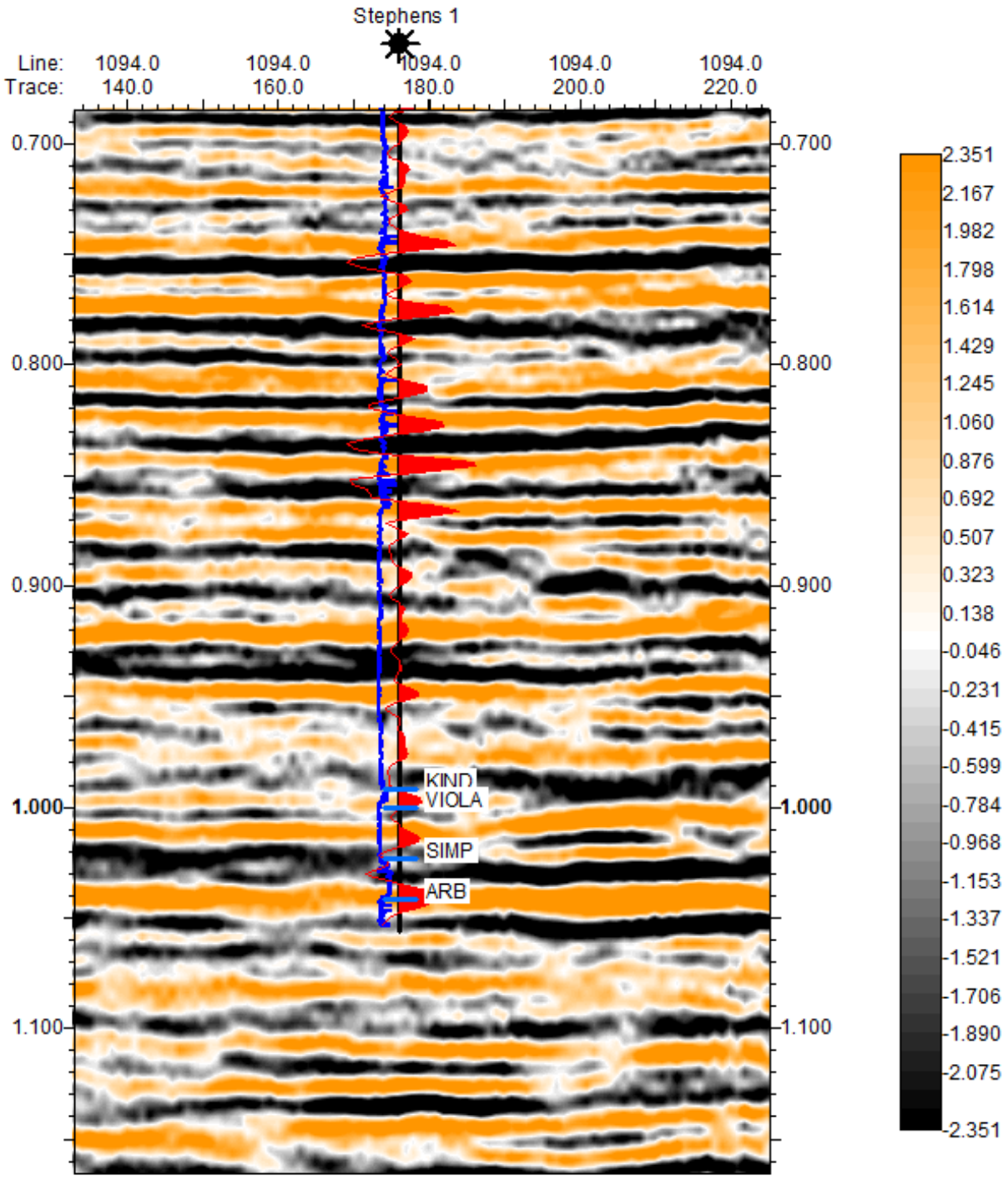

Figure 3-4 Amplitude cross section of a synthetic seismogram in red and gamma ray log in blue lain over the seismic trace data.

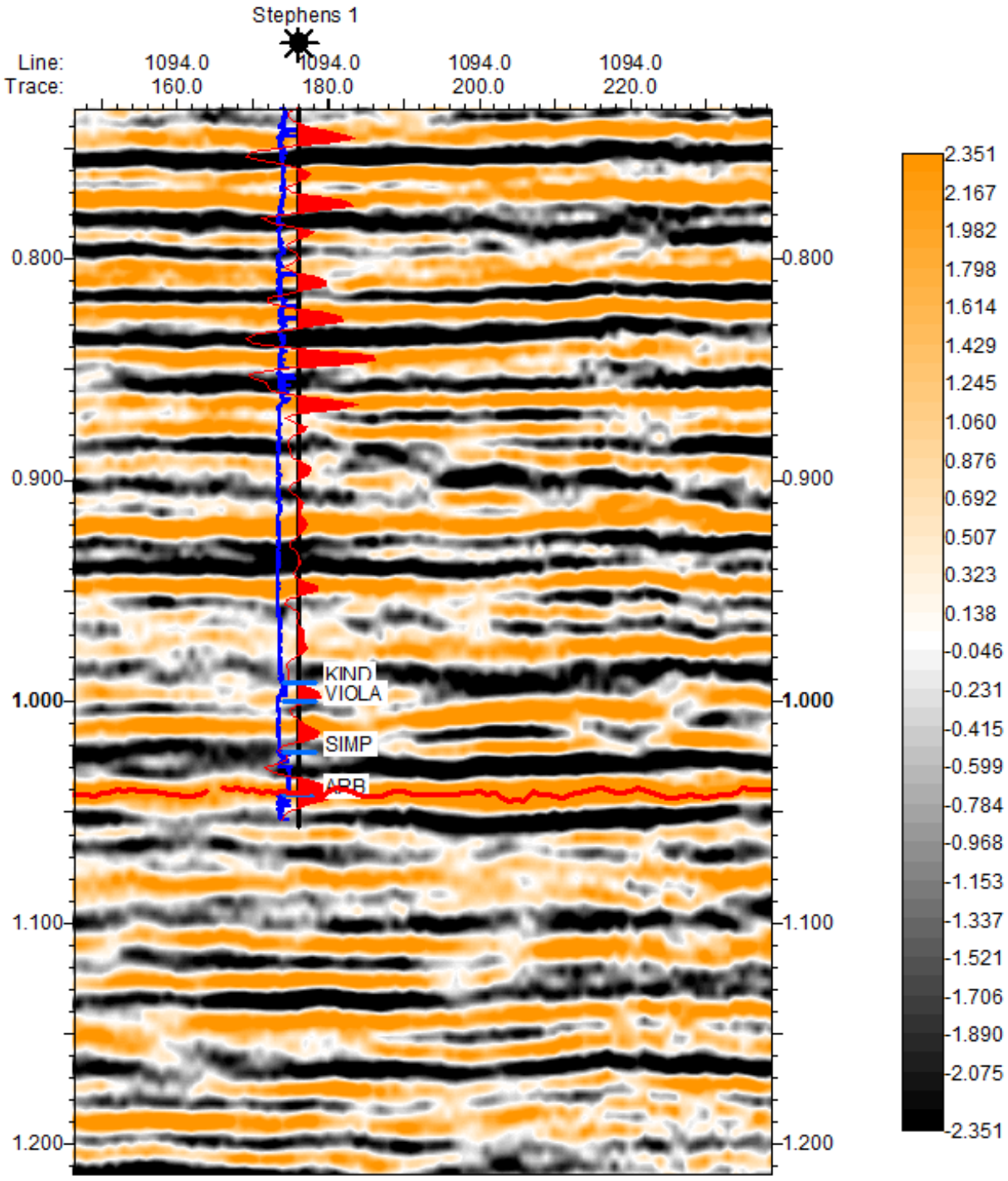

Figure 3-5 Amplitude cross section picking the Arbuckle (red line) based off of synthetic seismogram laid over the seismic trace data.

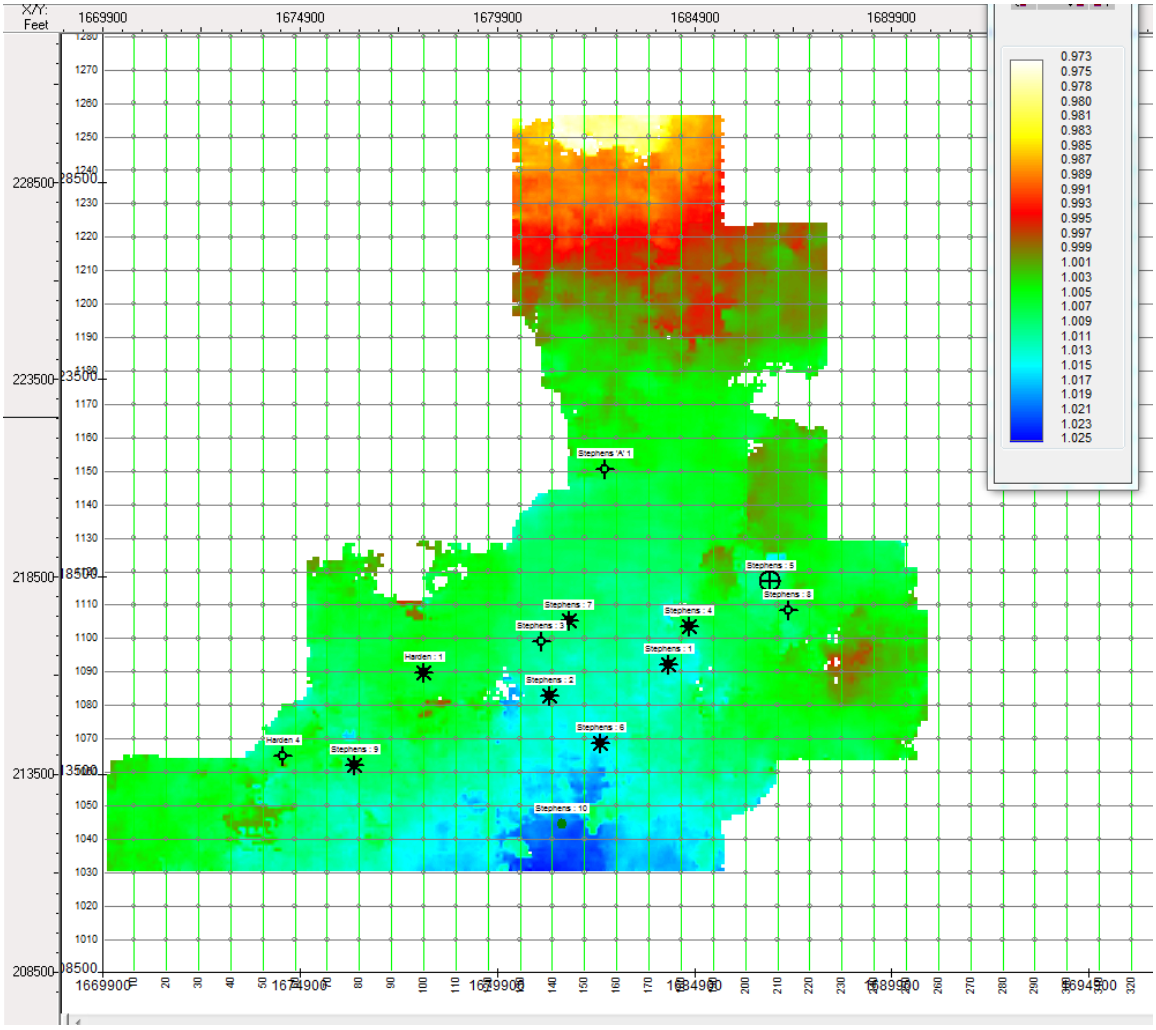

Figure 3-6 Time structure horizon generated by auto tracking. Generates a good idea for general structure of the Viola, but fails to recognize subtle changes in thickness that generate paleotopographic traps. Also, gaps are seen in the map as white space that must be manually interpreted.

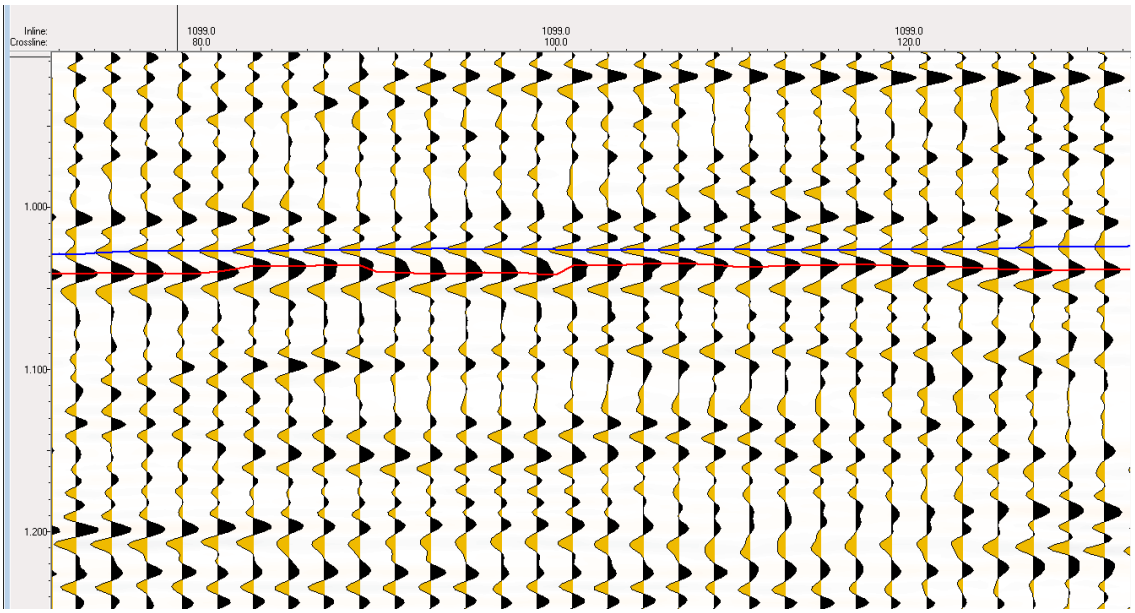

Figure 3-7 The Arbuckle (red line) follows a very consistent amplitude peak throughout the survey, which can be seen as a black peak on the wiggle trace above. The Simpson (blue line) follows a very consistent amplitude trough, which can be seen as a gold trough on the wiggle trace above.

3.2-4 Tuning Analysis

The shape of the reflection wavelet can vary when closely spaced reflecting interfaces interfere with each other. This variation in shape is known as the tuning effect. Tuning effects occur when the wavelength is greater than the bed thickness, causing the reflections to resonate and interfere (Hardage, 2009). A wedge model can explain the effect of bed thickness on seismic amplitude (Figure 3-8). As the wedge thins the lobes constructively interfere when the wedge thickness is one-quarter that of the effective source wavelet or one-half the thickness of the dominant period (Chopra & Marfurt, 2007). This constructive interference is causing a positive amplitude anomaly on the left side of the Figure 3-8 wedge model. Analysis of the effects of tuning can be done in the Kingdom Suite for each wavelet extracted at the borehole as well as for theoretical zero-phase wavelets (Figure 3-9)(Appendix A). This tuning analysis gives

an idea of where to be careful with regard to amplitude anomalies caused by interference of thin beds.

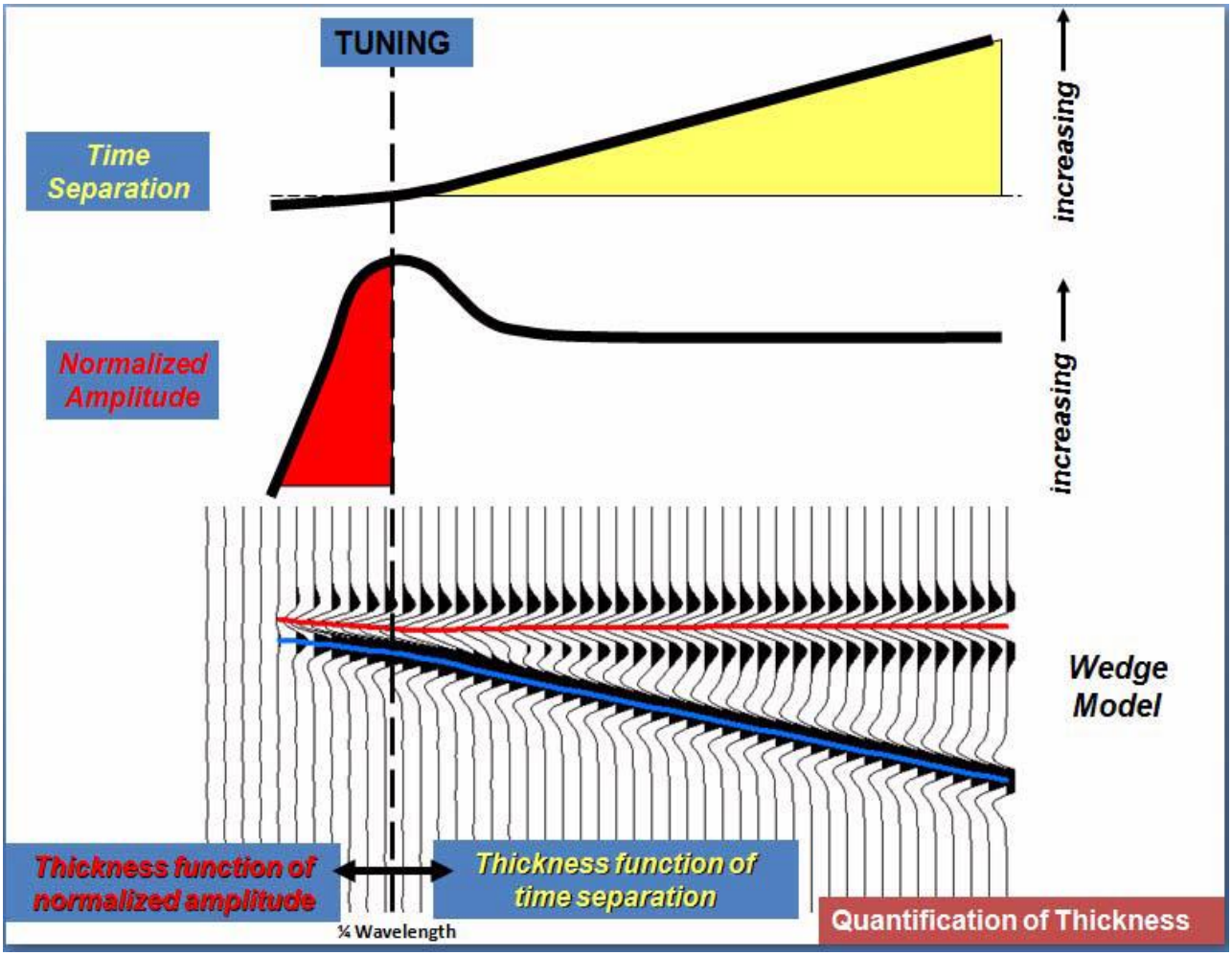

Figure 3-8 Example of wedge modeling on a seismic wiggle trace, tuning effects cause increased amplitude on left edge of the wedge model (IHS, 2012).

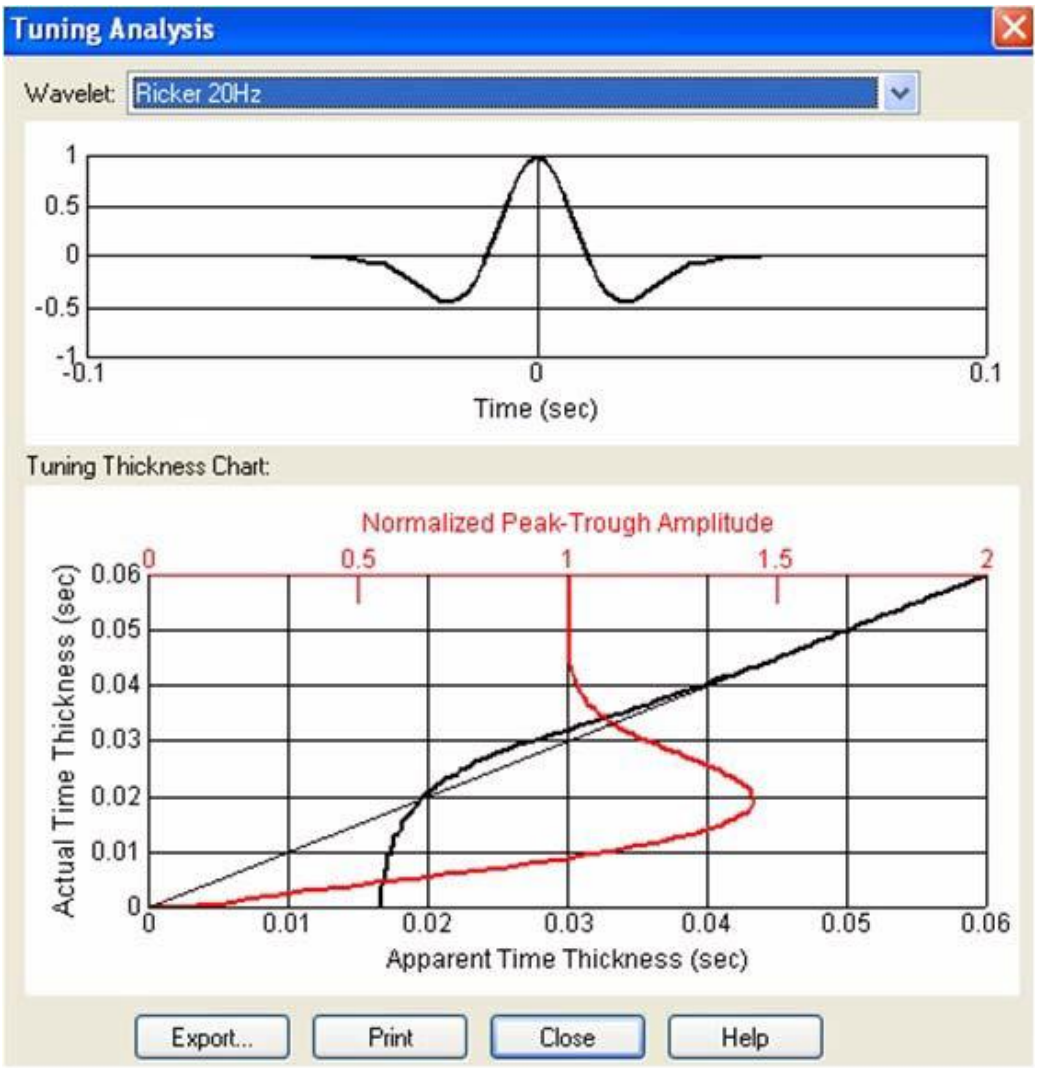

Figure 3-9 Tuning analysis chart for a theoretical Ricker wavelet of the above wedge model in Figure 3-8. Maximum tuning effects occur at approximately 8 milliseconds on all extracted wavelets (Appendix A) and at 20 milliseconds on the Ricker wavelet above (IHS, 2012).

3.2-5 Well Log Evaluation

Digital well logs (LAS Logs) were available for 11 wells targeting the Viola limestone within the 3D seismic survey area (Table 3-4). Within these digital well logs, sonic (DT) and density (RHOB) log values at all depths along the borehole were analyzed. This analysis

compared density, sonic, porosity and acoustic impedance log values between all wells with particular attention to comparing producing wells with non-producing or poor-producing wells. Formation tops and thickness were also analyzed with emphasis on the Viola and the overlying Maquoketa formation. Richardson, 2013 credits production in the Viola limestone to thinning within the Maquoketa and subsequent thickening in the Viola generating paleotopographic traps that preserve the productive porosity in the Viola (Figure 2-2).

Well	Gamma Ray (GR)	Density (RHOB)	Sonic (DT)	Photoelectric Effect (PE)	Resistivity Logs	Porosity Logs
Harden 1	Yes	Yes	Yes	Yes	Yes	Yes
Harden 4	Yes	No	Yes	Yes	Yes	Yes
Stephens 1	Yes	Yes	Yes	Yes	Yes	Yes
Stephens 2	No	No	No	No	No	No
Stephens 3	Yes	Yes	Yes	Yes	Yes	Yes
Stephens 4	Yes	Yes	Yes	Yes	Yes	Yes
Stephens 5	Yes	Yes	Yes	Yes	Yes	Yes
Stephens 6	No	No	No	No	No	No
Stephens 7	Yes	Yes	Yes	Yes	Yes	Yes
Stephens 8	Yes	Yes	Yes	Yes	Yes	Yes
Stephens 9	Yes	Yes	Yes	Yes	Yes	Yes
Stephens 10	Yes	Yes	Yes	Yes	Yes	Yes
Stephens ‘A’ 1	Yes	Yes	Yes	Yes	Yes	Yes

Table 3-4 Available LAS logs.

3.2-6 Seismic Attributes

3.2-6 a) Instantaneous Phase

Instantaneous phase is defined as the orientation angle of the amplitude vector at a particular time. Instantaneous phase represents the phase of a vector of individual simple harmonic motions. While individual vectors usually rotate clockwise, their resultant vector may at some instances appear to turn in the opposite direction. This usually the effect of interference of two closely arriving wavelets (IHS, 2012). A wave front is defined as a line of constant phase, which makes the phase attribute a physical attribute that can be used to describe geometrical shape (Taner, 2001). This makes instantaneous phase a useful attribute in indicating lateral continuity of rock layers and making a detailed visualization of bedding configurations (IHS, 2012). Instantaneous phase can make weak coherent events more clear (Taner et al, 1977). It is expressed by:

$$\Phi(t) = arc\ tan\ [y(z)/x(z)]$$

where t is time (or depth) and $y(z)$ and $x(z)$are the imaginary and real components of the complex seismic trace (Figure 3-10).

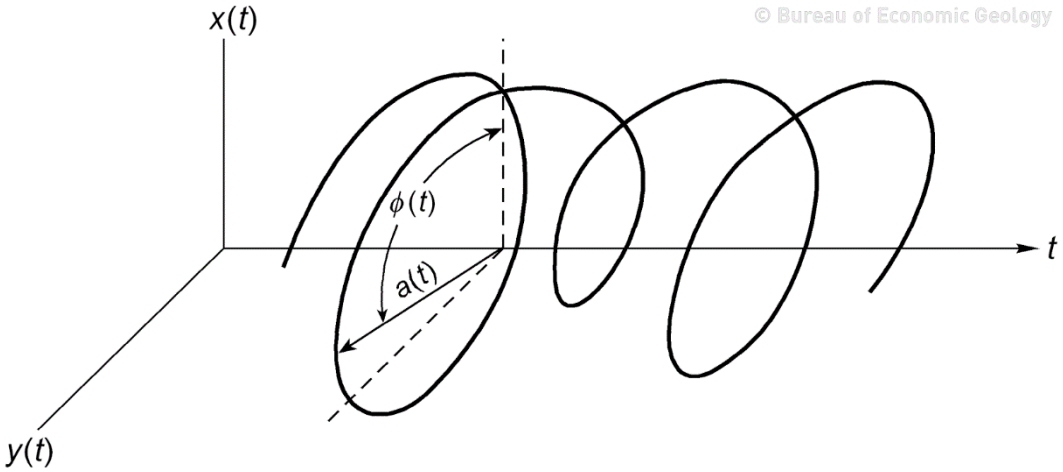

Figure 3-10 Close up of a complex seismic trace with the real seismic trace represented as x(t) on the x-axis and the imaginary seismic trace represented as y(t) on the y-axis. Instantaneous phase is represented as *Φ*(t) on the image. Instantaneous amplitude or envelope is also represented on the figure as a(t) (BEG, 2015).

3.2-6 b) Normalized Amplitude

Normalized amplitude is simply the cosine of the instantaneous phase angle. All of the details of instantaneous phase will be preserved in the normalized amplitude attribute, but the jumps inherent to instantaneous phase are avoided using normalized amplitude. Values of normalized amplitude will vary between -1 and +1. Normalized amplitude is useful in determining the direction of lateral continuity (IHS, 2012).

3.2-6 c) Amplitude

Amplitude data can be a useful attribute in hydrocarbon reservoir characterization. This is the most common seismic attribute, and amplitude is often correlated with porosity and liquid saturation. Amplitude is simply the height of a wave. A negative amplitude indicates a trough and a positive amplitude indicates a peak in the seismic trace. The bigger the peak or trough coincides with increasingly positive or negative amplitude values.

3.26 d) Instantaneous frequency

Instantaneous frequency is defined as the rate of change of phase over time (derivative of instantaneous phase). Wave propagation and depositional environments can be related to instantaneous frequencies. Uses of instantaneous frequency in this study are to indicate low impedance thin beds and relate those thin beds to tuning thicknesses (IHS, 2012). In zones of decreasing amplitude instantaneous frequency will peak and a surge in instantaneous frequency values can be an indicator of hydrocarbon saturation (Raef, 2001). Instantaneous frequency is calculated by the following equation:

$$w(t) = \frac{d|\Phi(t)|}{dt}$$

where Φ (t) is instantaneous phase and t is time (or depth)(BEG,2015).

3.2-6 e) Thin Bed Indicator

The thin bed indicator attribute shows interference zones in phase. It is computed as the difference between instantaneous frequency and time averaged frequencies following the equation

$$TBI = w(t) - \overline{w(t)}$$

where w(t) is instantaneous frequency values. Thin bed indicator can be used to indicate laterally continuous thin beds and give finer details of bedding patterns (IHS, 2012).

Attribute	Definition	Implication	Figure
Instantaneous Phase	Orientation angle of the amplitude vector at a given time	Indicates lateral continuity of rock layers, aids in creating a detailed visualization of bedding configurations and makes weakly coherent events more clear	Figures 4-2 & 4-3
Normalized Amplitude	Cosine of the instantaneous phase angle	Helpful in lateral continuity direction determination	Figure 4-4
Amplitude	Height of a peak or trough in a wavelet, wavelets respond to changes in impedance	Indicates low porosity zones and potential hydrocarbon presence	Figures 4-1, 4-6, 4-10 and 4-11
Instantaneous Frequency	Rate of change of phase over time (derivative of instantaneous phase)	Values peak with tuning thickness when amplitude is decreasing	Figure 4-14
Thin Bed Indicator	Difference between instantaneous and time averaged frequencies	Indicates laterally continuous thin beds and gives fine detail of bedding patterns	Figure 4-14

Table 3-5 Seismic attribute descriptions

Chapter 4 – Results and Discussions

Seismic attributes workflows were run to be correlated with the geological data derived from the borehole, and to determine why certain wells that were drilled did not produce or why one well produced so poorly that it was abandoned and subsequently converted into a salt water disposal well. Another objective of running seismic attributes workflows was to quality check the accuracy of the horizons of interest within the study area, most importantly the Viola limestone. As mentioned above the Arbuckle and Simpson formations are associated with consistent signature amplitude peaks or troughs, but the Viola limestone presents a problem when picking. Using a seismic attributes extraction solves this problem and can make the Viola horizon stand out. Previous work by Richardson, 2013 explains varying thickness in the Viola as it relates to preserving a productive porosity in a paleotopographic trap. These variations in thickness are subtle, and can be difficult to pick up on when visualizing broadband seismic amplitude data or wiggle traces but the variations in porosity as well as hydrocarbon presence can produce velocity anomalies that improve the resolution of the seismic data in potential productive zones. A decrease in the velocity of the seismic wave front would result in a shorter dominant wavelength according the equation:

$$\lambda = v/f$$

where λ is the dominant wavelength, f is the dominant frequency and v is the dominant velocity. A shorter dominant wavelength will improve the vertical resolution of the seismic trace data (Yilmaz, 1987). This more porous zone of the Viola limestone formation exist at the top of the formation increased seismic resolution should occur at the top of the Viola. The synthetic seismograms show a doublet occurring at the Viola "C" zone horizon and Viola top horizon

(Figure 3-2). This doublet is also seen in the wiggle trace displayed in Figure 4-1. The doublet is indeed seen in the wiggle trace, but the doublet is quite subtle and difficult to pick up on. However, after an attributes extraction, particularly instantaneous attributes, the picture becomes clearer and proper horizon picks of the Viola on the seismic trace data can be made. Instantaneous phase and normalized amplitude can then be used to emphasize the lateral continuity of seismic events, which allows for accurate picking of the Viola horizon.

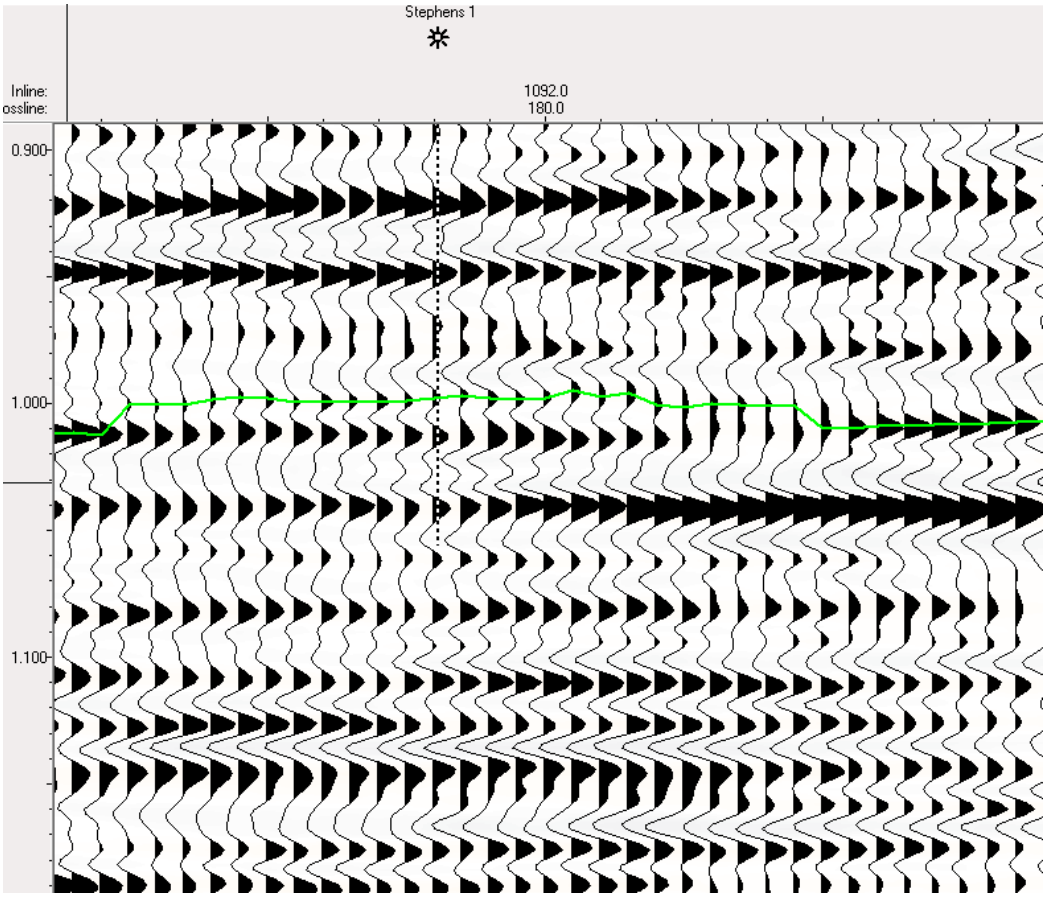

Figure 4-1 Amplitude wiggle trace cross section with the Viola limestone horizon in green. Increased resolution associated with a velocity anomaly within the Viola is difficult to pick up on in broadband amplitude data, and the strongest reflection event still occurs below the top of the Viola.

The instantaneous phase of a cross section through a well is shown in Figure 4-2. Events that show up as weakly coherent in amplitude cross sections are emphasized and shown to be coherent based on a consistent phase angle. Each color in the cross section represents a different degree of phase that relates to the propagation phase of the seismic wave front. A consistent phase angle near 45 degrees indicates the lateral continuity of the Viola limestone. The split in this phase angle value around the borehole location indicated the increased seismic resolution of the Viola which is interpreted as a velocity anomaly associated with increased porosity at the top of the Viola and/or the presence of hydrocarbons (Figure 4-3).

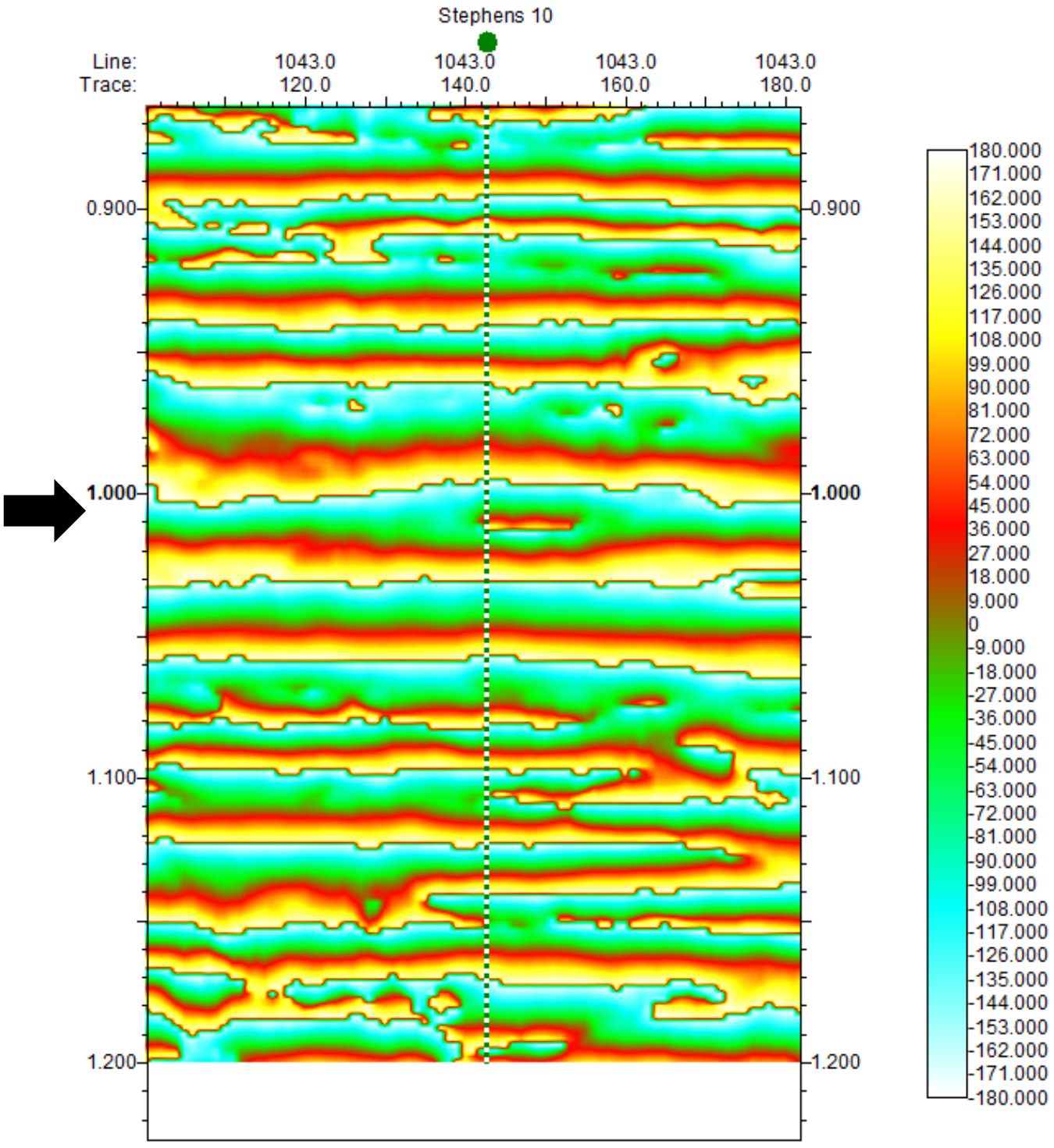

Figure 4-2 The above cross section shows the instantaneous phase without the picked horizons lain over it. The Viola lies at a time depth between 1.000 and 1.020 (indicated by black arrow). An instantaneous phase represented by a green horizon in this time range is interpreted as the Viola limestone, which thickens and splits at the Stephens 10 borehole representing a paleotopographic trap.

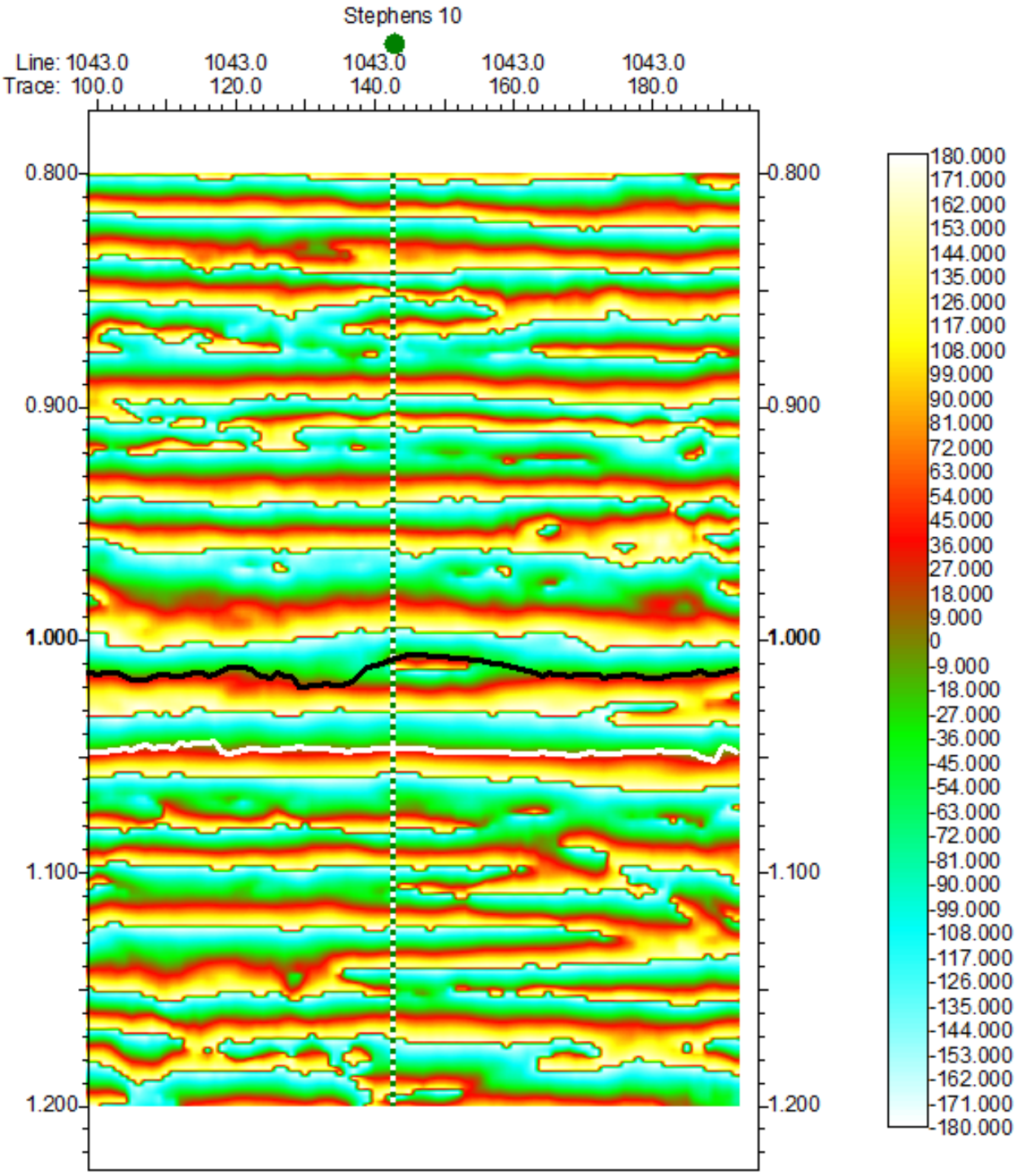

Figure 4-3 Instantaneous phase cross sections across Stephens 10 well. The Viola limestone is displayed in black following a consistent instantaneous phase and the Arbuckle formation is displayed in white also following a consistent instantaneous phase. Phase angles are represented by the color bar on the right.

Normalizing the amplitude of seismic trace data accurately shows the subtle changes in thickness at the top of the Viola limestone. Instantaneous phase and normalized amplitude allow for a much better pick of the top of the Viola limestone than can be done using just raw broadband seismic amplitude. A very pronounced doublet forms around borehole locations which implies a velocity anomaly associated with productive porosity and/or hydrocarbon presence at the top of the Viola (Figure 4-4). In looking at the wiggle overlay in Figure 4-1 which is just amplitude compared to the wiggle overlay in Figure 4-4, the usefulness of normalized amplitude in highlighting potentially productive zones within the Viola. The doublet is formed on either side of the well forming what some interpreters may refer to as a "buried football" shape that is a signature of a velocity anomaly within the horizon of interest. Doublets in the normalized amplitude cross section within the Viola have been interpreted as zones of increased porosity, and thus are targets for hydrocarbon exploration in Viola paleotopographic traps.

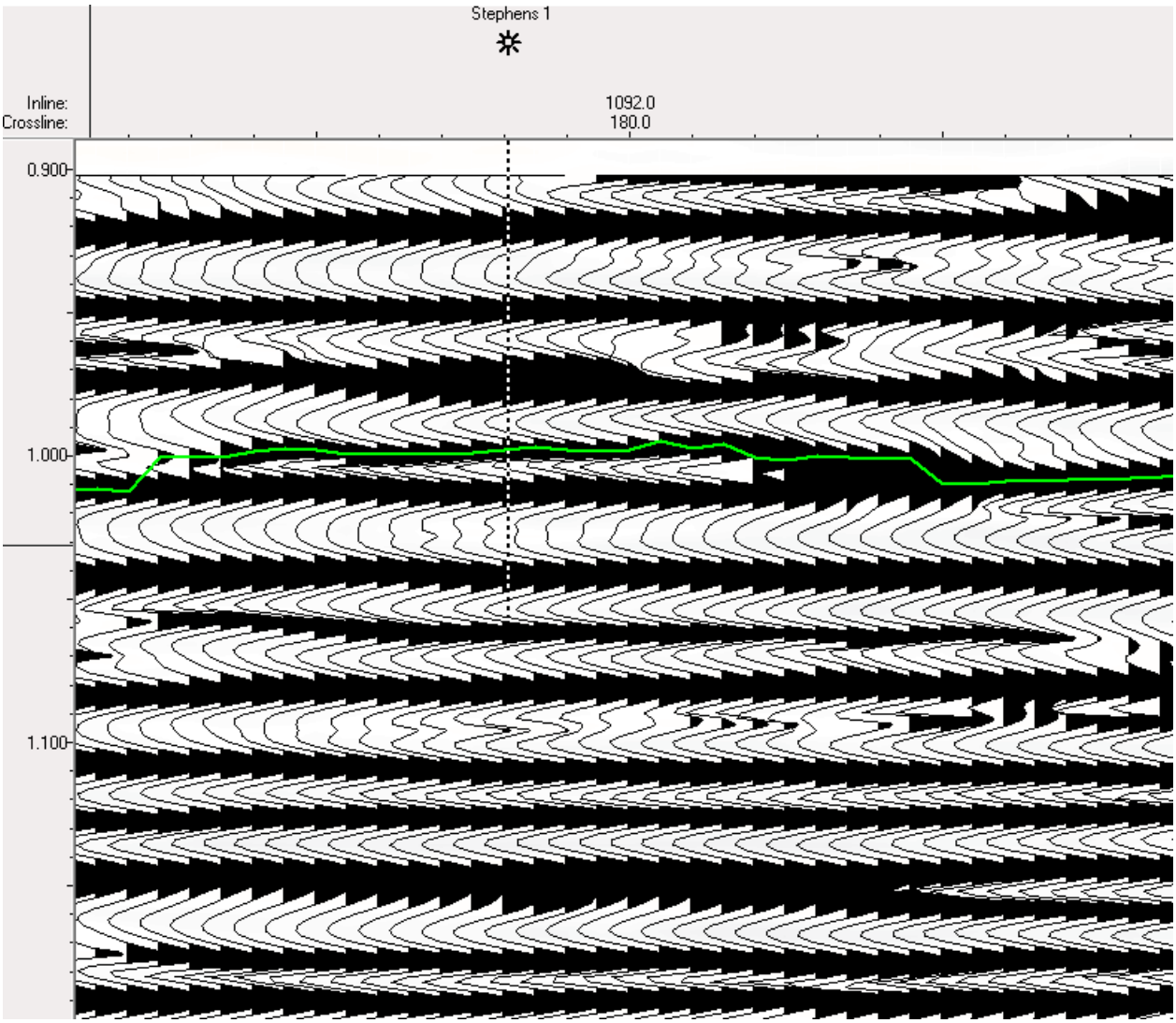

Figure 4-4 Normalized amplitude wiggle trace at the same location as Figure 3-6. A doublet in the wiggle trace is easy to pick up using the normalized amplitude attribute making the Viola limestone horizon easier to pick with greater confidence.

Figures 4-1, 4-2, 4-3 and 4-4 confirm a seismic doublet that forms around the borehole locations within the study area. Wells within the survey are targeting the upper Viola which exhibits the productive dolomite porosity. The productive porosity sits above the Viola "C" zone, deeming the Viola above the "A" and "B" zones (Richardson, 2013). This is where porosity is present and hydrocarbon traps are located. Figure 4-5 is a time structure map of the Viola "C" zone which shows no evidence of paleotopographic traps or velocity anomalies. A

cross section of this pick can be seen in Figure 4-6. On this cross section a doublet forms around the borehole location like the ones seen using instantaneous phase and normalized amplitude in the figures above (Figures 4-1, 4-2, 4-3 and 4-4). The doublet that forms is interpreted as a low velocity anomaly due to either 1) higher porosity and/or 2) lower impedance due to the presence of hydrocarbon. This low velocity anomaly improves the resolution of the seismic data allowing for the Viola to be more accurately picked as in Figures 4-7 and 4-8. Figure 4-9 gives a 3D image of the Viola "C" zone compared to the Viola "C" zone with the Viola top overlain. The 3D image in Figure 4-9 demonstrates the difference between the two tops picked as it relates to well placement. Picking the Viola top as opposed to the Viola "C" zone the introduced amplitude anomalies that correlated with well production.

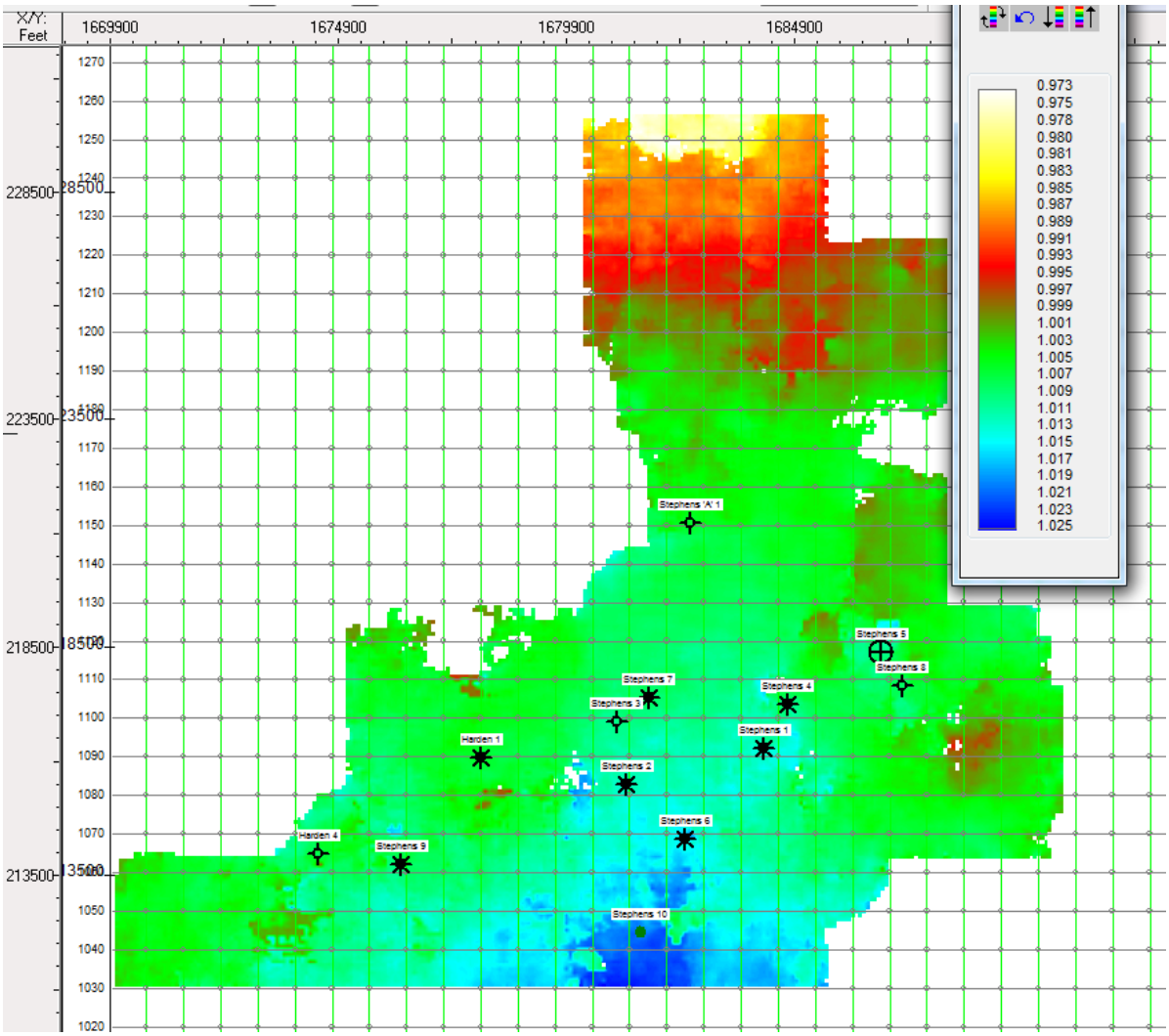

Figure 4-5 Time structure map of the Viola "C" zone formation top. No evidence of paleotopographic traps is seen when only the "C" zone is tracked.

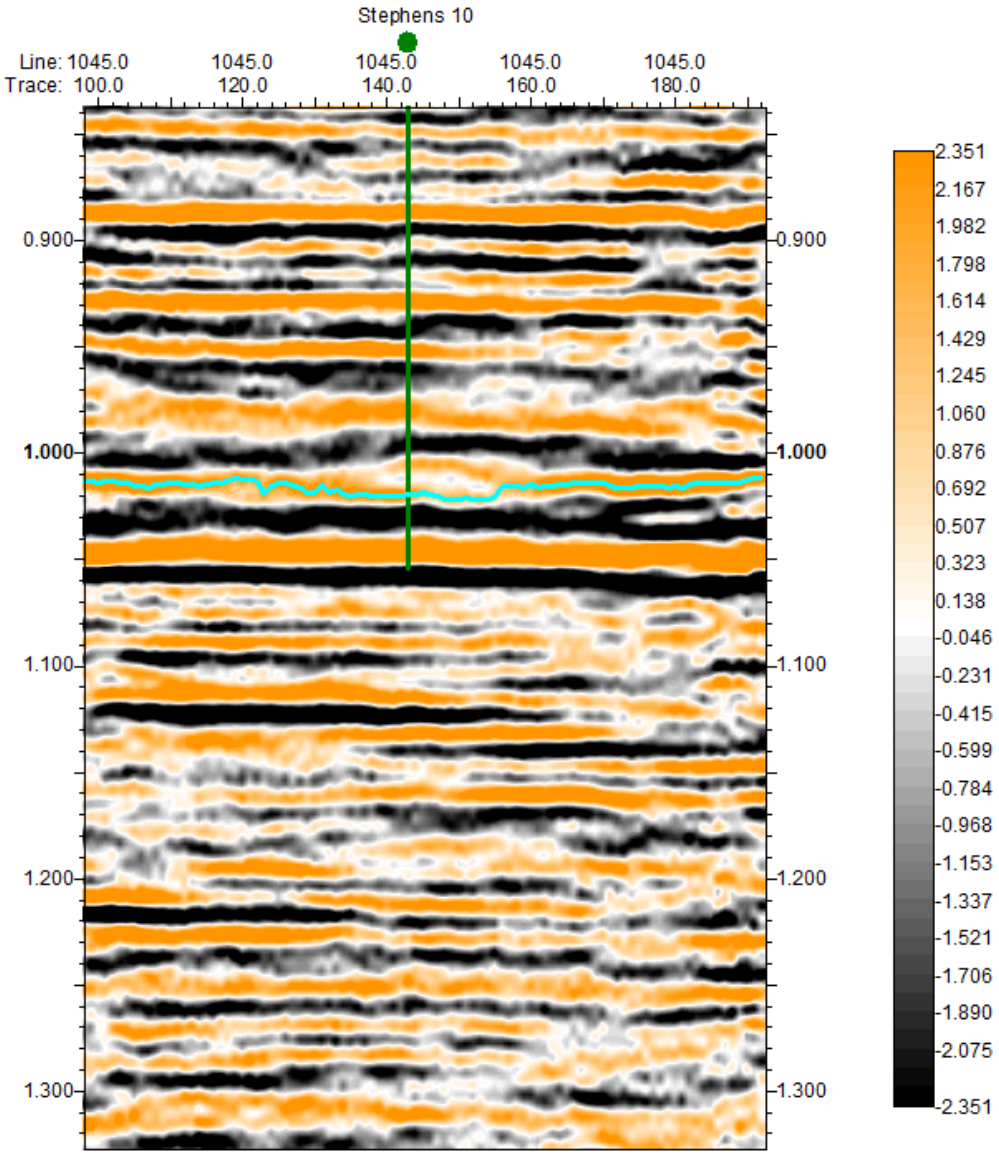

Figure 4-6 Amplitude cross section showing the Viola "C" zone pick.

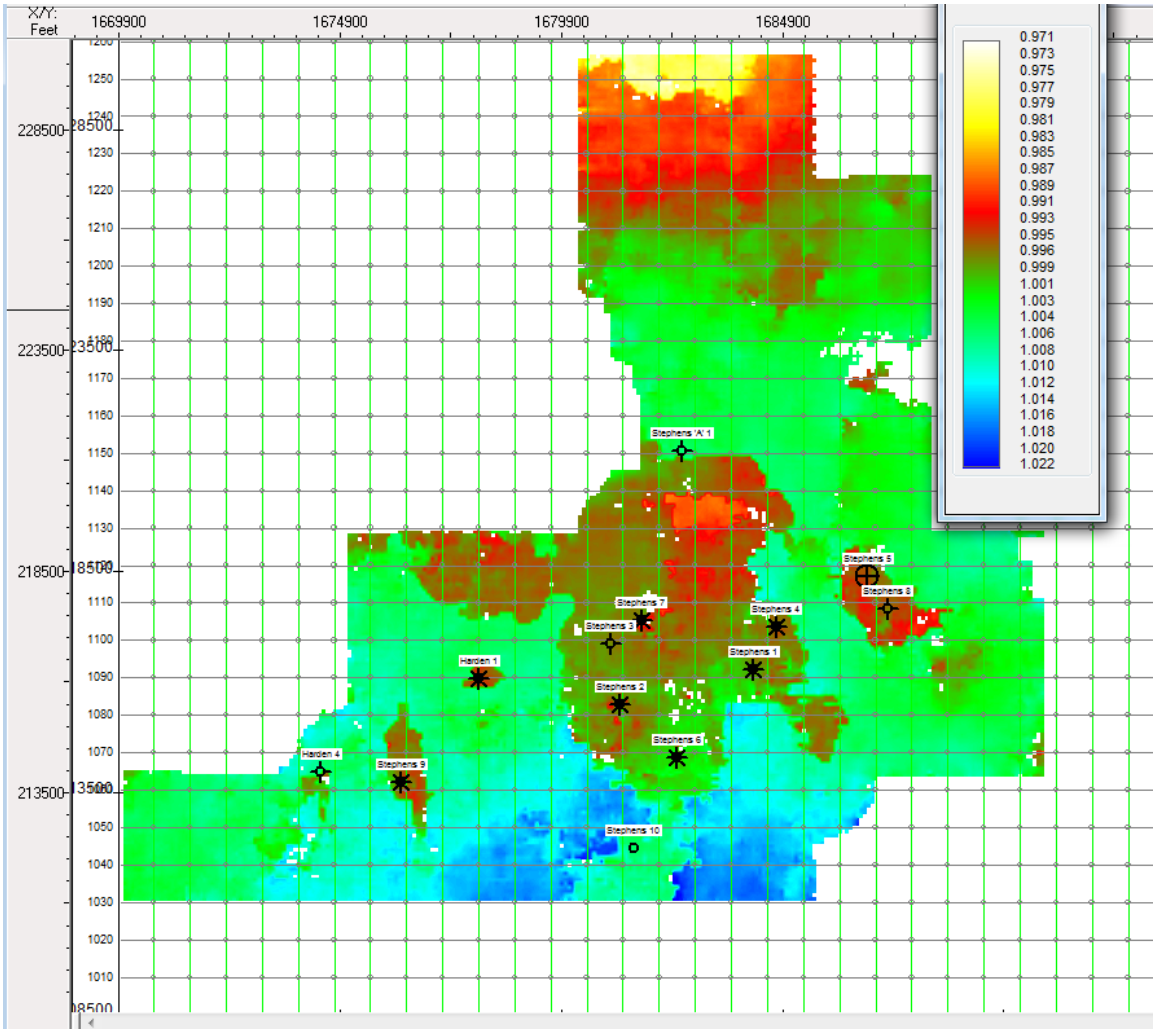

Figure 4-7 Time structure map of the Viola top showing paleotopographic traps, zones of productive porosity and/or hydrocarbon presence.

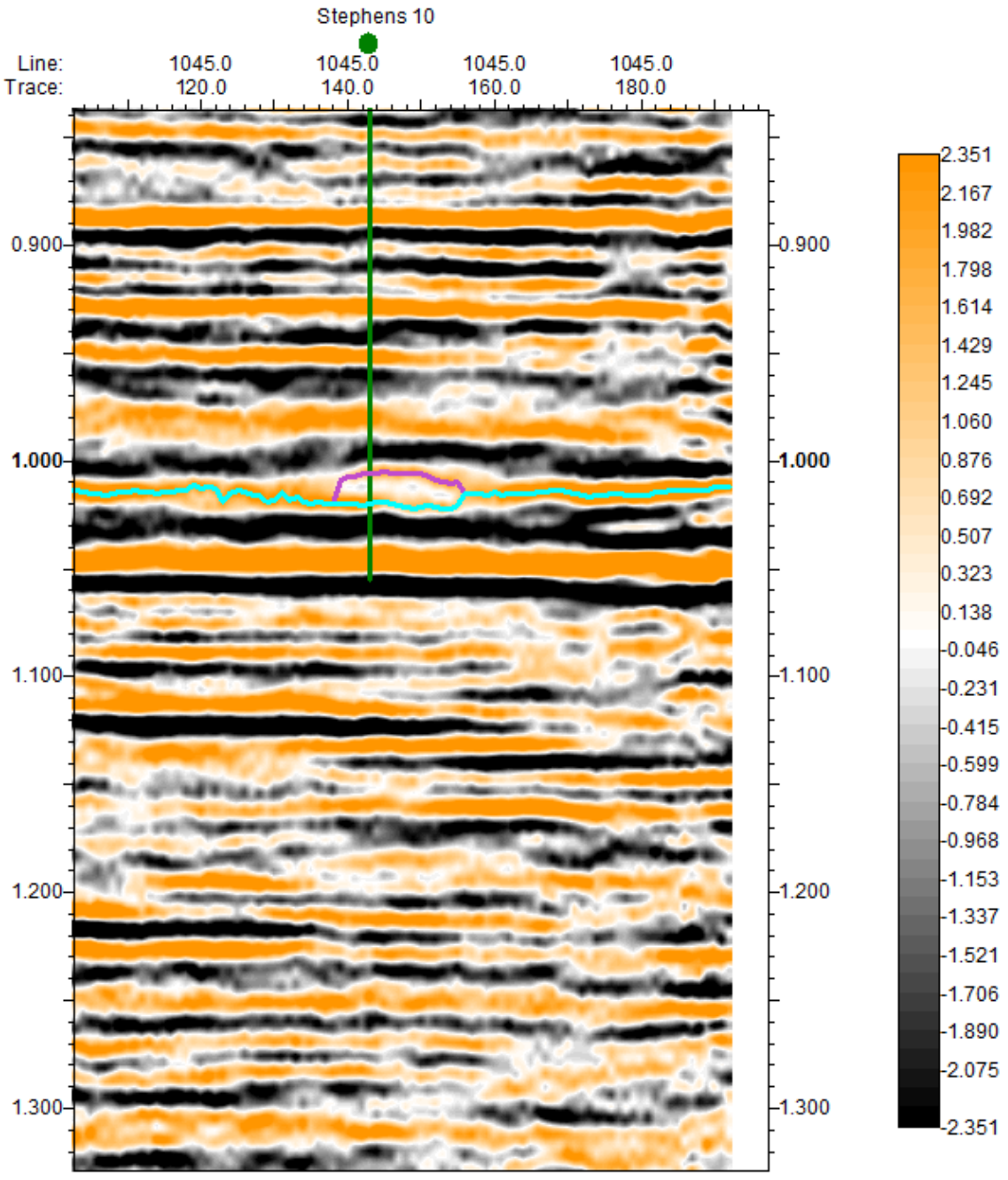

Figure 4-8 Amplitude cross section of the same inline as Figure 4-6 with the Viola top in purple lain over the Viola "C" zone in light blue.

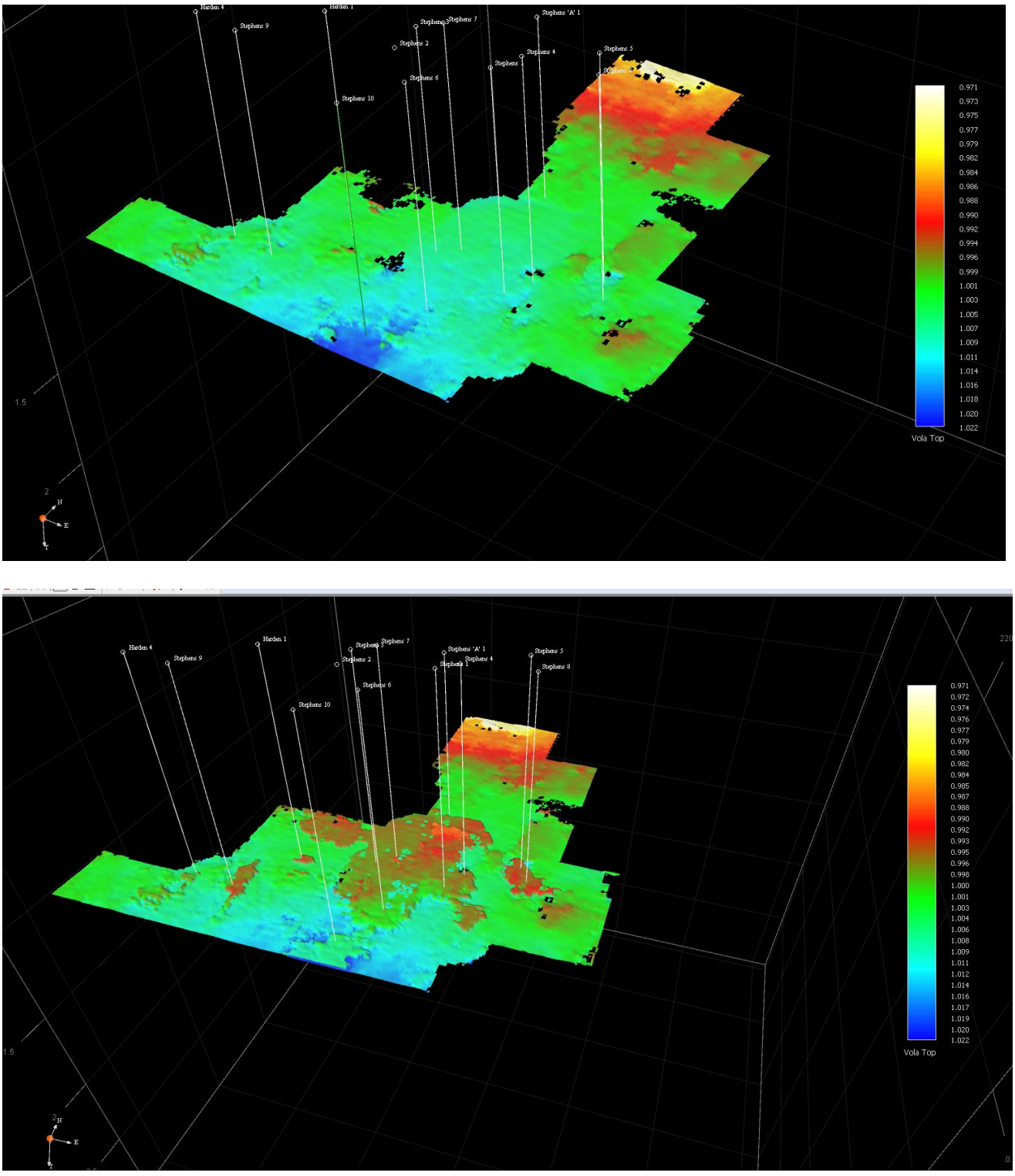

Figure 4-9 Top image is a time structure image of the Viola "C" zone and the bottom image is a time structure image of the Viola top overlain on the Viola "C" zone.

Attribute extraction was also carried out to evaluate well placement and to determine if attributes analysis could have avoided the completion of the dry holes in the survey and the well with poor economics seen in Stephens 5 (converted to SWD). The most useful attribute in discerning producing wells from uneconomic wells was amplitude. Amplitude maps were generate on both the Viola "C" zone and the Viola top horizon. Differences in the two amplitude maps can be seen when comparing Figure 4-10 to Figure 4-11. With the Viola top horizon marking the hydrocarbon bearing zone, amplitude anomalies within this horizon were of particular interest in this study. Producing wells in the Viola limestone had consistently lower amplitude values than dry holes and the well that was converted to a SWD well on the amplitude map for the Viola top horizon (Figure 4-11). These amplitude values are displayed on the graph in Figure 4-12. Producing wells in the Viola, in green, have relatively lower amplitudes than the non-producing wells in blue. These low amplitude anomalies that are highlighting the hydrocarbon bearing zone make sense because the presence of hydrocarbons would decrease the variation in acoustic impedance between the Viola and the overlying horizon. Tuning effects could explain the high amplitude anomalies seen in producing wells Stephens 1 and 4 as the peak to trough thickness of the wavelet at these locations was 8ms, which aligns with the maximum effect of tuning on amplitude for the wavelets extracted along the Stephens 1 and 4 (Figure 4-13). Further investigation into the effects of tuning thickness revealed that higher values of instantaneous frequency correlated with amplitudes near zero, specifically the amplitude values seen in the productive wells. As mentioned in studies by Raef, 2001, instantaneous frequency peaks with tuning effects in zones of decreasing amplitudes like what we see in the Viola limestone, also a surge in instantaneous frequency can be an indicator of hydrocarbon saturation (Figure 4-14). The thin bed indicator attribute was also applied to the 16ms time window at the

top of the Viola in Figure 4-14 to compliment the instantaneous frequency data. Thin bed indicator peaks with instantaneous frequency further strengthening the case for tuning effects occurring within the zone of deceasing amplitude as well as displaying productive wells associated with particular thin bed indicator values and instantaneous frequency values.

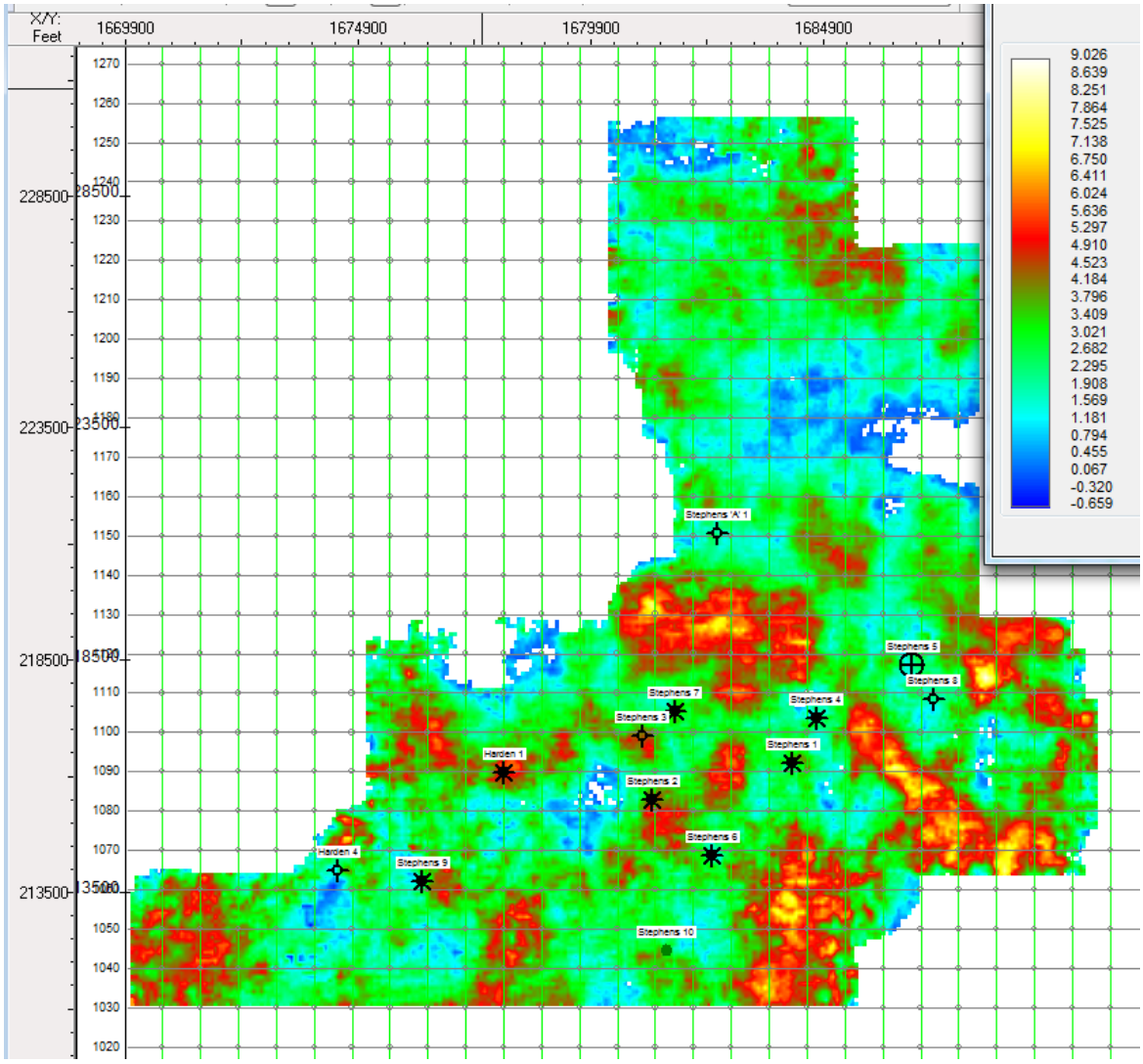

Figure 4-10 Amplitude map of the Viola "C" zone.

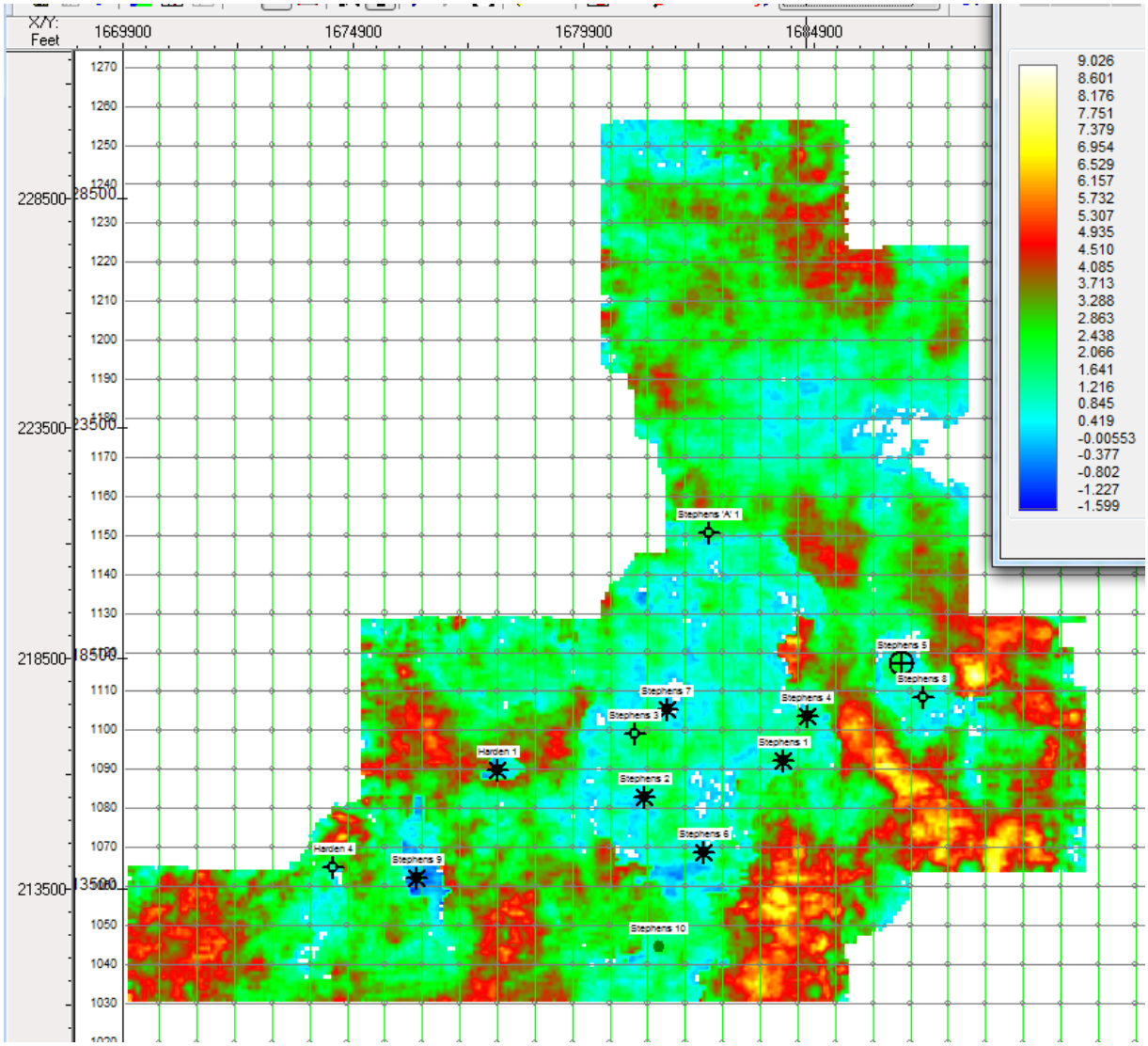

Figure 4-11 Amplitude map of the Viola top.

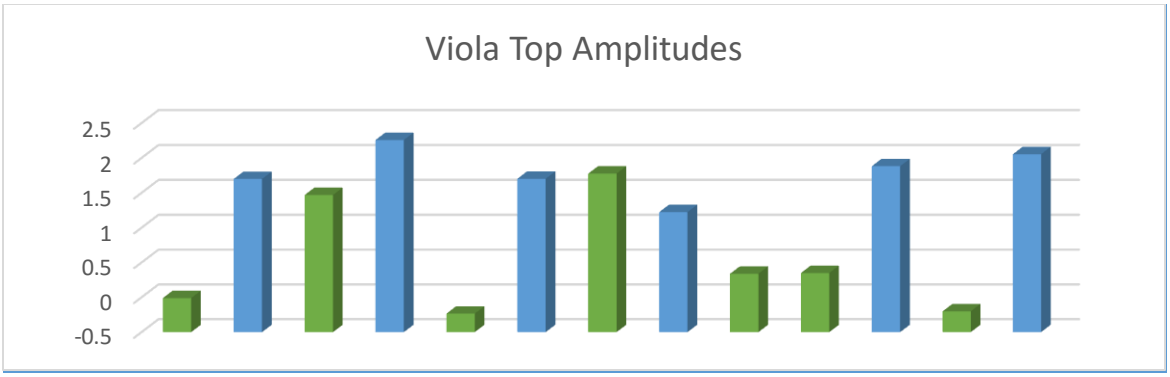

Figure 4-12 Amplitude values for the Viola top horizon at well locations with producing wells in the Viola green and non-producers are blue. Wells are from left to right: Harden 1, Harden 4, Stephens 1, Stephens 10, Stephens 2, Stephens 3, Stephens 4, Stephens 5, Stephens 6, Stephens 7, Stephens 8, Stephens 9 and Stephens "A"1.

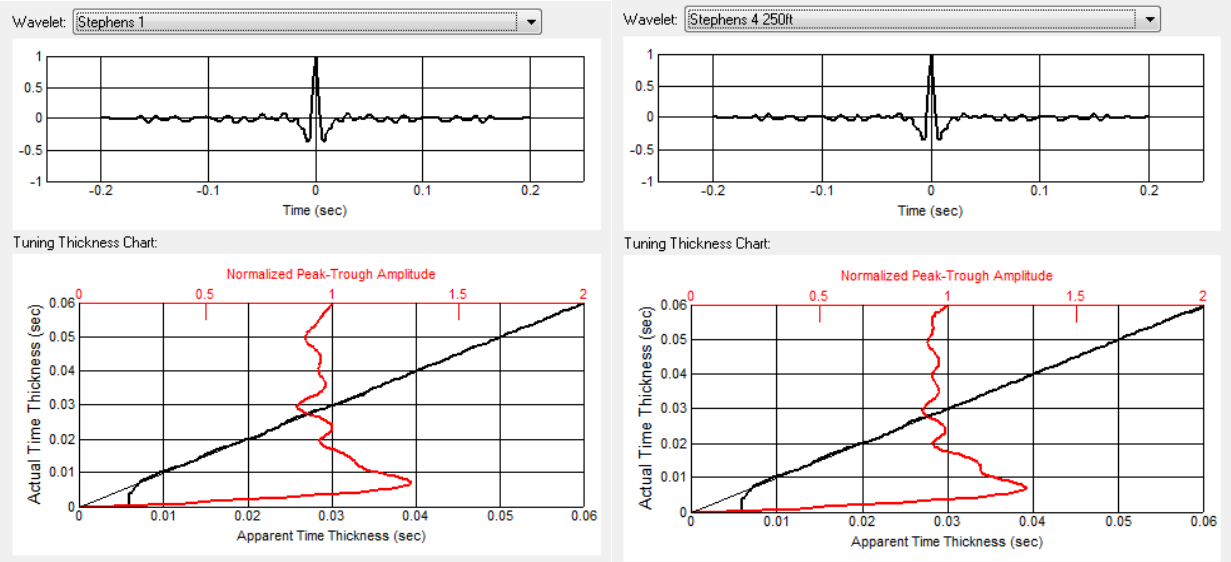

Figure 4-13 Tuning charts for Stephens 1, 4 and 10 showing maximum effects of tuning at approximately 8ms.

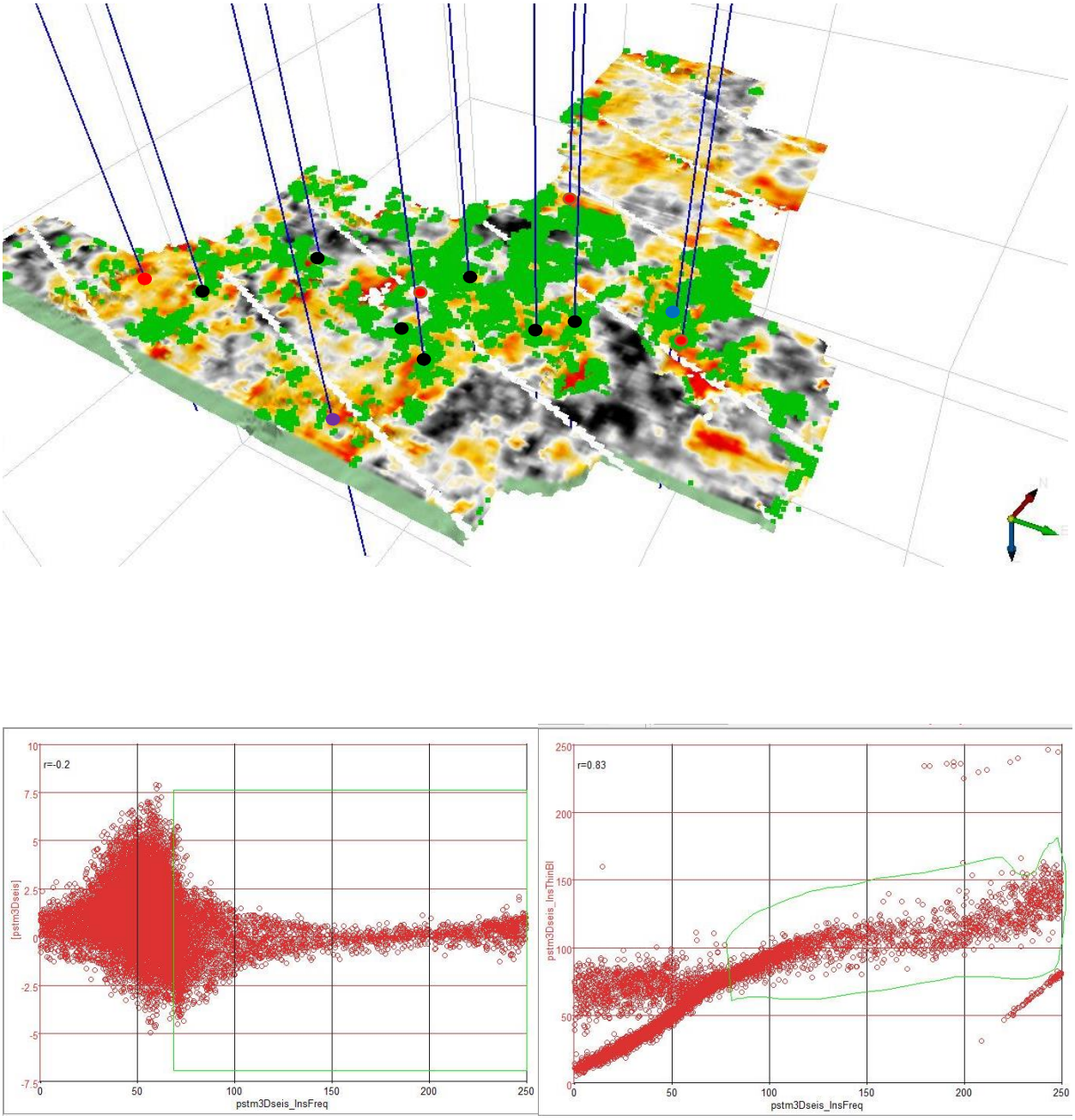

Figure 4-14 Map of a 16ms time-window within the upper Viola limestone showing effects of instantaneous frequency and thin bed indicator attributes. Green boundaries on the charts below are displayed on the horizon above in green. The chart on the left plots amplitude values on the y-axis against instantaneous frequency values on the x-axis. The chart on the right plots thin bed indicator on the y-axis against instantaneous frequency on the x-axis. Wells producing within the Viola are displayed in black, dry holes drilled in the Viola are displayed in red and the salt water disposal well is in blue, the purple well produces from the morrow formation and was originally a dry hole targeting the Viola.

Well log evaluation was conducted on both digital and raster logs. When evaluating logs with regard to thicknesses within the formations of interest, thinning within the Maquoketa seemed to correlate directly with production in wells with geologs including the Maquoketa. Relatively thick Maquoketa resulted in no production while relatively thin Maquoketa resulted in productive wells (Table 4-1). These Subtle changes in thickness are outside of the temporal resolution of the seismic survey so they cannot be noticed when prospecting using the seismic data.

Evaluation of digital (LAS) logs was completed with focus on how acoustic impedance (density log * sonic log) and porosity relate to lithology. This relationship was then correlated to well placement and production. Various cross plots of these values are shown in figures 4-15, 4-16, 4-17, 4-18 and 4-19. Figure 4-15 shows spontaneous porosity (SPOR) decreasing with depth through the pay zone with a correlation coefficient of r=-0.5 along with gamma ray log (GR) values trending the opposite direction for the Stephens 1 producing well, indicating the highest porosity is located at the top of the Viola. In figure 4-16 concentrated neutron porosity (CNPOR) and acoustic impedance is plotted against measured depth through the pay zone for Stephens 1. This shows the highest porosity values aligning with the lowest acoustic impedance values at the top of the Viola. Figure 4-17 emphasizes that conclusion drawn from figure 4-16 showing the linear trend between acoustic impedance and CNPOR (porosity increases while acoustic impedance decreases) for Stephens 1. In figure 4-18 and 4-19 the same well log values are evaluated, but for the dry hole Stephens 8. Figure 4-18 plots the gamma ray log and density porosity against measured depth similar to the cross plot in figure 4-15. The porosity log behaves similarly to the porosity log for Stephens 1 at depth (steadily increasing as depth decreases), but towards the top of the Viola, where the potential pay zone would be located, the

porosity values suddenly drops. Figure 4-19 emphasizes the difference between productive wells and dry holes seen in comparing Figure 4-19 to Figure 4-17 plotting CNPOR and acoustic impedance against density porosity (DPOR). This cross plot shows acoustic impedance increase as porosity decreases, but the two porosity logs don't align for Stephens 8 as they did in the cross plots for Stephens 1.

Well	Maquoketa Thickness	Well Status
Stephens 1	17 ft.	Producing
Stephens 2	11 ft.	Producing
Stephens 3	29 ft.	Dry Hole
Stephens 4	22 ft.	Producing
Stephens 5	28 ft.	Salt Water Disposal Well
Stephens 6	11 ft.	Producing
Stephens 7	19 ft.	Producing
Stephens 8	34 ft.	Dry Hole
Stephens 9	14 ft.	Producing
Stephens 10	18 ft.	Producing (Morrow)
Harden 1	17 ft.	Producing
Harden 4	N/A	Dry Hole

Table 4-1 Maquoketa thickness correlated to well production.

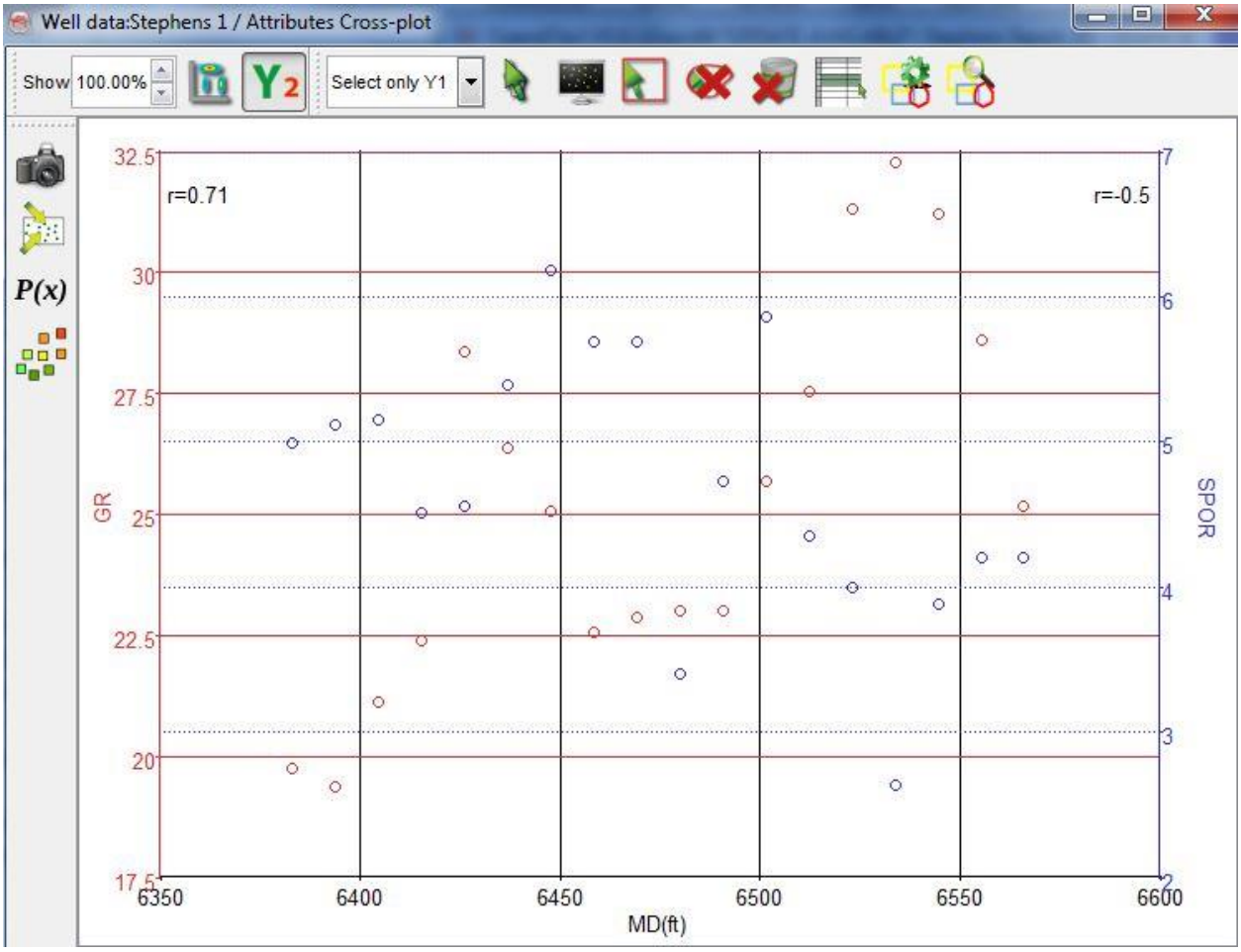

Figure 4-15 Gamma Ray (GR) and sonic porosity (SPOR) plotted against depth (MD) through the Viola limestone for Stephens 1.

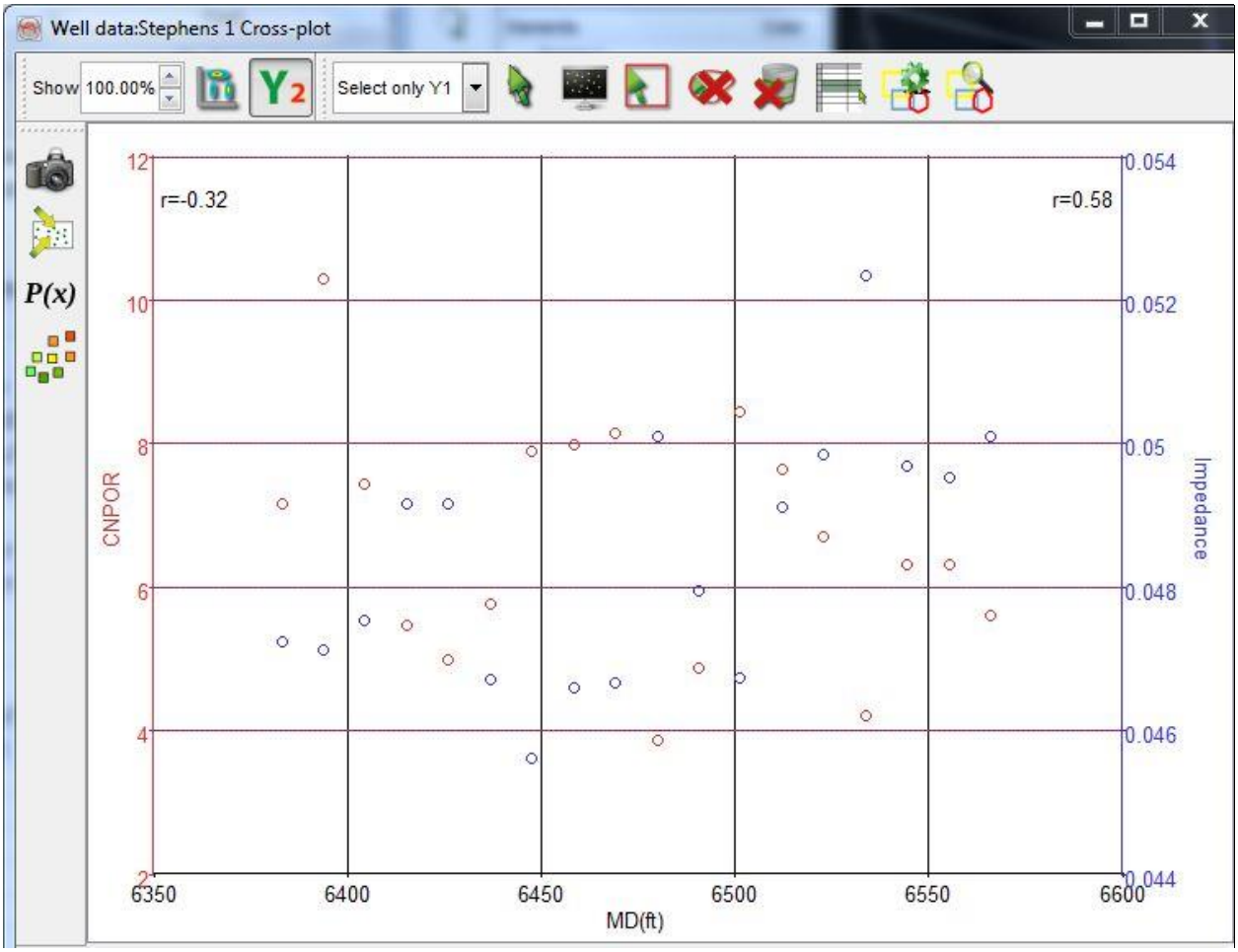

Figure 4-16 Concentrated neutron porosity (CNPOR) and acoustic impedance plotted against depth (MD) through the Viola limestone for Stephens 1.

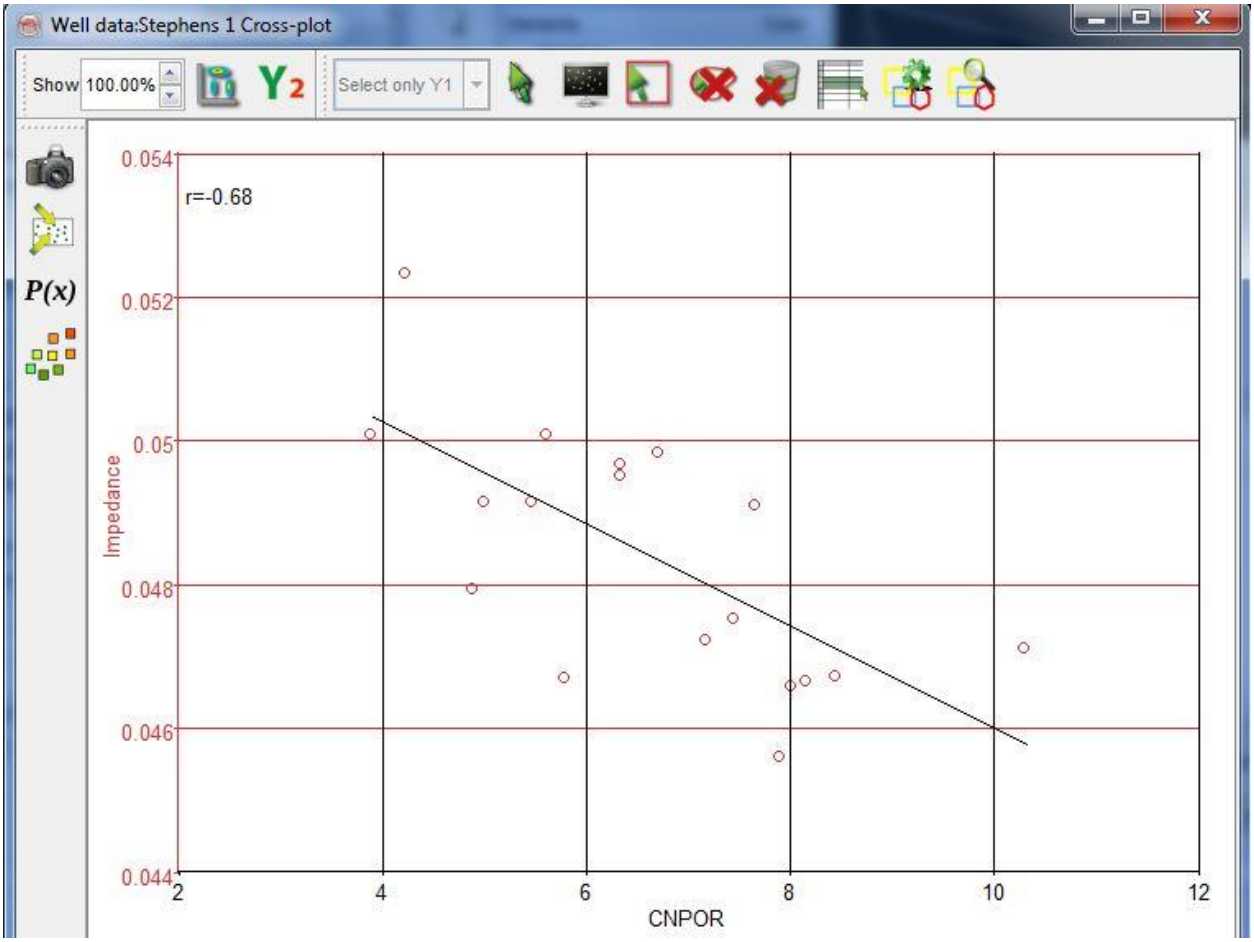

Figure 4-17 Acoustic impedance plotted against concentrated neutron porosity (CNPOR) through the Viola limestone for Stephens 1.

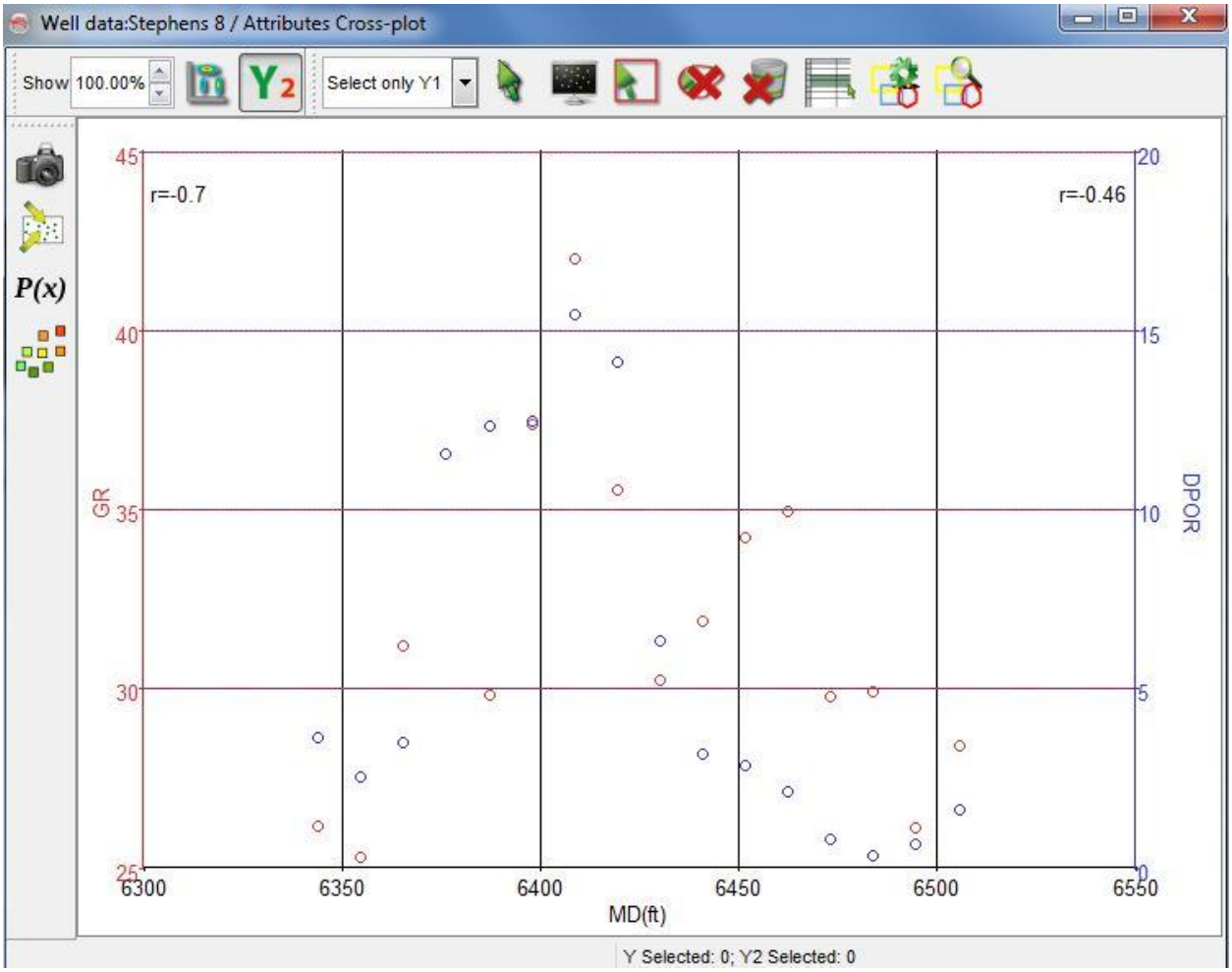

Figure 4-18 Gamma ray (GR) and density porosity (DPOR) values plotted against depth through the Viola limestone for Stephens 8.

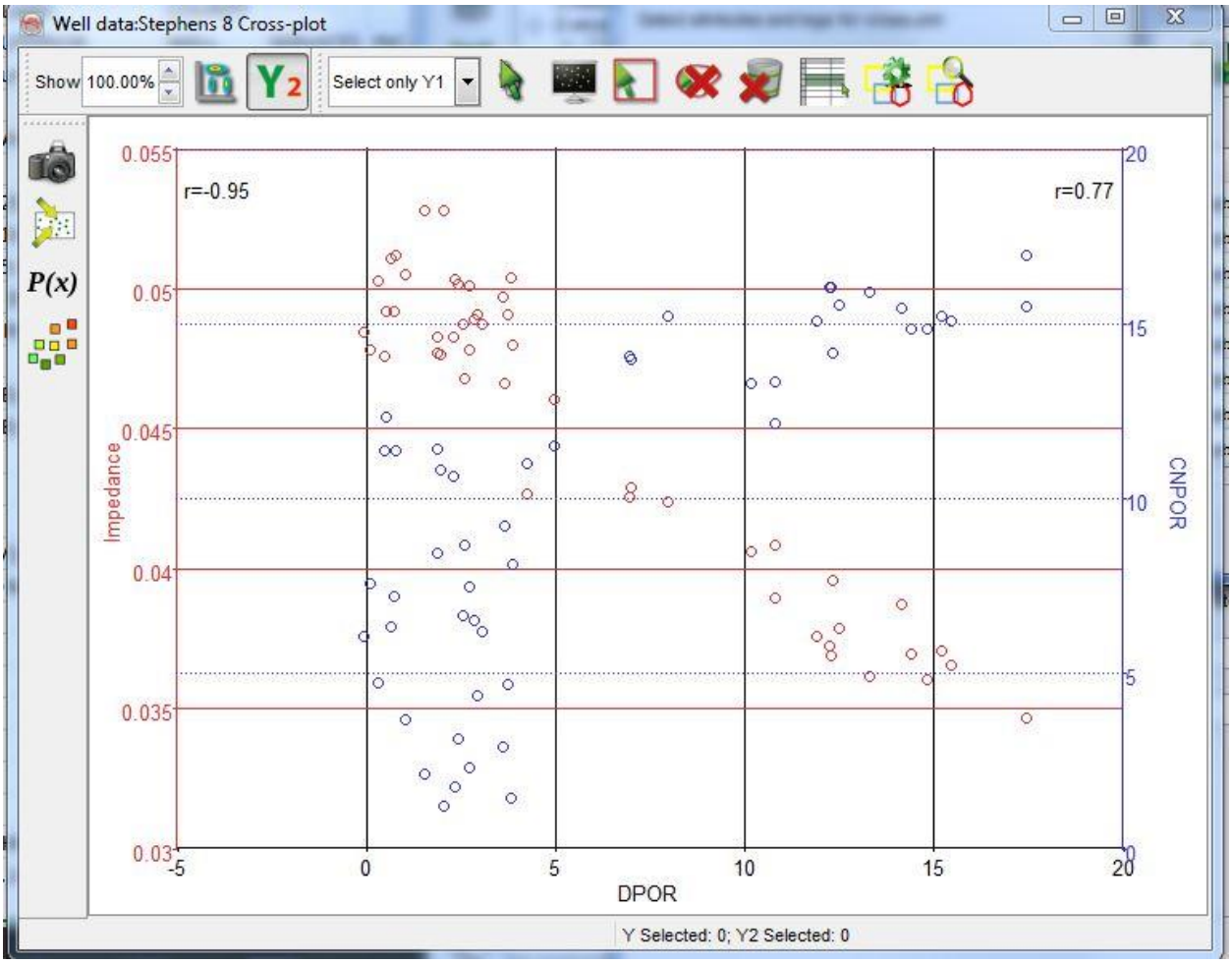

Figure 4-19 Acoustic impedance and concentrated neutron porosity (CNPOR) plotted against density porosity (DPOR) through the Viola limestone for Stephens 8.

Chapter 5 – Conclusions and Recommendation

Identification of potentially productive zones within the Viola limestone are based on instantaneous attributes analysis and amplitude anomalies. Using the workflow presented by this study could benefit future development plans in the Morrison and Morrison NE fields of east-central Clark County, KS as well as other locations in southwest and south-central Kansas. Identification of doublets forming at the top of the Viola imply a velocity anomaly associated with either the presence of hydrocarbons, the presence of more porous rock or a combination of the two. Low velocity anomalies increase the resolution of the seismic data which results in the doublets observed in the seismic trace data. Instantaneous phase and normalized amplitude attributes are helpful in identifying these velocity anomalies forming a doublet in the seismic trace data. The purpose of generating instantaneous phase and normalized amplitude attributes was to identify zones with hydrocarbon producing potential.

Amplitude was analyzed to identify a trend associating particular amplitudes with producing or non-producing wells in the study area. Lower amplitudes were associated with producing wells, while higher amplitudes were associated with dry holes and uneconomical wells with the exception of wells with a peak to trough thickness aligned with the greatest effects of tuning thickness.

The instantaneous frequency attribute when cross plotted with amplitude showed that high values in instantaneous frequency correlated with amplitude values associated with the wells completed in the survey area. This surge of instantaneous frequency values associated with decreasing amplitude values indicates hydrocarbon saturation. The thin bed indicator attribute compliments this point showing an increase in values as instantaneous frequency values increase.

Combining the attributes used in this study (amplitude, instantaneous phase, instantaneous frequency, normalized amplitude, and thin bed indicator) gives insight into the presence productive porosity and hydrocarbon saturation within the Viola limestone in the study area. Instantaneous phase and normalized amplitude highlight the doublet forming at the top of the Viola that indicates the potentially productive porosity is present. Amplitude anomalies correlate well with production, showing productive wells with amplitudes very low near zero while non-productive wells are associated with higher amplitudes. Combining low amplitude anomalies associated with the wells in the survey with instantaneous frequency and thin bed indicator shows tuning effects associated with the productive wells. This workflow demonstrates that hydrocarbon bearing zones in the Viola limestone within the study area behave as thin beds.

In future production plans within the field as well as other areas targeting the Viola limestone, combining instantaneous attributes for identification of zones of interest with amplitude analysis of these zones can lead to improved success in Viola limestone production by eliminating the completion of dry holes. The southwest corner and west-central portions of the Stephens Ranch survey are of particular interest for future well placement within the area. These two areas show the improved resolution seen in productive wells as well as the instantaneous frequency and thin bed indicator values associated with productive wells (Figure 5-1 & 5-2).

Coral Coast Petroleum has already acquired more seismic surveys in the area which are being developed. Exploration by Coral Coast could benefit from running this type of workflow at no extra cost. As more well control becomes available in these surveys this workflow should be repeated and if similar results are obtained, the workflow presented could become a valuable asset to Viola exploration in the area surrounding Clark County, Kansas.

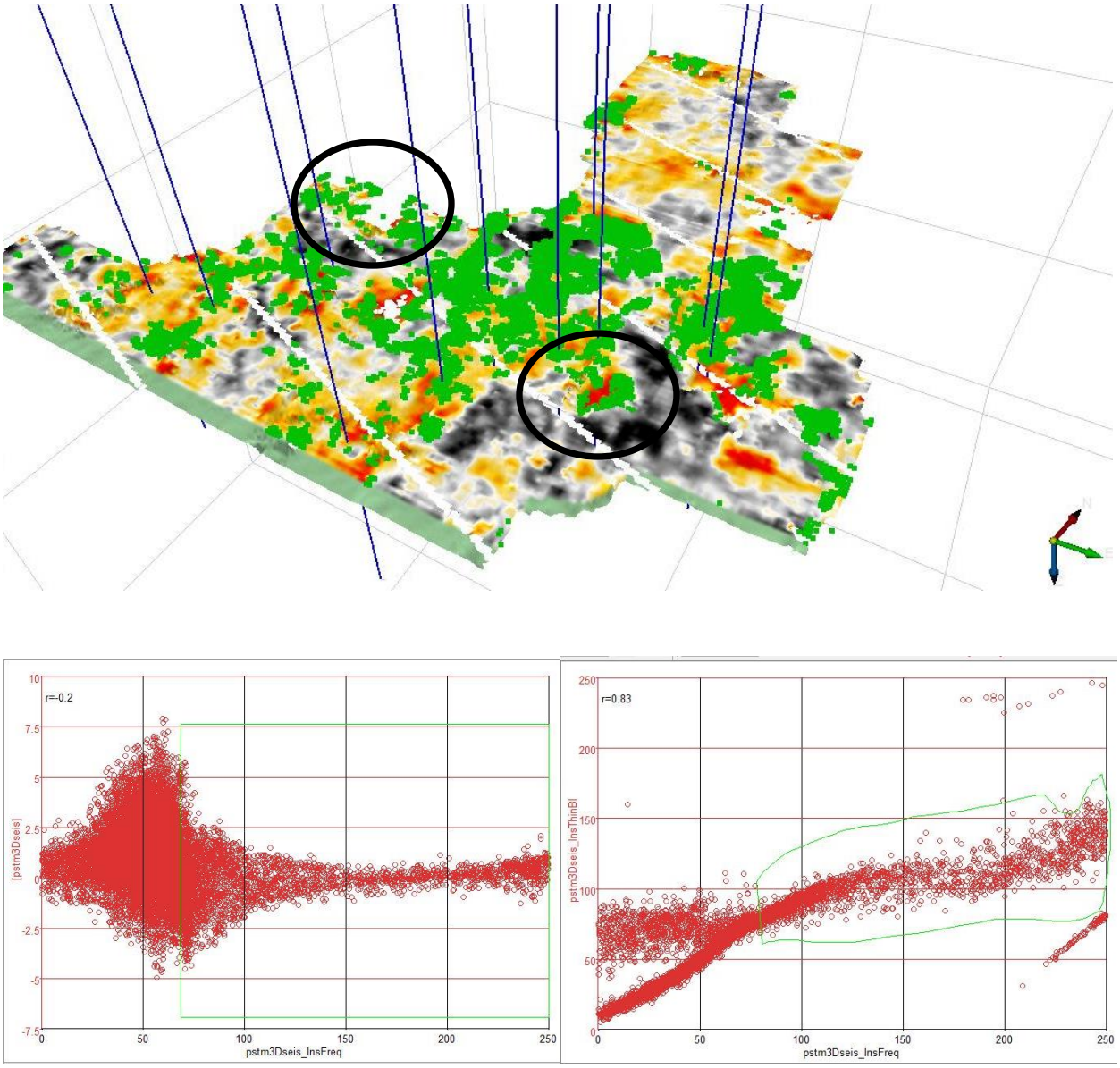

Figure 5-1 Viola Top modified from Figure 4-14. Green on the map represents areas where instantaneous frequency are peaking with thin bed indicator an indicated by the cross plots below. Circles represent potential future well placement areas.

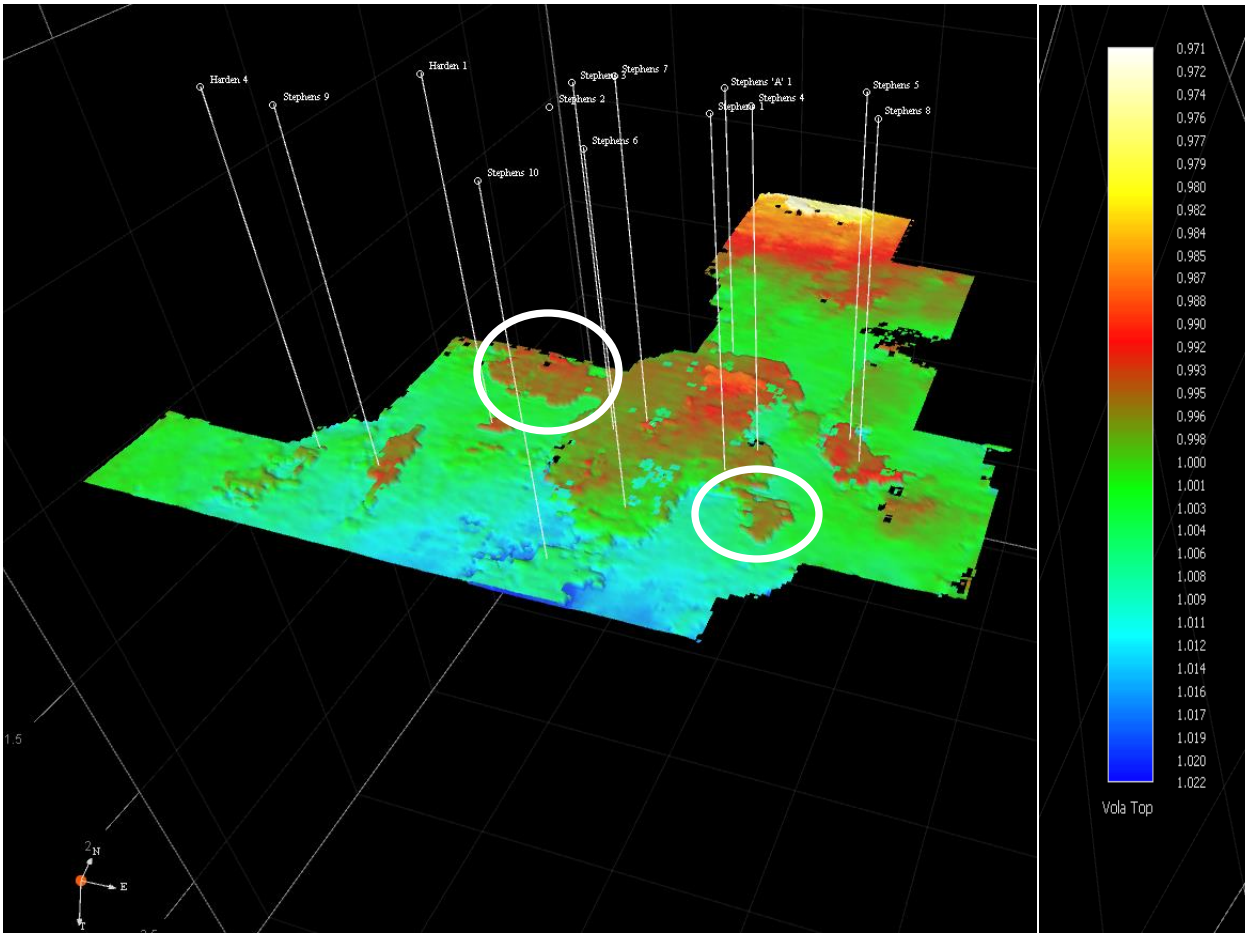

Figure 5-2 Time structure map of the Viola top. White circles represent areas for potential future well placement.

References

Adkinson, W.L., 1972, Stratigraphy and Structure of Middle and Upper Ordovician Rocks in the Sedgwick Basin and Adjacent Areas, South-Central Kansas. Geological Survey Professional Paper 702.

Anees, M., 2013, Seismic Attribute Analysis for Reservoir Characterization. 10th Biennial International Conference and Exposition.

Barnes, A.E., 1999, Instantaneous spectral bandwidth and dominant frequency with applications to seismic reflection data. Geophysics, vol. 59, no. 3, p. 419-428.

Barnes, C.R., Ordovician oceans and climates, in Webby, B.D. et al, The great Ordovician biodiversification event, Columbia University Press, 2004, p. 72-76.

Blakey, R., 2015, Northern Arizona Univesity <https://www2.nau.edu/rcb7/nam.html> Accessed, 2015.

Bureau of Economical Geology (BEG), 2015, <www.bed.utexas.edu> Accessed, 2015.

Bornemann, E., Doveton, J. H., St. Clair, P. N., 1982, Lithofacies Analysis of the Viola Limestone in South-central Kansas: Kansas Geol. Survey, Petrophysical Series 3, 50 p.

Cartwright, J. and Huuse, M., 2005, 3D seismic technology: the geological 'Hubble.' Basin Research, vol. 17, p. 1-20.

Castagna, J.P., Siegfried, R.W., and Sun, S., 2003, Instantaneous spectral analysis: detection of low frequency shadows associated with hydrocarbons. The Leading Edge, vol. 22, p. 120-127.

Chambers, R.L., and Yarus, J.M., 2002, Quantitative use of seismic attributes for reservoir characterization. The Leading Edge, vol. 21, no. 10.

Chopra, S. and Marfurt, K.J., 2005, Seismic attributes-a historical perspective. Attribute Review Paper, p. 1-71.

Chopra, S., and Kurt Marfurt, K.J., 2006, Seismic Attributes- A Promising aid for geologic prediction, CSEG Recorder, Special Edition, P. 110-121.

Chopra, S. and Marfurt, K.J., 2007, Seismic Attributes for Prospect Identification and Reservoir Characterization. SEG Geophysical Development Series No. 11. Tulsa, OK: Society of Exploration Geophysicists.

Chopra, S. and Marfurt, K.J., 2008, Emerging and future trends in seismic attributes. The Leading Edge, vol. 27, no. 3, p. 298-318.

Choquette, P.W., and Pray, L.C., 1970, Geological nomenclature and classification of porosity in sedimentary carbonates: American Association of Petroleum Geologists Bulletin, v. 54, p. 207-250.

Henry S., 2004. Understanding Seismic Amplitudes. AAPG Search and Discovery Article #40135.

IHS Global Inc., 2012, Rock Solid Attributes, Version 8.7,

Kansas Geological Survey (KGS), 2015, <http://www.kgs.ku.edu> Accessed, 2013-2015.

Partyka, G., Gridley, J., and Lopez, J., 1999, Interpretational applications of spectral decomposition. The Leading Edge, vol. 18, no. 3, p. 353-360.

Raef, A.E., 2001. Seismic modeling and multi attribute analysis – guiding applications of 3D seismic attributes to reservoir characterization. University of Science and Technology, Cracow, Poland

Raef, A.E., Mattern, F., Phillip, C., Totten, M.W., 2011. 3D seismic attributes and well-log facies analysis for prospect identification and evaluation: interpreted palaeoshoreline implications, Weirman Field, Kansas, USA. Kansas State University, Manhattan, KS.

Raef, A.E., Meek, T.N., Totten, M.W., 2015. Applications of 3D seismic attribute analysis in hydrocarbon prospect identification and evaluation: verification and validation based on fluvial paleochannel cross-sectional geometry and sinuosity, Ness County, Kansas, USA. Kansas State University, Manhattan, KS.

Richardson, L.J., 2013, The Herd Viola trend, Comanche County, Kansas. AAPG Search and Discovery Article #20220.

Rock Solid Images. Seismic Trace Attributes and Their Projected Use in Prediction of Rock Properties and Seismic Facies. (2010, January 1). Retrieved , from http://www.rocksolidimages.com/pdf/attrib.pd

Ross, R. J. Jr., 1976, Ordovician sedimentation in the western United States; *in*, The Ordovician System: Proceedings of a Palaeontologic Association Symposium, Birmingham, September 1974, M. G. Bassett, ed.: University of Wales Press and Natural Museum of Wales, Cardiff, p. 73-106.

St. Clair, P. N., 1981, Depositional history and diagenesis of the Viola Limestone in south-central Kansas: Unpub. M.S. thesis, University of Kansas., 66 p.

Subrahmanyam, D., and Rao, P.H., 2008, Seismic attributes-a review. Seventh International Conference and Exposition on Petroleum Geophysics.

Taner, M. T., Koehier, F., and Sheriff, R. E., 1977, Complex Seismic Trace Analysis, J. Geophysics., vol. 44, no. 6, pp.1041 -1063.

Taner, M.T., 2001, Seismic Attributes, Rock Solid Images, Houston, TX, U.S.A., CSEG Recorder, September, 2001, pp. 48-56.

Yilmaz, O., 1987, Seismic Data Processing: Society of Exploration Geophysicists: Tulsa, OK

Appendix A - Tuning Thickness Charts

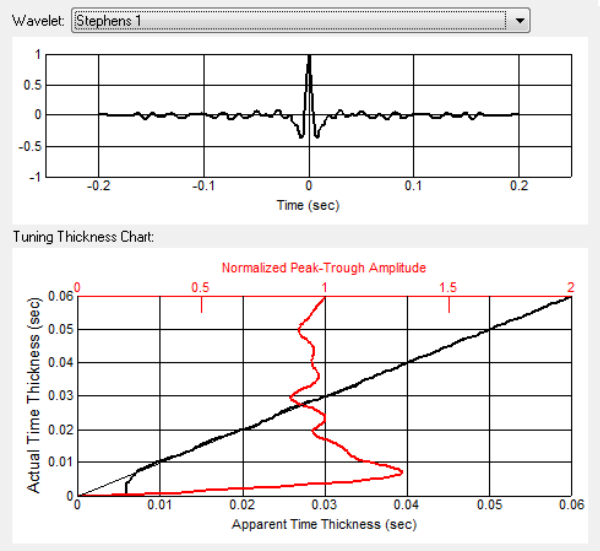

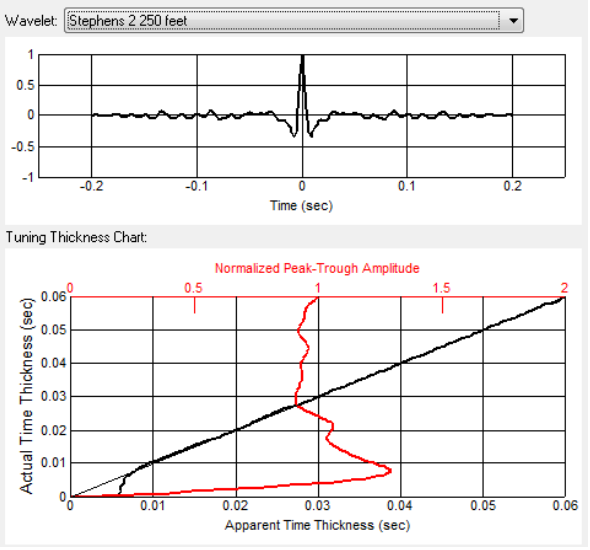

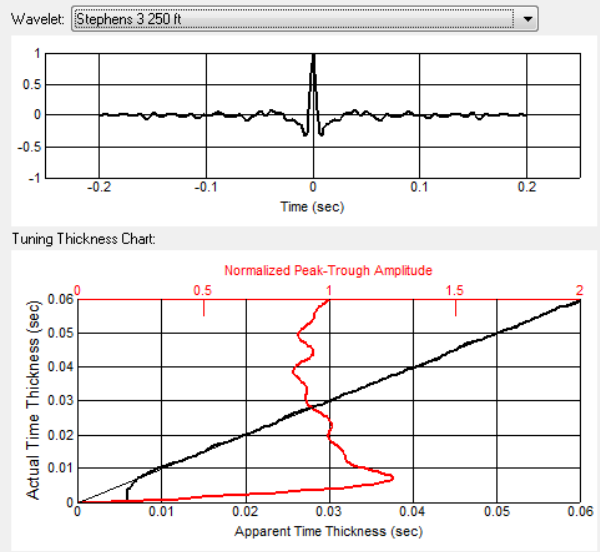

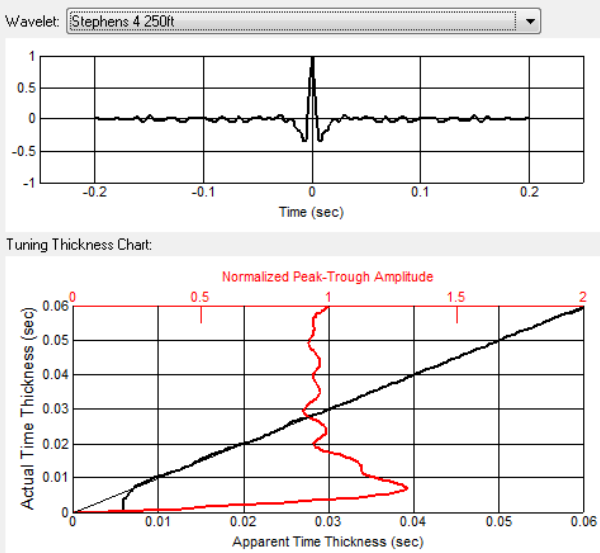

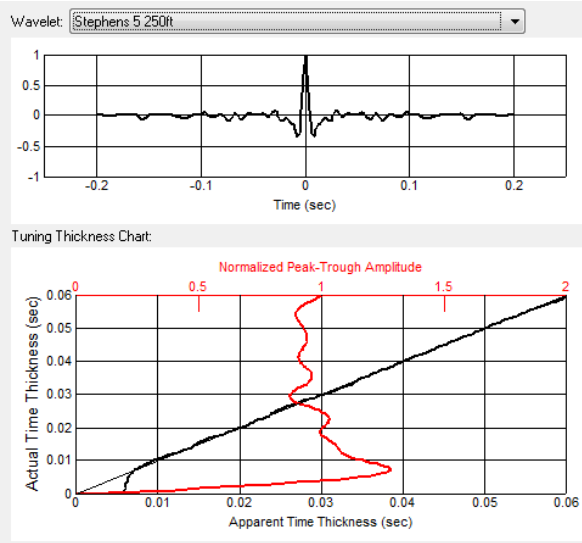
Wavelet: Stephens 5 250ft
Time (sec)
Tuning Thickness Chart:
Normalized Peak-Trough Amplitude
Actual Time Thickness (sec)
Apparent Time Thickness (sec)

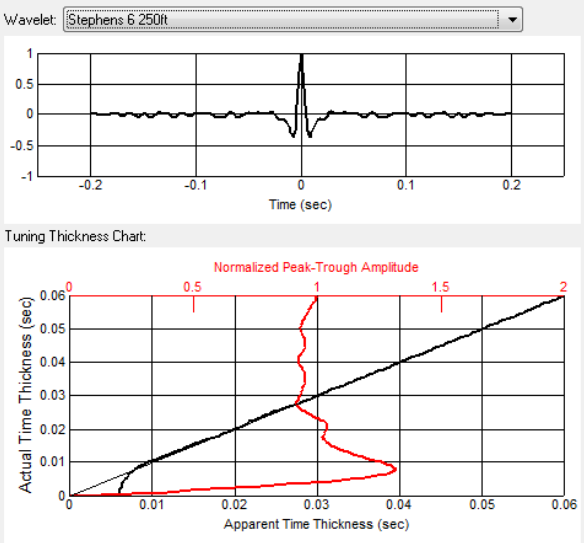
Wavelet: Stephens 6 250ft
Time (sec)
Tuning Thickness Chart:
Normalized Peak-Trough Amplitude
Actual Time Thickness (sec)
Apparent Time Thickness (sec)

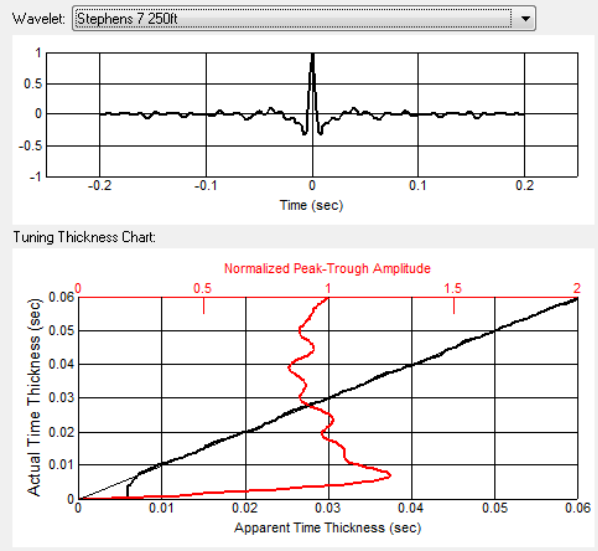
Wavelet: Stephens 7 250ft
Time (sec)
Tuning Thickness Chart:
Normalized Peak-Trough Amplitude
Actual Time Thickness (sec)
Apparent Time Thickness (sec)

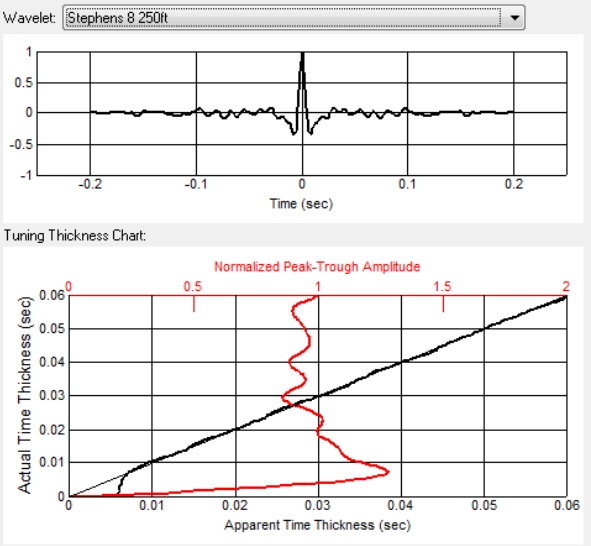
Wavelet: Stephens 8 250ft
Time (sec)
Tuning Thickness Chart:
Normalized Peak-Trough Amplitude
Actual Time Thickness (sec)
Apparent Time Thickness (sec)

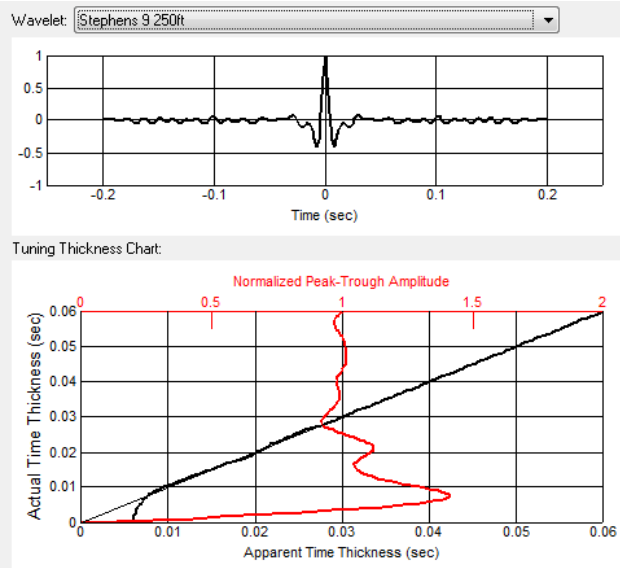
Wavelet: Stephens 9 250ft
Time (sec)
Tuning Thickness Chart:
Normalized Peak-Trough Amplitude
Actual Time Thickness (sec)
Apparent Time Thickness (sec)

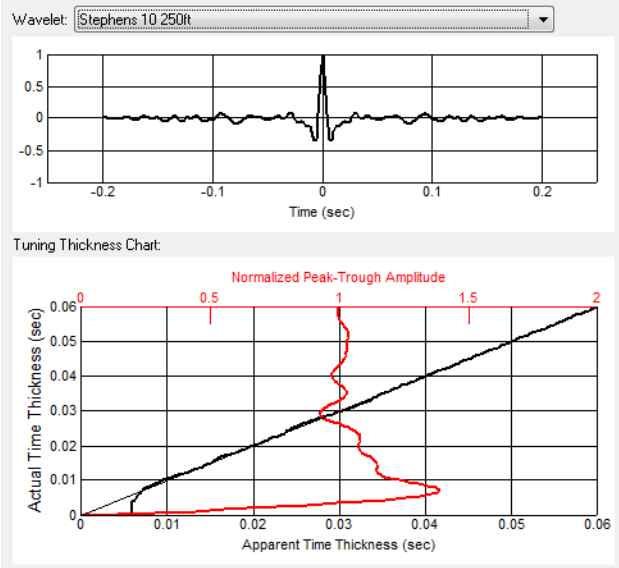
Wavelet: Stephens 10 250ft
Time (sec)
Tuning Thickness Chart:
Normalized Peak-Trough Amplitude
Actual Time Thickness (sec)
Apparent Time Thickness (sec)

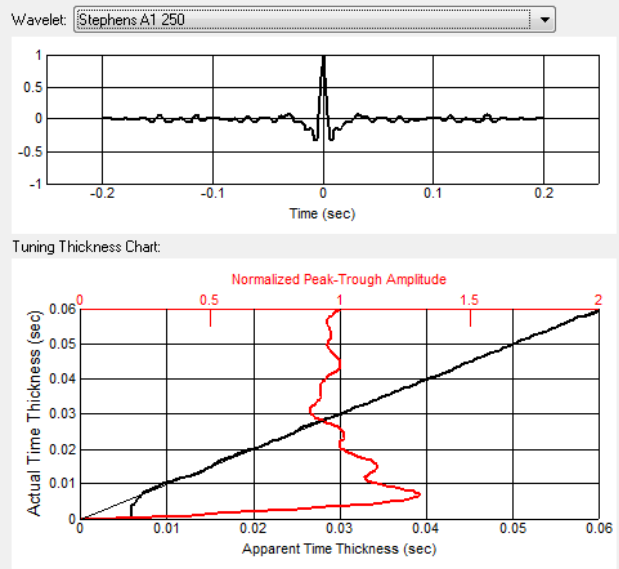
Wavelet: Stephens A1 250
Time (sec)
Tuning Thickness Chart:
Normalized Peak-Trough Amplitude
Actual Time Thickness (sec)
Apparent Time Thickness (sec)

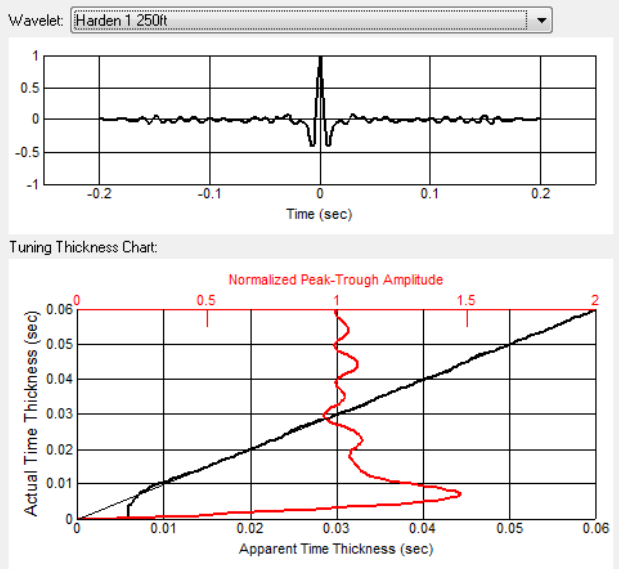
Wavelet: Harden 1 250ft
Time (sec)
Tuning Thickness Chart:
Normalized Peak-Trough Amplitude
Actual Time Thickness (sec)
Apparent Time Thickness (sec)

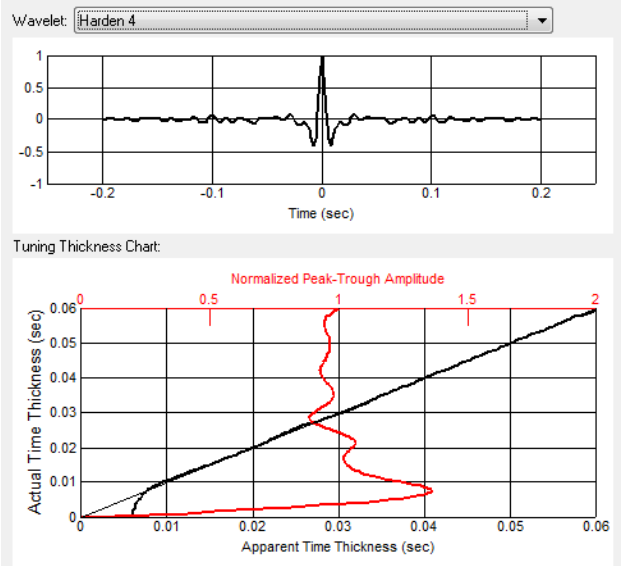

Figure A-1 Tuning thickness charts for wavelets extracted at each well within the survey area.

Appendix B - Synthetics on Seismic Trace Data

Figure B-1 Synthetic seismogram for Stephens 1 lain over trace data with tops data. Viola "C" zone in blue and Viola top in purple.

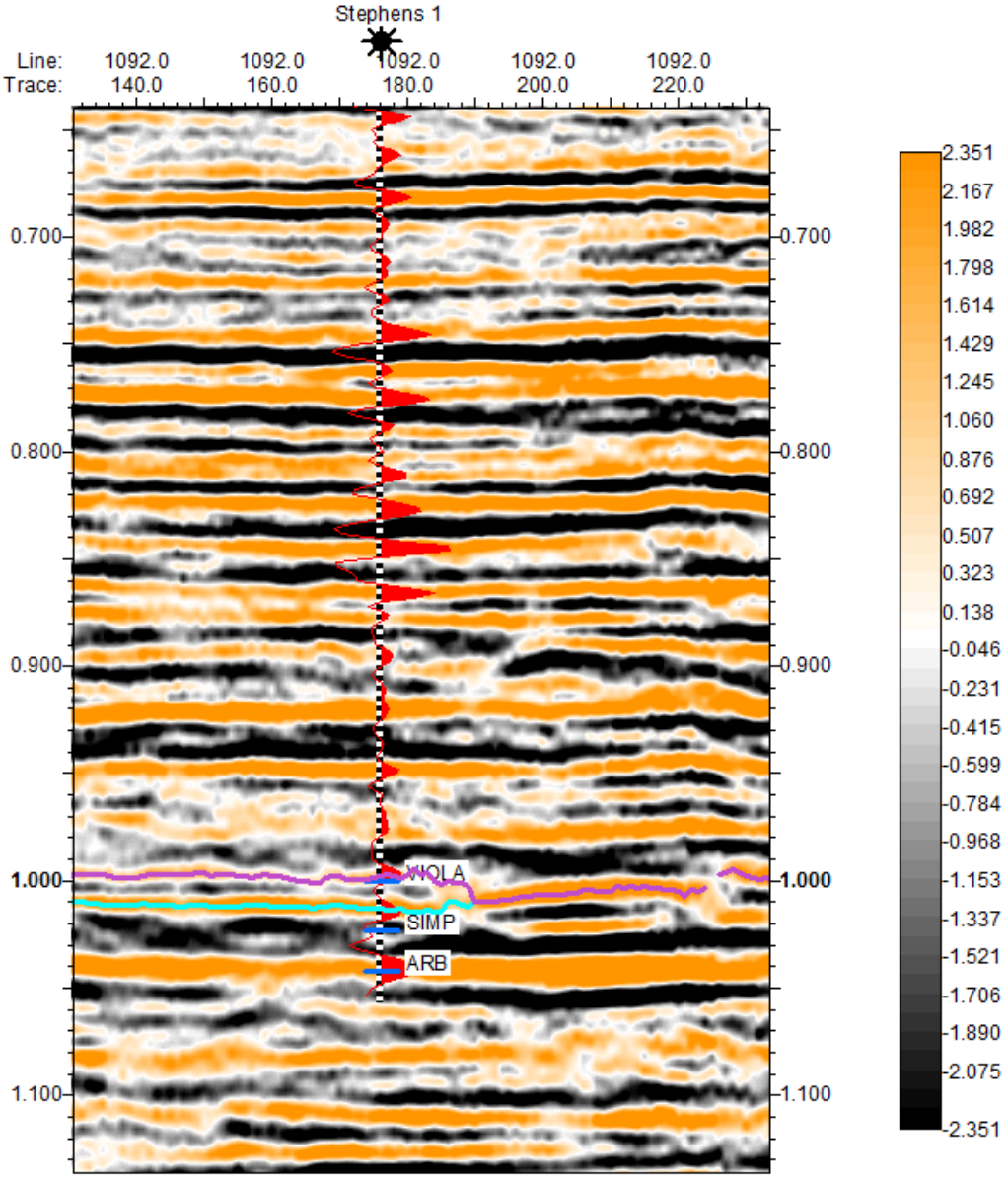

Figure B-2 Synthetic seismogram for Stephens 3 lain over trace data with tops data. Viola "C" zone in blue and Viola top in purple.

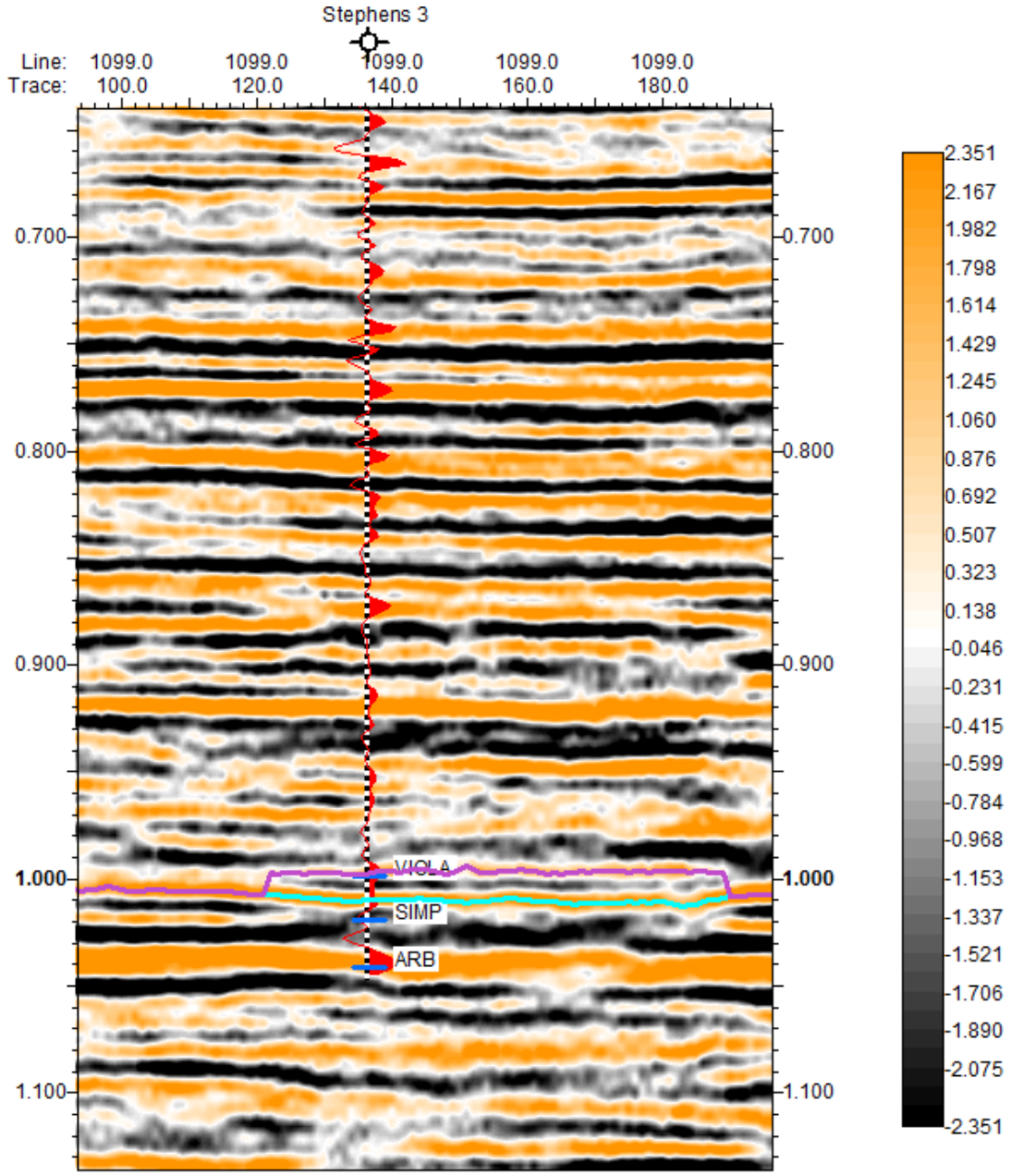

Figure B-3 Synthetic seismogram for Stephens 4 lain over trace data with tops data. Viola "C" zone in blue and Viola top in purple.

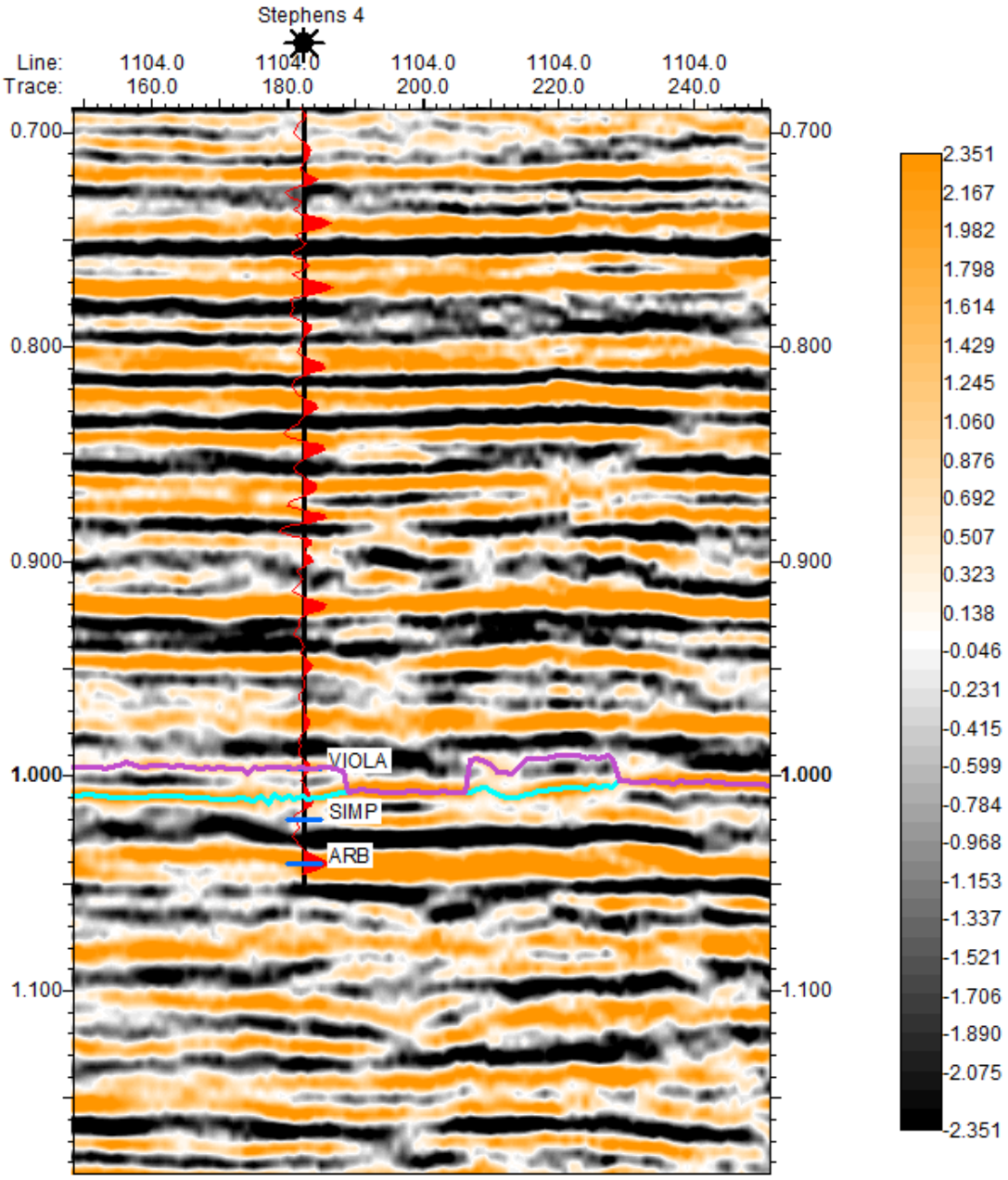

Figure B-4 Synthetic seismogram for Stephens 5 lain over trace data with tops data. Viola "C" zone in blue and Viola top in purple.

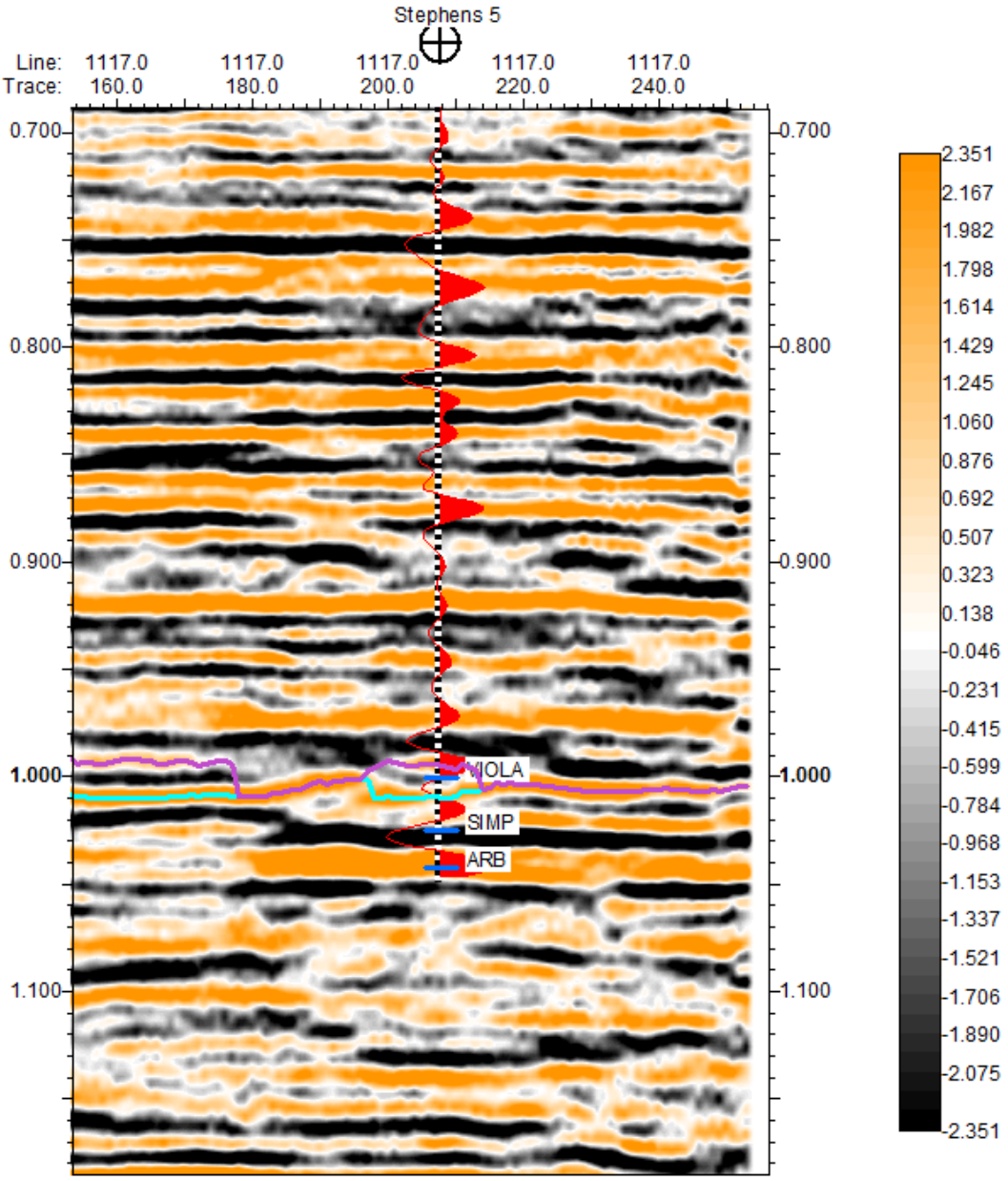

Figure B-5 Synthetic seismogram for Stephens 8 lain over trace data with tops data. Viola "C" zone in blue and Viola top in purple.

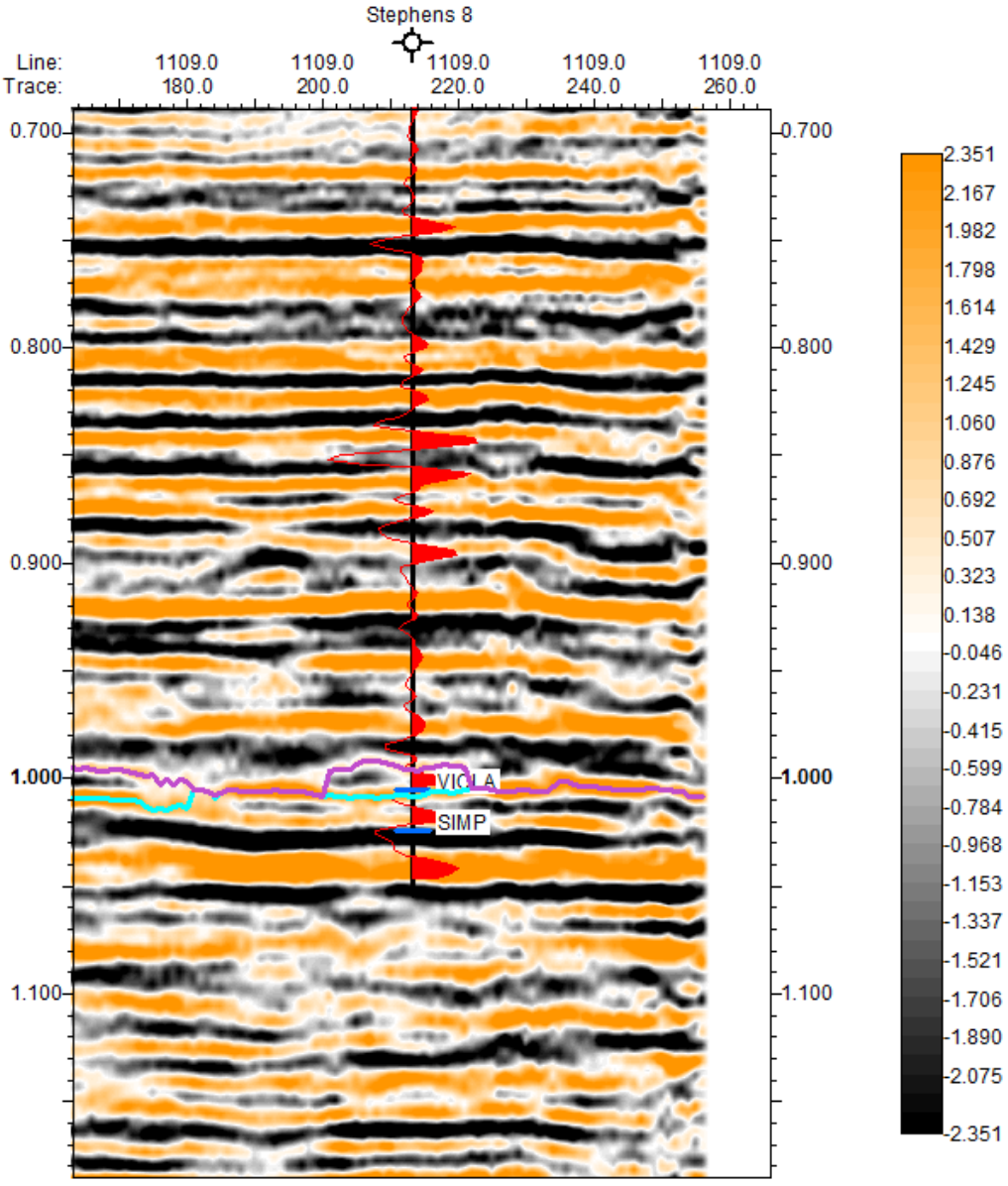

Figure B-6 Synthetic seismogram for Stephens 9 lain over trace data with tops data. Viola "C" zone in blue and Viola top in purple.

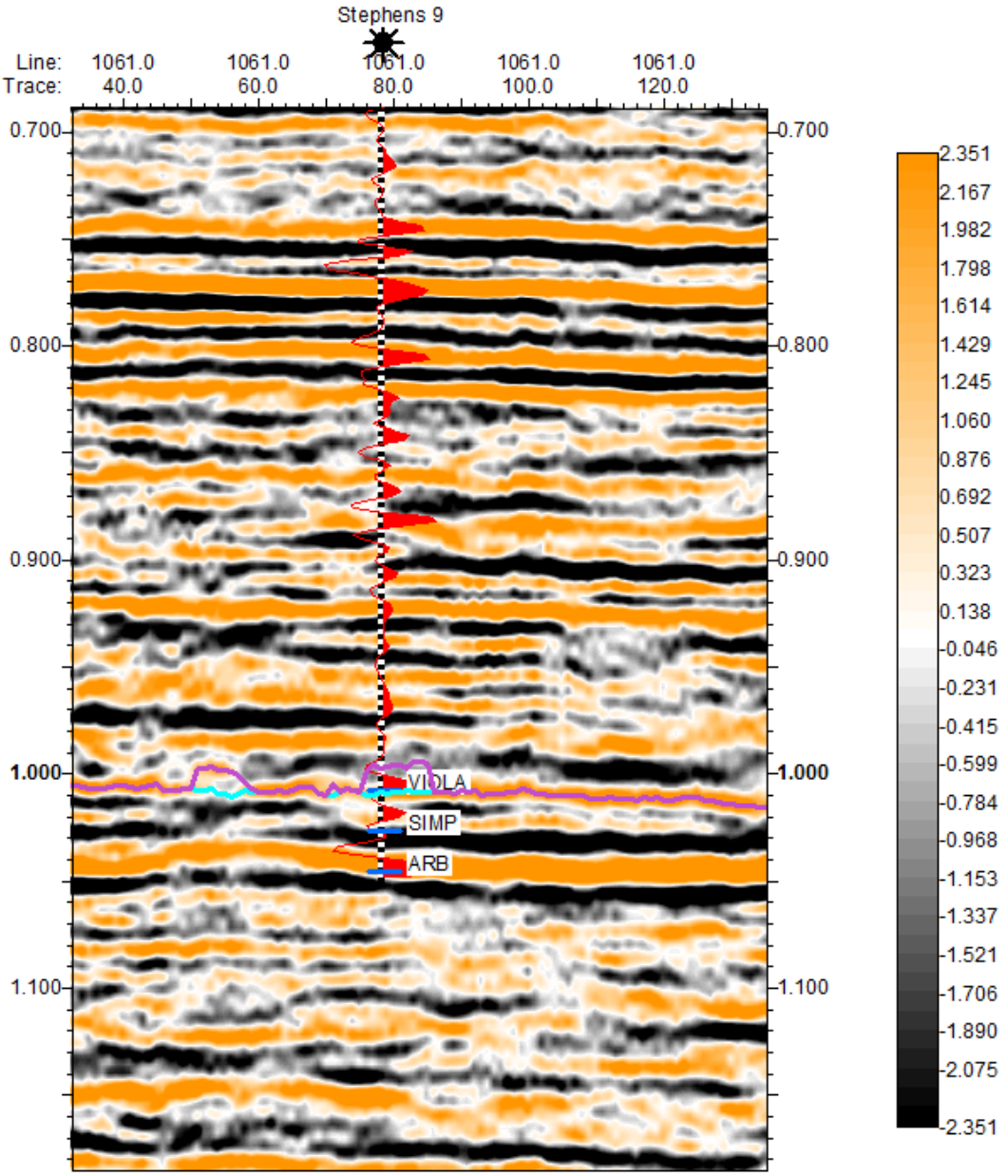

Figure B-7 Synthetic seismogram for Stephens 10 lain over trace data with tops data. Viola "C" zone in blue and Viola top in purple.

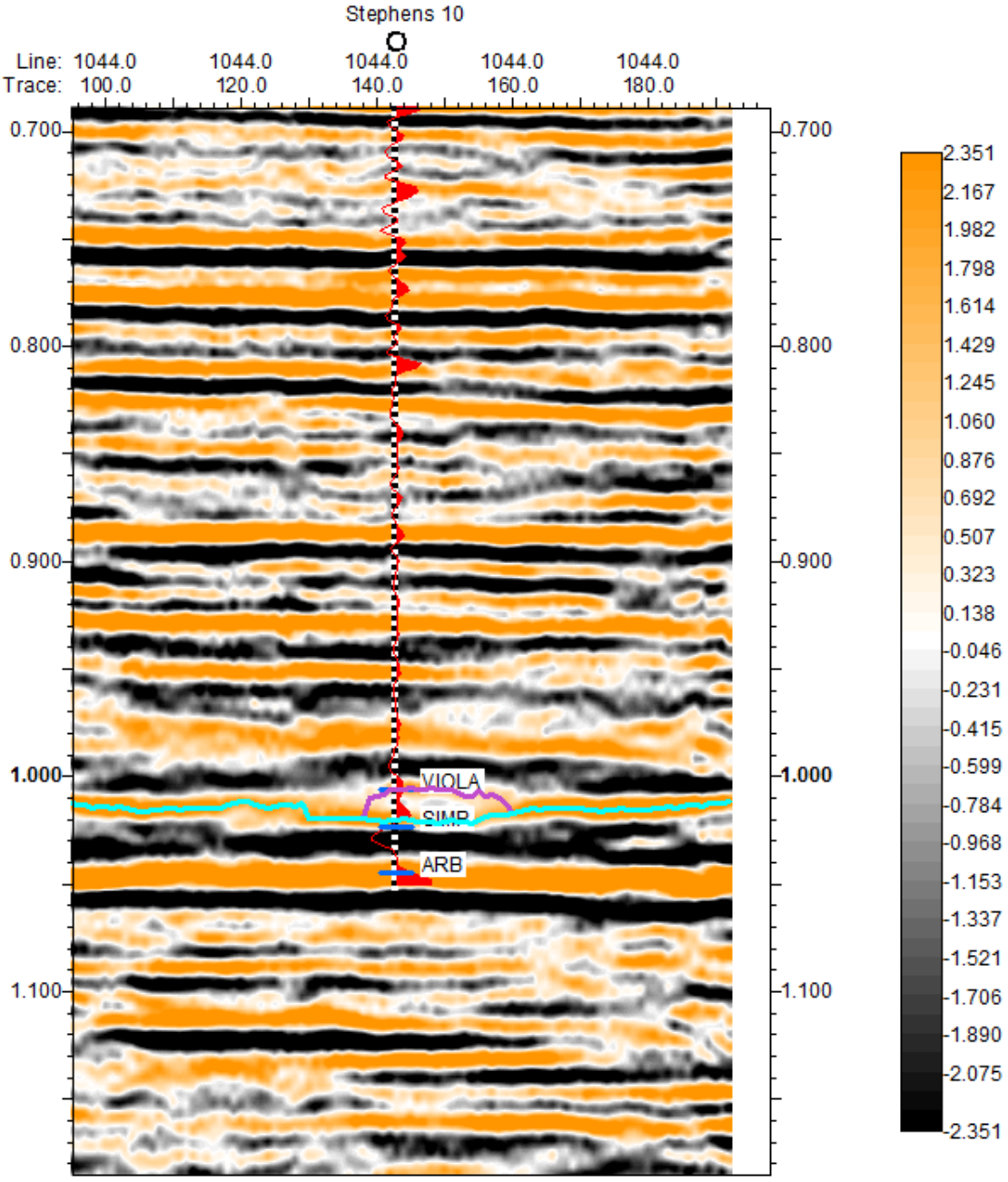

Figure B-8 Synthetic seismogram for Stephens 'A' 1 lain over trace data without tops data. Viola "C" zone in blue and Viola top in purple.